INVESTIGATION OF OIL RETENTION AND PRESSURE DROP IN SUCTION LINES USING R1234yf, R134a AND R410A WITH POE ISO 100

BY

ARAVIND RAMAKRISHNAN

THESIS

Submitted in partial fulfillment of the requirements
for the degree of Master of Science in Mechanical Engineering
in the Graduate College of the
University of Illinois at Urbana-Champaign, 2012

Urbana, Illinois

Adviser:

Professor Predrag S. Hrnjak

Abstract

Compressors of typical vapor compression refrigeration systems require the presence of oil, primarily for the purpose of lubrication. A small portion of this oil is transported out of the compressor by the high velocity refrigerant vapor exiting the compressor or by the refrigerant forming an equilibrium mixture with the oil. This results in a refrigerant/oil liquid mixture being circulated in the system, thereby leading to a decrease in system performance in terms of heat transfer coefficient and pressure drop. Of particular interest is studying the retention of oil at suction lines to the compressor, where conditions lead to a mixture that is rich in oil, consequently leading to high oil retention due to high mixture viscosity. The current work presents experimental data for oil retention and pressure drop in suction lines using R1234yf, the low Global Warming Potential (GWP) refrigerant which was developed as a consequence of the European Union's Mobile Air-Conditioning Directive. Tests were conducted in 10.2 mm internal diameter horizontal and vertical suction lines that were about 2 m long, using POE ISO 100 lubricant. A saturation temperature of 13 °C and a superheat of 15 °C were employed, while the superficial refrigerant vapor velocity was varied between 1-6 m/s. Experiments were also performed in R134a in order to study if R1234yf is a suitable drop-in replacement for R134a. Also, comparisons were made with data obtained using POE ISO 32 to study the effect of lubricant viscosity. Experimental tests in R410A using POE 32 and POE 100 served as data for further comparison. Results show that at similar operating conditions, the more viscous POE 100 yields upto 40 % more oil retention and upto 60 % more pressure drop in comparison to POE 32. It was also observed that at a similar system cooling capacity, R1234yf had upto 15 % more oil retention and upto 60 % more pressure drop in comparison to R134a. A semi-empirical model has also been proposed in order to predict oil retention and pressure drop in vertical suction lines.

An improved critical mass flux is also predicted in order to properly design vertical suction line sizes. Flow visualization studies were also performed in order to identify various regimes and the transitions between different regimes.

To My Parents and My Brother

Acknowledgement

This research work would not have been possible without the support of many individuals. I would like to thank my adviser, Professor Predag S. Hrnjak for giving me the opportunity to work with him. His constant support and guidance throughout this project, as well as the numerous insightful discussions that we had, ensured that I stayed motivated throughout my work. I would like to thank Ankit Sethi, my colleague and friend, whom I had the pleasure of working with. He has always found the time to patiently answer all my questions, despite having a busy work schedule. I would like to thank Dr. Scott Wujek, Augusto Zimmermann, Yang Zou, Rahul Kolekar and Shenghan Jin for their tremendous support, valuable advice and help throughout this research project. A special thanks to Bharat Budhiraja for the never-ending discussions that we had, and also for providing the mixture properties. I would also like to thank the various members of the Air Conditioning and Refrigeration Center at the University of Illinois for their support. The weekly group meetings that we had were always insightful, with new ideas and concepts always presenting themselves. I would also like to thank Navin Fogla, whose words of advice have always been of immense help.

Last but not certainly not the least, I thank my parents, Venkatraman Ramakrishnan and Jayanti Ramakrishnan, and my brother Anand, for their enduring love, affection and support, without whom I am incomplete. They have been there for me in every step of my life, and as a small token of appreciation, I dedicate this thesis to them.

Table of Contents

List of Tables

List of Figures

Nomenclature

a	=	constant	$\dot{m}$	=	mass flow rate, kg/s
b	=	constant	MO	=	Mineral Oil
c	=	constant	ISO	=	International Organization for Standardization
d	=	constant	OCR	=	Oil in Circulation Ratio
A	=	inner area of pipe, m^2	P	=	pressure, Pa
AB	=	alkyl benzene	P_{sat}	=	saturation pressure, Pa
D	=	diameter, m	PAG	=	PolyAlkylene Glycol oil
EES	=	Engineering Equation Solver	POE	=	PolyOl Ester oil
f_i	=	interfacial friction factor	r	=	radial distance from axis, m
f_s	=	smooth pipe friction factor	R	=	pipe radius, m
g	=	gravity, m/s^2	Re	=	Reynolds number
GWP	=	Global Warming Potential	SUS	=	Saybolt universal seconds
G	=	mass flux, kg/m^2-s	T_{bub}	=	bubble temperature, ^oC
HFC	=	hydrofluorocarbon	v	=	velocity, m/s
HFO	=	hydrofluoroolefins	w_{local}	=	local oil concentration in liquid film
j*	=	dimensionless superficial velocity	We	=	Weber number
K	=	constant	x	=	quality
L	=	length of suction pipe, m	z	=	axial distance
m_{oil}	=	mass of oil, kg			

Greek Symbols

α	=	void fraction	ρ	=	density, kg/m^3
δ	=	liquid film thickness, m	σ	=	surface tension, N/m
δ^+	=	dimensionless film thickness	τ	=	shear stress, Pa
μ	=	dynamic viscosity, Pa-s	τ_i	=	interfacial shear stress, Pa
υ	=	kinematic viscosity, m^2/s			

Subscripts

c	=	refrigerant vapor core	z	=	axial coordinate
l	=	liquid film	v	=	refrigerant vapor
r	=	radial coordinate	mix	=	mixture

Chapter 1-INTRODUCTION

1.1Background

One of the major components of a Vapor Compression Refrigeration System (VCRS) is the compressor. The compressor has the primary function of maintaining refrigerant flow in the system. The compressor serves to raise the exit vapor pressure and consequently the temperature as well. The compressor, predominantly positive displacement types, requires oil for their operation. The primary purpose of the oil is to serve as a lubricant for the various moving components in the compressor, by providing a thin oil-film. Secondary functions include serving as a tightness element, noise limiter, acting as a heat transfer medium to cool the compressor, as well as transporting away debris/contaminants from the compressor (Youbi-Idrissi and Bonjour, 2008).

As the vapor entering into the compressor is compressed, a portion of this oil is carried away by the refrigerant vapor. This primarily occurs due to two reasons: 1) the lubricant forms an equilibrium mixture with the refrigerant vapor and is hence carried away, 2) the high vapor momentum forces oil out of the compressor. In any case, at the exit of the compressor, refrigerant vapor is accompanied by an oil-rich liquid mixture. The fraction of oil in this mixture depends on the solubility of the refrigerant vapor in the oil, which in turn depends on the specific refrigerant/oil choice, saturation temperature and the degree of superheat. Thus in any Vapor Compression Refrigeration System (VCRS), a refrigerant/oil mixture is always in circulation. This evidently will lead to changes in the heat transfer characteristics, since the mixture is highly zeotropic, as oil will not vaporize under general operating conditions.

Another important aspect of this issue is lubricant return to the compressor. As the oil is transported out of the compressor, the compressor is gradually depleted of oil. This would lead to compressor failure due to lubricant starvation. Thus in order to avoid this situation, the lubricant should ideally be returned back to the compressor, which in general will happen by steady state principles. The amount of oil that is measured in any given component at a given operating condition is the 'oil retention' of that component. The inlet/suction lines to the compressor have conditions of high quality and low temperature, which give rise to the highest liquid mixture viscosity. This condition of high viscosity leads to the highest oil retention at the suction line for the system. This problem is further compounded by operation at part load conditions, where low vapor momentum condition is insufficient to transport the liquid mixture back to the compressor, leading to increased oil retention. Another impact of oil is the increase in pressure drop across components in the system, since vapor momentum is utilized for oil transport.

The current work looks at oil retention and pressure drop in horizontal and vertical suction lines in a R1234yf system. R1234yf is a HFO (HydroFluoroOlefin) that has been developed to be used in automotive air-conditioning systems, replacing the existing refrigerant, R134a in accordance with the European Union's Mobile Air-Conditioning Directive. The main characteristic of R1234yf is its extremely low GWP (Global Warming Potential) of 4, in comparison to 1430 of R134a. It also has an atmospheric lifetime that is about 400 times less than that of R134a. However, there is also an inherent interest to compare performance in R1234yf with that of R134a. For this reason, oil retention and pressure drop measurements were made in R134a as well. The lubricant employed for the current work was POE 100. POE (PolyOl Ester) and PAG (PolyAlkylene Glycol) are classes of lubricants referred to as synthetic oils. These were developed so that they would be compatible with the new HFCs (HydroFluoroCarbons) like

R410A, R407C, etc. which were introduced as replacements for R22. The MOs (Mineral Oils) that were used with R22 were immiscible with these new HFCs - leading to increased retention, thus paving the way for synthetic lubricants. Thus in reality, the oil retention is a strong function of the liquid mixture properties, namely mixture viscosity and mixture density. In order to capture the effect of lubricant viscosity, the current work has been compared with those results obtained by using POE 32 (Sethi and Hrnjak, 2011). The effect of lubricant viscosity is also studied by employing POE 32 and POE 100 in a R410A system.

1.2 Literature Review

1.2.1 Experimental Investigations on Oil Retention

Jacobs *et al.* (1976) investigated the oil retention phenomenon in vertical suction risers, in order to determine the veracity of the minimum tonnage requirements necessary for oil transport, which had been presented in the ASHRAE Handbook (1973). They simulated a wide range of common suction and discharge conditions using R12 and R22 refrigerants with prescribed amounts of 150 and 300 SUS naphthenic oils. A 2.5 cm diameter, vertical test section was used with an injector and separator present at the inlet and outlet respectively. The test fluid entering the test section was refrigerant vapor, into which the lubricant was injected and oil transport was visually observed through a sight glass. It was ensured that the conditions of oil transport were independent of both the method of injection as well as the injector position. An increase in the amount of oil accumulated with decreasing refrigerant mass flux was observed through the sight glass, thus indicating lack of oil transport. This was continued until the test section was flooded. Thus the minimum conditions necessary for liquid transport were formulated analytically. They correlated the experimental data by employing the commonly used Wallis flooding correlations (Wallis, 1969). This was performed by considering a force balance between vapor momentum

flux and the hydrostatic forces, namely buoyancy and gravitational force. Based on the experimental data obtained, a conservative estimate for the dimensionless flooding correlation for the vapor flow was suggested as

$$(j_g^*)^{1/2} = 0.85 \tag{1.1}$$

Thus the minimum mass flux required for oil transport and return is represented in the following convenient form.

$$G = ((j_g^*)^{1/2})^2 \left[\rho_v g D(\rho_l - \rho_v)\right]^{0.5} \tag{1.2}$$

This has been recast in the form of minimum tonnage required to ensure proper oil return, with the authors presenting this data in the form of charts, along with the minimum pipe diameters required. The drawback of this correlation is that it does not consider the effect of oil concentration as well as the lubricant viscosity on oil return.

Annular film flow reversal in an 8 mm internal diameter, vertical pipe was investigated by Mehendale and Radermacher (2000). This work investigated the critical refrigerant mass flow rates at which the oil-rich annular film started reversing, both experimentally as well as theoretically, with extensive flow visualizations being conducted. For the experiments, miscible refrigerant-oil combinations of R410A/POE, R22/MO and R407C/POE were considered in addition to the immiscible refrigerant-oil combinations of R410A/MO and R407C/MO. Lubricant was injected into the test section as a percentage of the refrigerant mass flow rate and was separated at the end of the test section. It was observed that when the refrigerant mass flow rate was reduced below a critical value, the stable upward moving annular liquid film became unstable, started oscillating and then reversed its direction of motion by flowing downwards. It

was also noted that these critical flux limits were higher than those predicted by Jacobs *et al.* (1976). This would seem to indicate that the Jacobs critical mass flux is perhaps not the ideal choice based on which suction lines should be designed. An analytical model was developed in order to determine the critical mass flux for lubricant return, for which the Wallis interfacial friction factor correlation was used. The model predictions were found to lie within -4 % and +7 % of the experimental data (without considering experimental uncertainties). Parametric variation of the model showed that the critical refrigerant mass flux should decrease with an increase in film viscosity.

Biancardi *et al.* (1996) conducted experimental as well as analytical investigations to understand lubricant circulation and return characteristics in HVAC (Heating, Ventilation and Air-Conditioning) systems, thereby identifying 'worst case' oil return scenarios, where no oil return was observed. For this purpose, R22/MO was employed as the baseline test, and comparisons were made with R407C/POE and R407C/MO, which simulated high miscibility and low miscibility mixtures respectively. Both heating mode as well as cooling mode operations was simulated, with a 19 mm inner diameter suction line being employed and the lubricant concentration being varied from 0-10 %. For the heating mode, the flow velocity corresponding to the worst oil return was approximately 0.5 m/s, which was observed both visually as well as by measurements for oil circulation rates between 0.25-0.5 %. For higher oil circulation rates, this flow velocity went up to 1 m/s. The cooling mode was characterized by worst case flow velocities of about 1.84 m/s. With miscible lubricants, both R22 and R407C were found to exhibit similar oil return characteristics, which were confirmed by both minimum velocity measurements as well as visual observations. They also made the surprising conclusion that the

immiscible R407C/MO mixture could be operated at lower velocities in comparison to the miscible R407C/POE and R22/MO mixtures.

Kesim *et al.* (2000) investigated oil return in vertical suction lines, by determining the minimum refrigerant speed required to carry the lubricant up the vertical line. An analytical model was developed in order to predict the minimum refrigerant vapor velocity required to carry oil back to the compressor. The oil velocity at the refrigerant vapor interfacial surface is determined by deriving the oil velocity profile across the film thickness. This is performed by applying cylindrical Navier-Stokes equation as well as continuity equation on the oil film, from which the volumetric flow rate expression is obtained by integrating over the film thickness. It was assumed by the authors that the limiting condition at which no oil return is observed corresponds to the case where the oil volumetric flow rate goes to zero. The closure equation was obtained by relating the frictional pressure drop to the refrigerant vapor velocity. The friction factor employed was given by the Blasius correlation, which was for turbulent flow in smooth pipelines. Results were tabulated in the form of minimum capacity (kW) tables required for oil entrainment, for various vertical copper tube diameters. The condensing temperature was maintained at 40 °C, while the evaporator temperatures were varied among the values of -35, -25, -15, -5 and 5 °C respectively, while the oil film thickness was assumed to be 2 % of the pipe inner diameter. As pointed out by Sethi and Hrnjak (2011), the application of the Blasius correlation may not be really suitable since it is suited for turbulent flow in smooth pipes, while in reality flow visualizations show that the point of film reversal is characterized by an extremely wavy interface, which is not smooth.

Lee et al. (2001) conducted experimental investigations on lubricant retention in vertical suction lines, by employing R134a refrigerant and AB ISO-8, AB ISO-10 and MO ISO-10 as the

lubricants. The refrigerant/oil mixtures in the study were immiscible in nature, with the oil concentration being varied between 0.2-5.4 % by weight. Three different refrigerant mass flow rates of 0.10 g/s, 0.37 g/s and 0.57 g/s were employed while the volumetric flow rate of the oil was operated at conditions of 4 ml/hr, 12 ml/hr and 20 ml/hr respectively. The test methodology was the injection-separation method. Liquid oil was introduced at the bottom of the vertical suction line at a specified flow rate by means of a syringe pump, while an oil separator at the end of the suction line extracts oil from the flow stream. The amount of oil retained was computed based on the rates of injection and extraction. It was observed that for MO, the oil retention in the suction line accounted for 3.8-17.6 % of the initial oil charged into the compressor. The amount of oil retention in the case of AB decreased, with the vertical retention accounting for 2.3-12.8 % of the initial compressor oil charged. It was clearly observed that the higher viscous AB ISO-10 oil had more oil retention than AB ISO-8 oil. Results were also presented in the form of mean oil film thickness ratio (MOFTR), which is the annular film thickness non-dimensionalized by the tube radius. For conditions of the same superficial vapor velocity, AB ISO-10 had a larger MOFTR in comparison to AB ISO-8. In general, it was observed that the MOFTR values decreased with increasing refrigerant flow rates, while increasing oil volumetric flow rates lead to an increase in MOFTR, which consequently yielded higher oil retention. The poor solubility of MO with R134a, in comparison to that of AB yielded higher oil retention. It was also observed that at a high vapor velocity of 4.6 m/s, the influence of viscosity and type of oil on the retention characteristics was insignificant. Flow visualizations indicated that the flow regime was annular at high vapor velocities, with the flow transitioning into churn flow at low refrigerant flow conditions.

Cremaschi *et al.* (2005) conducted experimental investigations on oil retention in different components of a typical air-conditioning system, namely the condenser, evaporator, liquid line and suction line. Suction line experiments were conducted using injection-separation methodology, similar to Lee et *al.* (2001). Tests were conducted with miscible and immiscible refrigerant/oil combinations, and the effects of oil mass fraction (OMF), the refrigerant vapor mass flux and mixture viscosity ratio were investigated. The refrigerant/oil mixtures included R22/MO, R410A/MO, R410A/POE, R134a/POE and R134a/PAG, while both horizontal and vertical suction lines were employed having inner diameters of 13-19 mm. The OMF was varied between 0.7-8 % by weight, the refrigerant mass flux was changed between 150-400 kg/m^2-s while mixture viscosity ratio was varied between 20-48. The mixture viscosity ratio was the liquid film viscosity divided by the refrigerant vapor viscosity ($\nu_{liq,film}/\nu_{vapor,ref}$). This mixture viscosity ration was further non-dimensionalized by that of R22/MO to give the viscosity ratio factor (vrf). For the R22/MO mixture, it was observed that at an OMF of 5 %, increasing the mass flux from 150 kg/m^2-s to 206 kg/m^2-s decreased the horizontal suction line oil retention by 30 %, while the vertical oil retention decreased by 23 %. It was also observed that the oil retention of the immiscible R410A/MO mixture was 55 % larger than that observed in the case of R410A/POE, and this was characterized by a larger vrf for R410A/MO. It was also observed that at an OMF of 3 %, increasing the vrf from 17 % to 55 % yielded an increase in oil retention volume from 20 % to 120 %. At the same OMF, miscible mixtures like R134a/POE and R134a/PAG had 20 % lower oil retention in comparison to R22/MO due to their lower vrf values. Gravitational effects caused a 50 % higher oil retention in vertical suction lines in comparison to horizontal lines. Flow visualization studies were also conducted to identify the various flow regimes present. Flow regime instability was also observed, with the annular liquid

film becoming wavy when the mass flux was reduced to 63 kg/m^2-s for the 19 mm vertical suction line.

Lee (2003) experimentally and theoretically investigated the horizontal oil retention in various components for a CO_2 refrigerant system. PAG ISO 43 was employed as the lubricant in the investigation, with the suction line being 3.8 m in length and 7.1 mm in inner diameter. Analogous to Lee *et al.* (2001), injection-separation methodology was employed for estimating suction line oil holdup. Typical automotive air-conditioning operating conditions were simulated, with the initial amount of oil charged into the compressor being 250 ml, with the OCR being varied between 1-7 % by weight. Oil retention results were expressed in terms of oil retention volume ratio, which is the volume of oil retained, divided by the initial charged volume. For a mass flux of 290 kg/m^2-s, it was noticed that the oil retention volume ratio increased from 0.05 to 0.15, when the OCR was changed from 1.4 % to 6 % by weight. It was also noticed that the oil retention volume ratio decreased with an increase in mass flux for a particular OCR. Also, an increase in the vapor quality at the suction line inlet leads to an increase in oil retention volume ratio, due to an increase in liquid film viscosity.

1.2.2 Oil Retention Investigations at ACRC, University of Illinois at Urbana-Champaign

Crompton *et al.* (2004) conducted oil retention experiments in horizontal, round copper tubes of various internal geometries, namely internally smooth tube, axially microfinned tube and helically microfinned tube. Different refrigerant/oil mixtures were employed, namely R134a/POE, R134a/PAG, R134a/AB, R22/AB and R410A/POE. Tests were conducted in a 9 mm inner diameter tube, with the mass flux predominantly varying between 75-150 kg/m^2-s, while the oil concentration and the suction line inlet vapor quality were changed in general between 0-4 % and 0-100 % respectively. For the mixture of R134a/PAG, the oil concentration

was varied upto 15 %. Experiments were performed by employing the direct measurement technique. The oil concentration and the mass flux were controlled by mixing liquid refrigerant and oil and sending the mixture to the heater, thereby controlling the superheat. The oil-rich mixture is then sent to the suction lines and once equilibrium flow conditions have been attained, the test section was closed off at the ends simultaneously, by means of employing ball valves. The test section is then disconnected from the system and refrigerant vapor is removed by following ASHRAE Standard 41.4, after which the mass of oil retained in the suction line is measured. It was consistently observed that when the quality was varied between 0-100 %, the oil retention initially decreased with increasing quality, reached a minimum value at about 50 % quality value, beyond which the oil retention again increased with increase in quality. The minimum oil retention at the mid-quality range was attributed to the stretching of the liquid layer by the increased refrigerant vapor velocity. For a given quality near 50 %, it was observed that the oil retention at 75 kg/m^2-s was greater than that observed at 150 kg/m^2-s while an increase in oil concentration percentage also yielded an increase in oil holdup. These trends were not observed at high quality values. It was also noticed that the tube internal geometry did not affect oil retention significantly at low to medium vapor quality, while at higher vapor quality the smooth geometry tube had lower retention in comparison to the finned tubes. Also, the immiscible refrigerant/oil combination of R134a/AB had much larger oil retention in comparison to the miscible combinations. It was also concluded that smooth tube configuration as well as higher mass flux values yielded higher void fraction values. Flow visualization experiments were conducted in order to identify various trends in the flow regime.

Zoellick and Hrnjak (2010) conducted oil retention and pressure drop experiments in horizontal and vertical suction lines which were about 2 m in length. A refrigerant/oil mixture of

R410A/POE 32 was employed for the study, with two different suction line inner diameters being used, namely 7.1 mm and 18.5 mm respectively. In this study, the effect of mass flux, OCR and apparent superheat on the oil retention and pressure drop were observed. Similar to method described by Crompton *et al.* (2004), the direct measurement technique was employed to determine oil retention in the horizontal and vertical suction lines. The mass flux was varied between 100-250 kg/m^2-s in the 7.1 mm tube while it was varied between 60-100 kg/m^2-s in the 18.5 mm tube. The OCR was varied between 1-5 %, while the apparent superheat values used were 0 °C, 5 °C, 10 °C and 15 °C respectively. These superheat values were observed to correspond to suction line inlet vapor qualities between 0.85-0.95. It was observed in the vertical test section that the flow regime transitioned from annular flow to churn flow, when the mass flux was reduced to the Jacobs critical mass flux condition. Interestingly, it was also noticed that on increasing the mass flux, the flow transitioned back into annular flow at a 30 % higher mass flux, indicating the presence of a hysteresis loop at the Jacobs limit. Flow visualizations were conducted in the transparent test sections, which showed higher liquid film thickness for higher OCR flows, which thereby lead to an increase in oil retention. It was also observed that for a given OCR value, increase in the mass flux yielded a decrease in oil retention. Increase in the apparent superheat leads to an increase in the liquid mixture viscosity, which consequently leads to an increase in oil retention. It was observed that increasing the OCR from 1 % to 3 % lead to a 20-50 % increase in oil retention. It was noticed that the oil retention increased by 15 % when the apparent superheat increased by 5 °C. The vertical suction line had 10 % more oil retention than the horizontal line due to gravitational effects. It was also observed that the pressure drop in the suction lines increased with an increase in OCR. In the horizontal suction lines, the pressure drop decreased with decrease in mass flux, while in the vertical suction line, the pressure drop

decreased initially and went to a minimum value, beyond which it again started increasing when the mass flux was increased.

Sethi and Hrnjak (2011) conducted oil retention experiments with R134a/POE 32 and R1234yf/POE 32 in horizontal and vertical suction lines. The transparent suction lines were 2 m in length and had an internal diameter of 10.2 mm. The operating conditions were maintained at a saturation temperature of 13 °C, with a superheat of 15 °C. The mass flux was varied between 33-140 kg/m^2-s for R134a and between 36-170 kg/m^2-s for R1234yf, which corresponded to variation in the superficial vapor velocity between 1.5-7 m/s. Experimental results showed similar trends to those observed in Zoellick and Hrnjak (2010). Comparisons were made between R1234yf and R134a for similar conditions and it was observed that at the same system cooling capacity, the two refrigerants had similar oil retention while R1234yf possessed 20-30 % higher pressure drop than R134a. These results have severe implications in employing R1234yf as a drop-in replacement for R134a refrigeration systems. Experiments were conducted on inclined suction lines as well, with the angle of inclination being 45° and 60°. It was observed that the inclined suction lines possessed larger oil retention in comparison to the vertical and horizontal test sections at the same conditions of operation, thus implying that inclined pipes should be avoided at compressor inlets. Extensive flow visualizations were performed in the transparent test sections. It was again observed that the flow in the vertical test section was annular at high vapor velocities, transitioning into churn flow at the lower Jacobs critical mass flux limit. It is thus safe to say that the Jacobs critical limit is one where the annular flow transitions into churn flow in the vertical suction line. In the horizontal suction line, the flow regime was annular at high mass fluxes, which transitioned into stratified-wavy with decrease in mass flux.

1.2.3 Modeling Oil Retention and Pressure Drop in Suction Lines

Modeling oil retention and pressure drop in both horizontal and vertical suction lines is of utmost importance. Prior knowledge of oil retention is required in order to prevent compressor failure due to lubricant starvation. In general, modeling of oil retention is performed for annular flow in vertical suction lines. This is due to the higher oil retention in vertical lines in comparison to horizontal suction lines. The ultimate aim of a system designer would be to minimize oil retention, which is best carried out by sizing the suction lines appropriately, so that the flow conditions that lead to large oil retention are avoided. Experimental investigations have shown that the oil retention is significantly lesser in the annular flow regime, making it much preferable than the churn flow regime. Thus the optimal method to minimize oil retention would be to size the vertical suction lines in a better way.

Many modeling efforts have been made to predict oil retention in vertical suction lines. In a majority of these models, the cylindrical form of the Navier-Stokes equation and the continuity equation is applied to the annular liquid film, with appropriate boundary conditions being applied to give an expression for the liquid film mass flow rate. This mass flow rate is a function of the pressure drop, annular liquid film thickness and the liquid/vapor interfacial shear stress. A momentum balance is then performed on the refrigerant vapor core, with a friction factor correlation serving as the closure equation. The pressure drop and oil film thickness are implicitly calculated from the closed set of equations, from which the oil retained is calculated. The friction factor correlation is perhaps the most important aspect of the model. Many such correlations have been proposed by different authors, based on their experimental data.

One of the most commonly used friction factor correlations is the Wallis (1969) correlation. Here, the interfacial friction factor is expressed as a function of the film thickness, for upward

vertical flows with a gas core and a thin liquid film. Wongwises and Kongkiatwanitch (2001) proposed an interfacial friction factor which was expressed as a function of the vapor core Reynolds number (Re_v) and the non-dimensional annular liquid film thickness. Air/water mixture had been employed for the experiments in this work, and it was observed that the correlation was able to predict the experimental data within ± 25 %. Lee (2001) proposed an analytical model to predict oil retention in the horizontal suction line for CO_2/PAG mixture. The interfacial friction factor was expressed as a function of the vapor core Reynolds number and the non-dimensional film thickness (δ/D). This model was valid for a vapor Reynolds number in the range of $(1.6\times10^5 < Re_v < 3.5\times10^5)$. It was observed that the model was able to predict the experimental results within a limit of ± 20 %. The non-dimensional liquid film thickness was found to vary between $(0.02 \leq \delta/D \leq 0.10)$. Cremaschi (2004) expressed the interfacial friction factor for both horizontal and vertical suction lines as a function of the vapor Reynolds number, the non-dimensional film thickness as well as the mixture Weber number. This correlation was found to be suitable for a non-dimensional thickness in the range of $(0.001 \leq \delta/D \leq 0.06)$, a vapor core Reynolds number in the range of $(1.7\times10^5 \leq Re_v \leq 4\times10^5)$, a mixture Weber number of $(13.8 \leq We_m \leq 221)$. The correlation was also deemed suitable for a viscosity ratio in the order of $(20 \leq \nu_{liq,film}/\nu_{vapor,ref} \leq 48)$. The correlation for the horizontal suction lines was found to predict the experimental results within ± 31 %. This correlation was found to converge to the Wongwises correlation when the liquid film thickness increases.

Zoellick and Hrnjak (2010) proposed a friction factor correlation for their R410A/POE 32 test mixture in horizontal and vertical suction lines. They employed the Wallis friction factor correlation in their model, with the non-dimensional film thickness being related to the liquid film Reynolds number by using the van Rossum (1959) correlation. The oil retention data was

predicted within ± 20 % of the experimental values, while no verifications were made for the pressure drop data. Sethi and Hrnjak (2011) proposed a friction factor model that expressed the interfacial friction factor as a function of the vapor core Reynolds number, the liquid film Reynolds number and the non-dimensional film thickness. Oil retention and pressure drop data were predicted within ± 20 % of the experimental data. The model was validated for a non-dimensional thickness of $(0.01 \leq \delta/D \leq 0.07)$, a vapor Reynolds number of $(0.48\times10^5 \leq Re_v \leq 2.1\times10^5)$ and a liquid film Reynolds number of $(0.3 \leq Re_{lf} \leq 10)$. In the previous two works, the annular liquid film thickness was non-dimensionalized by the liquid film viscosity and the frictional velocity, in order to get a better effect of the suction line diameter on the interfacial friction factor.

1.3 Goals of Current Work

The primary objective of the current work is to experimentally measure oil retention and pressure drop in horizontal and vertical suction lines for R1234yf in POE 100 lubricant and compare it with the results obtained in R134a/POE 100 and R410A/POE 100 mixtures. For this purpose, 10.2 mm internal diameter suction lines are employed that are approximately 2 m in length. Different conditions are simulated by varying the refrigerant mass flux and the OCR, while the saturation temperature and superheat were kept constant for all the tests. In order to investigate the effect of lubricant viscosity, comparisons were made with experimental data obtained using POE 32 lubricant. Flow visualization studies were conducted so that the flow regimes associated with different conditions were observed, along with flow reversal and flow regime transitions. An analytical model was also proposed to predict oil retention and pressure drop in vertical suction lines.

CHAPTER 2 – EXPERIMENTAL TEST FACILITY

2.1 Description of the Experimental Setup

The experimental test facility employed in the presented work was initially developed by Zoellick and Hrnjak (2010) to study oil retention of POE 32 in R410A, in 7.2 mm and 18.5 mm internal diameter, horizontal and vertical suction lines. This setup was subsequently modified by Sethi and Hrnjak (2011), by installing a R22 condensing unit to improve the range of refrigerant mass flow rate over which data could be obtained. The current setup consists of horizontal and vertical suction lines made up of transparent PVC, each approximately 2 m long, with an internal diameter of 10.2 mm. Figure 2.1 shows the current setup in use. The refrigerants considered for the current study were R134a, R1234yf and R410A, while the lubricants considered were nominally 100 cSt POE and 32 cSt POE oils. Thus the refrigerant/oil mixtures considered in the current study were R134a/POE 100, R1234yf/POE 100, R410A/POE 100 and R410A/POE 32.

The amount of oil retained in the suction lines was determined by the direct measurement method. This is facilitated by means of providing ball valves at both ends of each suction line. Ball valves were chosen in a manner such that their orifices had the same diameter of the pipe, thereby minimizing flow disturbances. At a particular operating condition, once equilibrium had been attained, these ball valves were simultaneously closed, thus trapping a mixture of refrigerant and oil. Subsequently, the amount of oil retained was measured in accordance with ASHRAE Standard 41.4. The pressure drop across each suction line is measured by means of differential pressure transducers, which are connected to pressure taps provided at the ends of each test section. Pressure taps were furnished by drilling 1/16 ” holes into 1/2 ” unions, to which copper pipes were brazed in a manner such that its orientation was perpendicular to the flow direction, thus reducing disturbances to the flow.

Subcooled, liquid refrigerant was pumped by means of a Magnetek type gear pump. A MicroMotion CMF25 Coriolis flow meter was employed to measure the refrigerant flow rate and density. The CMF25 had the accuracy and repeatability of the mass flow measurements as ± 0.1 % and ± 0.05 % of the flow rate measurement respectively, while the accuracy of the density reading was ± 0.5 kg/m^3. A variable speed drive was used to vary the refrigerant mass flow rate. Liquid oil, with some quantity of refrigerant dissolved in it, is pumped by means of a Micropump GJ series gear pump from the oil tank. The flow rate and density of this liquid mixture was estimated by means of a MicroMotion CMF 10 Coriolis flow meter, with the mass flow measurements having an accuracy and repeatability of ± 0.01 % and ± 0.05 % of the measured reading respectively. Density readings had an accuracy of ± 0.5 kg/m^3. The temperature of the liquid mixture was measured by a T-type thermocouple (± 0.5 ºC) as it entered the flow meter. By knowing both the density and the temperature of the liquid mixture, the fraction of refrigerant present in the mixture was determined as mentioned in Zoellick and Hrnjak (2010). The gear pump was driven by a fixed frequency AC motor, with the flow rate of the oil mixture being varied by using a ball valve as well as a bypass valve. The mixture was also subcooled before it entered the gear pump, in order to prevent fluctuations in the flow. The OCR (oil in circulation ratio) was varied by changing the refrigerant and oil mixture mass flow rates. Uncertainty analysis showed that the typical uncertainty in OCR measurements was generally in the order of 0.05 ± 0.0002.

The liquid refrigerant and the oil rich mixture were mixed in a T-junction before entering the evaporator. This ensures proper mixing as well as equilibrium between the two streams before it enters the suction lines. This simulates the actual conditions in a real system, better than those systems which incorporate simulation by the injection-separation method. The evaporator is a 12

plate, counter flow heat exchanger, with the cold refrigerant/oil mixture being heated up by hot water. The flow orientation to the evaporator was such that the liquid flowed vertically downwards to the evaporator, thus reducing the oil retention in the evaporator. The superheat condition at the inlet of the suction line is controlled by means of varying the flow rate of the hot water. To ensure that both the refrigerant and oil are in thermal equilibrium with each other, the flow temperature was measured at the tube center and compared with the tube wall temperature. Besides the suction lines, all components and tubes are provided with insulation. A 100 diameter development length was provided to ensure that the mixture was in thermal and hydrodynamic equilibrium before entering the horizontal suction line. The concentration of oil in the liquid phase was dependent on the evaporator exit temperature as well as the saturation pressure, both of which were maintained within ± 3 % or ± 1 ºC of the testing temperature.

On exiting the vertical suction line, the liquid – vapor mixture was passed through a helical separator, where the refrigerant vapor is separated and the passed on to a 12-plate, counter flow condensing heat exchanger. The oil rich liquid mixture is directed back into the oil tank. The condenser served as the evaporator for a R22 condensing unit, the capacity of which was controlled by a variable speed drive. The saturation temperature of the system was maintained by means of the condensing unit, which controlled the rate at which refrigerant vapor condensed. The condensate then flows vertically downwards into a receiver, from where it was again pumped.

The system saturation pressure at the inlet of the suction lines was measured by means of a Honeywell TJE absolute pressure transducer, which had a range of 0-3477 kPa and an accuracy of ± 8.6 kPa. Both the horizontal and vertical pressure drops are measured using a Honeywell Z type differential pressure transducer, which had a range of 0 ± 69 kPa and an accuracy of ± 0.1

kPa. Oil retention measurements were conducted using an electronic mass balance and have been found to possess an uncertainty of ± 0.03 g.

Outputs from various measurements such as thermocouples, flow meters and pressure transducers were read by a Yokogawa HR 1300 data-logger. This interfaces with a computer running a LabVIEW program, thus displaying and recording live data. A detailed description of the testing procedure involved has been provided by Zoellick and Hrnjak (2010).

2.2 Operating Conditions

In the present study, the refrigerant/oil mixtures considered were R134a/POE 100, R1234yf/POE 100, R410A/POE 100 and R410A/POE 32. The saturation temperature was maintained at 13 ºC, while the degree of superheat was 15 ºC. The OCR was varied between 1-5 %. The total mass flux was varied between 33-140 kg/m^2-s for R134a, between 35-145 kg/m^2-s for R1234yf and between 45-165 kg/m^2-s for R410A. The lower limits presented all correspond to the Jacobs critical mass flux. Clear PVC pipes, with an internal diameter of 10.2 mm and an approximate length of 2 m, were employed as the horizontal and vertical test sections. Flow visualization was performed by means of a high speed camera, which was used to determine the flow regimes at different mass fluxes. The test conditions are tabulated in Tables 2.1, 2.2 and 2.3. It is also observed that the test matrix for R410A/POE 32 and R410A/POE 100 remain the same.

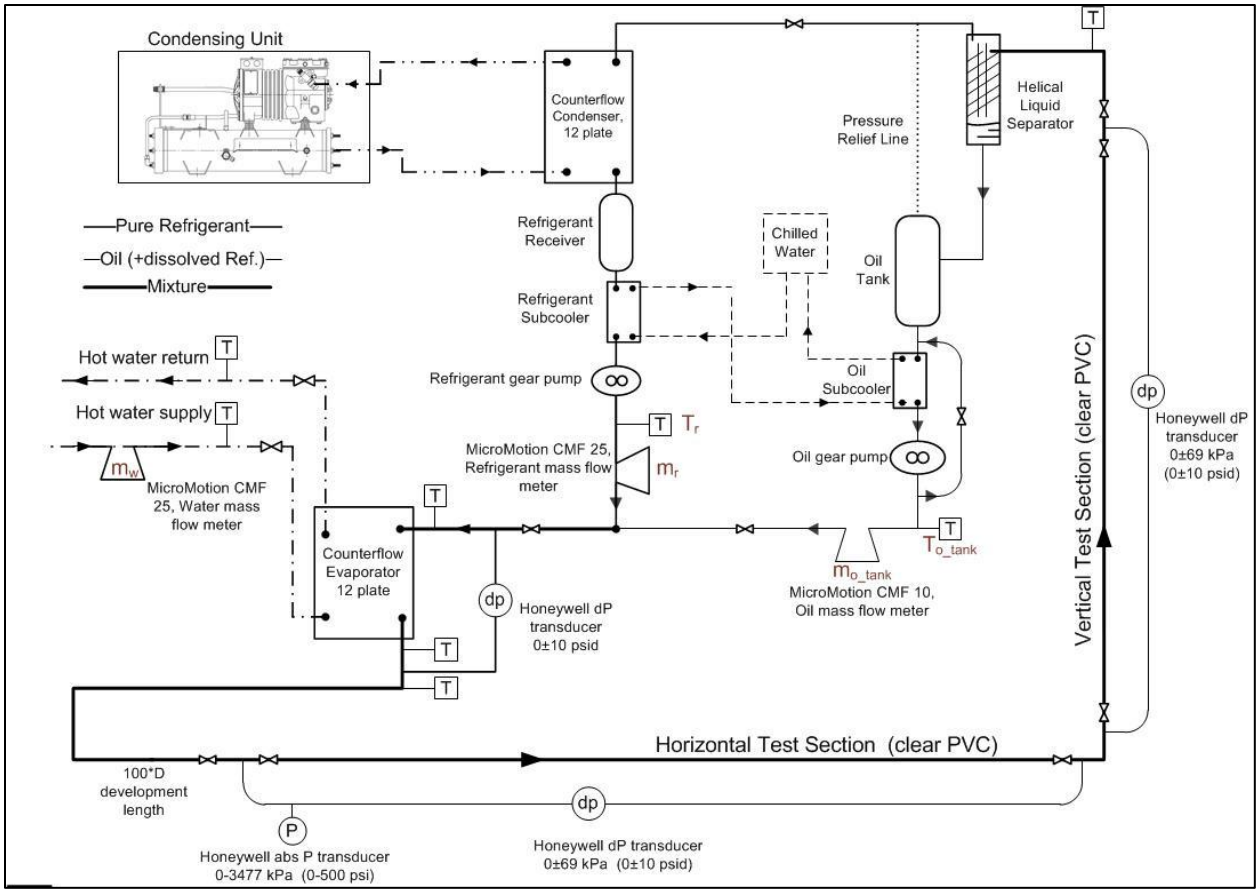

Figure 2.1 – Schematic representation of test apparatus

Table 2.1 – Test Conditions for R134a/POE 100

Total Mass Flux	**Superficial Vapor Velocity**	**Total Mass Flow Rate**
kg/m^{2}s	**m/s**	**g/s**
33(Jacobs Limit)	1.5	2.69
50	2.5	4.08
60	3	4.90
80	4	6.53
100	5	8.14
120	6	9.77

Table 2.2 – Test Conditions for R1234yf/POE 100

Total Mass Flux	**Superficial Vapor Velocity**	**Total Mass Flow Rate**
kg/m^{2}s	**m/s**	**g/s**
35(Jacobs Limit)	1.5	2.86
50	2	4.08
60	2.5	4.90
75	3	6.13
100	4	8.17
120	5	9.80
145	6	11.84

Table 2.3 – Test Conditions for R410A/POE 100 and R410A/POE 32

Total Mass Flux	**Superficial Vapor Velocity**	**Total Mass Flow Rate**
kg/m^{2}s	**m/s**	**g/s**
45(Jacobs Limit)	1	3.66
60	1.5	5.00
82.5	2	6.72
125	3	10.09
165	4	13.45

CHAPTER 3 - EXPERIMENTAL RESULTS

3.1 Flow Visualization Studies

Flow visualization studies were conducted by employing a high speed camera, capturing high speed videos. The main aim of flow visualization studies is to identify the regime of flow corresponding to each mass flux, and also capture the transition from one flow regime to another. Changes in the flow pattern observed due to change in OCR were also studied, with the OCR being maintained at 5 %, 3 % and 1 % respectively.

3.1.1 Horizontal Suction Line Flow Visualization

In horizontal suction lines, two predominant flow regimes were observed under the conditions of operation. In general, at high mass fluxes, the flow was observed to be annular in the horizontal pipe, while at lower mass fluxes, the flow transitioned into stratified flow, with characteristic waves observable on the oil film surface. Similar flow patterns were observed for all refrigerant/oil mixtures under consideration, namely R134a/POE 100, R1234yf/POE 100, R410A/POE 100 and R410A/POE 32. Figures 3.2, 3.4, 3.6 and 3.8 show pictures of various flow visualization experiments conducted, for the test matrix under consideration. For R134a/POE 100, an annular flow regime exists for a superficial vapor velocity of 5 m/s and above. Below a superficial vapor velocity of 5 m/s, the flow transitioned into a stratified wavy flow regime. In the case of R1234yf/POE 100, one can observe the annular flow regime upto a velocity of 4 m/s, below which it transitions into stratified wavy regime. Similar observations were made in R410A/POE 100, with the flow transitioning at 3 m/s superficial vapor velocity. It must be mentioned that the oil-rich film is purely annular only at high mass flux values. A reduction of mass flux is characterized by the thickening of the annular film present at the bottom of the suction line, which progressively increases with further decrease in mass flux. This is due to the

fact that the vapor core no longer possesses sufficient momentum to spread the oil film equally across the inner circumferential surface. Further reduction of mass flux leads to the condition where the oil film is only present in the bottom portion of the tube. Also, the variation of flow regimes with change in OCR is also observed. It can be observed for the case of R1234yf/POE 100 from Figure 3.4 that the flow regime is annular at 100 kg/m^2-s for 5 % and 3 % OCR, while the flow regime has transitioned to stratified wavy regime at 1 % OCR. This observation leads to the conclusion that the mass flux corresponding to the transition of the annular flow regime into stratified flow regime is lower for higher OCR values. Also, it was noticed that higher OCR flows depicted larger wave structures in the annular flow regime. In reality, the presence of larger ripple waves would lead to more oil entrainment in the refrigerant vapor core. These would lead to an increase in total pressure drop at higher mass fluxes, which can be observed from the experimental data. Similarly in the stratified wavy flow regime, higher OCR flows were characterized by thicker oil films, thus leading to higher oil retention. Another interesting observation was made in the stratified flow regime. From Figure 3.2 it can be observed that for the mass fluxes of 80 kg/m^2-s, 60 kg/m^2-s and 50 kg/m^2-s, the oil film thickness remained approximately the same at a given OCR, in the case of R134a/POE 100. Thus one would ideally expect the oil retention to be the same at these flow conditions, which was confirmed by experimental measurements. These observations were also consistent with those made by Sethi and Hrnjak (2011).

The horizontal flow regimes may be represented diagrammatically by means of a flow map. Figure 3.1 represents the Baker's (1954) flow map which has been modified as shown in Thome (2004), for a refrigerant/oil mixture of R134a/POE 100. The flow map is clearly able to predict the influence of OCR on the flow regime, indicating that the annular flow transitions into

stratified wavy flow more quickly at 1 % OCR with decrease in mass flux, in comparison to 3 % and 5 % OCR values. This trend is consistent with the observations made in the flow visualization studies, as shown in Figure 3.2. The modified Baker's flow map also shows the trend with change in mass flux, with higher mass flux flows tending to be annular in nature.

3.1.2 Vertical Suction Line Flow Visualization

Figures 3.3, 3.5, 3.7 and 3.9 show pictures obtained from flow visualization studies, for R134a/POE 100, R1234yf/POE 100, R410A/POE 100 and R410A/POE 32. In vertical suction lines, in general it was observed that the flow regime was annular at all mass fluxes except the Jacobs limit. At high mass fluxes, an annular film was observed, which possessed surface ripples. It was observed that reducing the mass flux led to the thickening of these waves, which would lead to increased oil retention. The vertical suction line flow visualization of R1234yf/POE 100 is shown in Figure 3.5. At 145 kg/m^2-s and 5 % OCR, one can see that the regime is annular. At the same OCR, reduction of the mass flux to 100 kg/m^2-s, 75 kg/m^2-s and 60 kg/m^2-s shows that the ripple waves become subsequently thicker. At a mass flux of 50 kg/m^2-s, it was observed that there was flow direction reversal in the oil-rich film, as some of the film was seen travelling downwards. Hence, the mass flux of 50 kg/m^2-s coincided with the onset of flow reversal in the 10.2 mm vertical suction line. Similar flow reversal was also observed at the same mass flux for R134a/POE 100, while in the case of R410A/POE 100, flow reversal was observed at 60 kg/m^2-s. Further reduction of the mass flux below the flow reversal point led to a transition in the flow regime from annular into the churn flow regime. The observation of the churn flow regime coincided with the mass flux being equal to the Jacobs critical mass flux. Similar observations were made by Zoellick and Hrnjak (2010), who conducted similar tests with R410A/POE 32 in a 18.5 mm vertical tube, and by Sethi and Hrnjak

(2011). The churn flow is characterized by chaotic two-phase flow, with the oil-rich film subjected to large flow reversal. In the churn flow regime, the presence of vapor bubbles as well as entrained oil droplets was also observed. Thus as one would have expected, the churn flow regime was associated with the maximum oil retention. As pointed out by Sethi and Hrnjak (2011), even before the churn flow regime is reached, there is appreciable increase in liquid film thickness, where the oil retention would also start increasing. Thus considering the Jacobs limit as the criterion for designing/sizing vertical suction risers does not seem suitable, since there is heightened oil retention even before that limit is reached. Thus evaluating a newer critical flux based on which suction lines are to be designed is an important requirement. The variation of the flow profile with OCR is also observed. Higher OCR flows have thicker ripple wave profiles and were also characterized by thicker annular films. Due to its slightly higher vapor density in comparison to R134a, R1234yf will undergo flow reversal at a higher mass flux, though visualization indicates flow reversal at 50 kg/m^2-s for both refrigerants. In the same vein, since R410A vapor has much higher density, flow reversal was initiated at an even higher mass flux.

3.2 Lubricant Retention and Pressure Drop

This section presents the experimental values for oil retention and pressure drop in horizontal and vertical test sections. Refrigerant-oil mixtures are presented in the order R134a/POE 100, R1234yf/POE 100, R410A/POE 100 and R410A/POE 100 respectively. Discussions of the experimental observations are also included in this section.

3.2.1 Lubricant Retention and Pressure Drop for R134a/POE 100

Figure 3.10 shows the variation of oil retention with mass flux, for both horizontal and vertical suction lines. The unit of choice for oil retention is grams per meter length of the suction pipe.

Pressure drop variation is shown in Figure 3.11. Data is presented for three different OCR's, namely 1 %, 3 % and 5 %. The mass flux was varied from 120 kg/m^2-s to 33 kg/m^2-s for 3 % and 5 % OCR. For 1 % OCR, the mass flux was varied between 120 kg/m^2-s and 50 kg/m^2-s. The lower limit of 33 kg/m^2-s corresponds to the Jacobs limit for vertical suction risers. At the Jacobs limit, the flow transitioned from annular flow regime to churn flow regime in the vertical test section.

3.2.1.1 Horizontal Pipe

In the horizontal suction line, an initial increase in oil retention was observed when the mass flux was decreased, at high mass fluxes. The variation of oil retention data with mass flux can be observed in Figure 3.10. The oil retention was expressed in terms of the mass of oil retained per unit length of the suction line (g/m). At an OCR of 5 %, the horizontal oil retention at 118 kg/m^2-s was 5.32 g/m, which increased to 5.76 g/m at a mass flux of 100 kg/m^2-s. But interestingly, this trend did not continue on further reduction of the mass flux. It was noticed that subsequent reduction of mass flux led to a reduced oil retention of 5.15 g/m at a mass flux of 81 kg/m^2-s. On reducing the mass flux even lower, the oil retention remained fairly constant at 5.08 g/m for a mass flux of 62 kg/m^2-s and at 5.27 g/m at a mass flux of 51 kg/m^2-s. The oil retention was observed to increase as the mass flux was further reduced, approaching the Jacobs critical limit. A mass flux of 32 kg/m^2-s yielded oil retention of 10.9 g/m. These observations were compared with the flow visualizations conducted. High speed videos indicated the transition of the flow regime from annular to stratified-wavy at a mass flux of 80 kg/m^2-s. The flow visualization indicated that the oil film thickness in the stratified wavy regime does not change much, when the mass flux is reduced to 62 kg/m^2-s and 51 kg/m^2-s. This accounts for the relatively constant oil retention measurements at these mass fluxes. However, the oil film thickness appreciably

increases at 32 kg/m^2-s, thus leading to an elevated oil retention value. Similar trends were observed for all OCR's, with the magnitude of oil retention increasing with increase in OCR. At a mass flux of 120 kg/m^2-s, the oil retention was found to increase by 25 % when the OCR was increased from 1 % to 3 %. Similarly, an increase in the OCR from 1 % to 5 % led to a 50 % increase in oil retention. For a lower mass flux of 100 kg/m^2-s, the oil retention increased by 45 % when the OCR is changed from 1 % to 3 %, and increased by 80 % when the OCR is increased from 1 % to 5 %. Thus at lower mass fluxes, the percentage increase in oil retention with increase in OCR is higher.

The variation of pressure drop with mass flux is represented in Figure 3.11. The pressure drop was expressed per unit length of the suction line (kPa/m). The pressure drop was found to decrease with reduction in mass flux. This is because at higher mass fluxes, the flow regime is annular, which transitions to stratified wavy at lower mass fluxes. In horizontal test sections, the frictional component of pressure drop is the dominant factor, which purely depends on the superficial vapor velocity. Reduction in mass flux leads to a reduction in vapor velocity, which in turn leads to a reduction in the frictional pressure component. At a particular mass flux, the pressure drop was also found to increase with increase in OCR. For instance, the pressure drop increased from 70 Pa/m to 2500 Pa/m, when the mass flux was changed from 35 kg/m^2-s to 120 kg/m^2-s at 3 % OCR. Also at 120 kg/m^2-s, the pressure drop increased by 50 % when the OCR was changed from 1 % to 3 %, and increased by 70% when the OCR is increased from 1 % to 5 %. All of the observations made were consistent with those made by Sethi and Hrnjak (2011) for the case of R134a/POE 32 and R1234yf/POE 32.

3.2.1.2 Vertical Pipe

In the vertical test sections, an increase in oil retention was observed with decrease in mass flux. In general, oil retention in vertical suction risers is higher than the retention in horizontal lines, due to the influence of gravity, especially at lower mass fluxes. Hence while designing a refrigeration system, the critical mass flux above which the system should be operated depends on the vertical oil retention. At 5 % OCR, the oil retention was 5.46 g/m at a mass flux of 120 kg/m^2-s. This oil retention increased to 6.02 g/m when the mass flux was lowered to 100 kg/m^2-s. At a mass flux of 51 kg/m^2-s, oil film reversal can clearly be observed from the flow visualization, which corresponds to an oil retention of 9.21 g/m. Further reduction of the mass flux to 32 kg/m^2-s, which corresponds to Jacobs critical flux, gave an oil retention of 16.39 g/m. Similar to results in the horizontal test section, oil retention in the vertical pipe increased with increase in OCR. At a mass flux of 120 kg/m^2-s, the oil retention increased by 13 % when the OCR was changed from 1 % to 3 %, while an increase of 37 % was achieved when the OCR was changed from 1 % to 5 %. Another interesting observation was made in terms of oil retention. At high mass fluxes, the oil retention in the vertical test section was similar to that observed in the horizontal test section. On reducing the mass flux, the oil retention in the vertical test section was always greater than that in the horizontal test section, due to the influence of gravity.

Pressure drop variation is seen in Figure 3.11. It was observed that the pressure drop decreased initially with decrease in mass flux, reaches a minimum close to 50 kg/m^2-s, beyond which it increases at the Jacobs critical flux of 35 kg/m^2-s. This observation may be explained on the basis of different components of pressure drop and their dependence on the regime of flow. At high mass fluxes, the regime of flow of the liquid film is annular, at which the predominant component of pressure drop is the frictional pressure drop. Reduction of the mass flux, leads to a

decrease in superficial vapor velocity, which consequently leads to a drop in the frictional pressure drop. Thus the overall pressure drop decreases. This trend is seen to continue till 50 kg/m^2-s, where flow reversal of the oil film starts. Further reduction leads to transition of the flow regime of the annular film into the chaotic churn flow regime. In the churn flow regime, the hydrostatic component of pressure drop dominates over the frictional component. Thus further reduction of mass flux below the point of flow reversal results in an increase in the hydrostatic pressure drop component, which translates as an increase in the overall pressure drop. Thus the pressure drop attains a minimum value close to 50 kg/m^2-s, below which it again starts to increase. For a 3 % OCR, the pressure drop is 3090 Pa/m at 120 kg/m^2-s and drops to 2395 Pa/m at 100 kg/m^2-s. The pressure drop decreases and reaches a minimum of 1250 Pa/m at 51 kg/m^2-s, below which it again increases to 1600 Pa/m at 35 kg/m^2-s. At a given mass flux, the pressure drop increases with increase in OCR. From the flow visualization studies conducted, it was observed that higher OCR values were characterized by thicker surface ripple waves as well as thicker oil films. The thicker ripples would lead to more area of interaction between the vapor refrigerant core and the liquid film. Consequently more momentum would be transported to the liquid film, thus leading to an increase in pressure drop. For instance, at a mass flux of 120 kg/m^2-s, the pressure drop increases by 43 % when the OCR is changed from 1 % to 3 %, while an OCR change from 1 % to 5 % leads to an increase in pressure drop by 65 %. It was also observed that this percentage increase in pressure drop with increase in OCR, reduced with a decrease in mass flux. This trend continues till the point of flow reversal at about 50 kg/m^2-s. At this mass flux, the pressure drop is 1075 Pa/m at 1 % OCR and goes upto 1405 Pa/m at 5 % OCR, which accounts for only a 31 % increase in the overall pressure drop.

3.2.2 Lubricant Retention and Pressure Drop for R1234yf/POE 100

Figure 3.12 shows the change in oil retention with change in mass flux, for both horizontal and vertical suction lines, while Figure 3.13 shows variation in pressure drop. Both quantities are represented per meter length of the suction line. The OCR was maintained at three different values, namely 1 %, 3 % and 5 %. The mass flux was varied from 145 kg/m^2-s to 35 kg/m^2-s for all OCR values. The lower limit of 35 kg/m^2-s corresponds to the Jacobs critical mass flux limit for vertical suction risers. At the Jacobs limit, it was observed that the flow transitioned from annular flow regime to churn flow regime in the vertical test section.

3.2.2.1 Horizontal Pipe

Similar results were obtained in comparison to those observed in the case of R134a/POE 100. At 5 % OCR, the oil retention at a mass flux of 144 kg/m^2-s was observed to be 6.08 g/m, which increased to 6.32 g/m at 119 kg/m^2-s. Further reduction in mass flux to 100 kg/m^2-s led to an increased oil retention of 6.76 g/m. This was followed by a reduction in oil retention, when the mass flux was further decreased, due to transition in the flow regime from annular to stratified wavy. Thus at a mass flux of 74 kg/m^2-s, the oil retention reduced to 6.41 g/m. Subsequent reduction in mass flux to 63 kg/m^2-s and 50 kg/m^2-s yielded relatively constant oil retention values of 6.11 g/m and 6.76 g/m respectively. Further reduction of the mass flux upto the Jacobs mass flux yielded a much higher oil retention of 11.25 g/m. The effect of OCR on the oil retention is also observed, with higher retention obtained at a higher OCR. At a mass flux of 120 kg/m^2-s, the oil retention increased by 42 % when the OCR was varied from 1 % to 3 %, while an oil retention increase of 60 % was observed when the OCR was changed from 1 % to 5 %. At a lower mass flux of 50 kg/m^2-s, the oil retention increased by 48 % when the OCR was changed from 1 % to 3 %, while an 89 % change was observed when the OCR was varied from 1 % to 5

%. This again represents that at lower mass fluxes, the percentage increase in oil retention with increase in OCR is higher. Similar trends were also observed in the pressure drop variation, in comparison to R134a/POE 100. The pressure drop continuously decreased with a reduction in mass flux. For instance at 5 % OCR, the pressure drop decreased from 3270 Pa/m to 1520 Pa/m, when the mass flux was reduced from 144 kg/m^2-s to 100 kg/m^2-s. Also, an increase in pressure drop was observed with increasing OCR values. For instance, at 120 kg/m^2-s, the pressure drop increased from 1240 Pa/m to 2050 Pa/m when the OCR was changed from 1 % to 3 %, while the pressure drop increased up to 2280 Pa/m when OCR was changed to 5 %.

3.2.2.2 Vertical Pipe

Oil retention was observed to increase consistently with a decrease in mass flux, similar to the previous case of R134a/POE 100. At an OCR of 5 %, the oil retention was observed to be 6.23 g/m at a mass flux of 144 kg/m^2-s, which increased to 7.33 g/m when the mass flux was decreased to 100 kg/m^2-s. Further reduction in the mass flux up to 74 kg/m^2-s led to an oil retention of 9.07 g/m. The flow reversal point of 50 kg/m^2-s was characterized by an oil retention of 11.65 g/m, which was an 18 % increase in oil retention compared to that observed at 63 kg/m^2-s. The Jacobs critical mass flux was characterized by the churn flow regime, as observed from the flow visualization studies conducted. At this mass flux, the oil retention was a very high value of 18.31 g/m. Similar to the horizontal test section, increase in OCR yielded an increase in oil retention. At a mass flux of 120 kg/m^2-s, the oil retention increased by 27 % when the OCR was varied from 1 % to 3 %, while an increase in 41 % was observed when the OCR was changed from 1 % to 5 %. On lowering the mass flux to 75 kg/m^2-s, the oil retention increased by 33 % when the OCR was altered from 1 % to 3 %, while an increase in oil retention of 57 % was observed when the OCR was altered from 1 % to 5 %. The pressure drop was found to

decrease up to the flow reversal point, beyond which it again increased due to change in flow regime. For instance, at an OCR of 3 %, the pressure drop decreased from 3790 Pa/m to 2820 Pa/m when the mass flux was changed from 144 kg/m^2-s to 121 kg/m^2-s. Further decrease in mass flux to 76 kg/m^2-s yielded a pressure drop of 1510 Pa/m. At 50 kg/m^2-s, the pressure drop was 1010 Pa/m, which increased to 1490 Pa/m at 36 kg/m^2-s. It is evident from these observations that designing suction lines based on the Jacobs critical mass flux is not prudent, due to the high oil retention observed as well as the fact that the pressure drop is not a minimum value. Increasing OCR values led to increased pressure drop, as evident from Figure 3.13. It was noted that the difference in oil retention of the vertical suction line with respect to the horizontal suction line was only 4 % in the case of 3 % OCR, 144 kg/m^2-s mass flux. At the same OCR value, this difference went up to 7 % at 120 kg/m^2-s, showing that the influence of gravity on oil retention in the vertical suction line increases with decreasing mass flux. Pressure drop data for pure refrigerant flow is shown in Figure 3.13. In this case, both the horizontal as well as the vertical pressure drop decrease with a reduction in mass flux. These are compared with the predictions made using the smooth pipe friction factor correlation, which are represented by means of the dotted lines. The predicted values match the experimental data, thus verifying the pressure transducer data.

3.2.3 Lubricant Retention and Pressure Drop for R410A/POE 100

Figure 3.14 and 3.15 show the change in oil retention as well as variation in pressure drop with change in mass flux, for both horizontal and vertical suction lines in the case of R410A/POE 100. Both quantities are represented per meter length of the suction line. The OCR was varied between 1-5 %. The mass flux was varied from 165 kg/m^2-s to 45 kg/m^2-s for all OCR values, which corresponded to the superficial vapor velocity being varied from 1-4 m/s. The lower limit

of 45 kg/m^2-s corresponds to the Jacobs critical mass flux limit for vertical suction risers. Visualization studies showed that the flow transitions from annular flow into churn flow at the Jacobs limit for vertical suction lines.

3.2.3.1 Horizontal Pipe

At 1% OCR, the oil retention decreased from 3.16 g/m to 2.55 g/m when the mass flux was decreased from 166 kg/m^2-s to 125 kg/m^2-s. The mass flux of 125 kg/m^2-s corresponded to the transition point where the flow regime changed from annular to stratified wavy. Further reduction of the mass flux to 83 kg/m^2-s yielded a relatively constant oil retention of 2.81 g/m, and on reaching the Jacobs critical mass flux, the oil retention increased to 13.46 g/m. Increase in OCR also led to increase in oil retention. At 125 kg/m^2-s, an increase in oil retention of 81 % was observed when the OCR was changed from 1 % to 3 %, while the oil retention more than doubled when the OCR was changed from 1 % to 5 %. The pressure drop continuously decreased with decrease in mass flux. For instance at 5 % OCR, the pressure drop changed from 2220 Pa/m to 1070 Pa/m when the mass flux was decreased from 165 kg/m^2-s to 125 kg/m^2-s. The pressure drop ultimately reduced to 90 Pa/m when the mass flux was reduced to 46 kg/m^2-s. Also, the pressure drop increased with increase in OCR. At a mass flux of 125 kg/m^2-s, the horizontal suction line pressure drop increased by 40 % and 73 % respectively, when the OCR was changed from 1 % to 3 % and 1 % to 5 % respectively. It was also noticed that the magnitude in percentage decrease in pressure drop was much higher in R410A in comparison to R134a and R1234yf.

3.2.3.2 Vertical Pipe

An increase in oil retention was observed when the mass flux was reduced. At 3 % OCR, the oil retention increased from 4.95 g/m to 5.95 g/m when the mass flux was reduced from 165 kg/m^2-s

to 125 kg/m^2-s. At a mass flux of 62 kg/m^2-s, the oil retention increased to 10.94 g/m while at the Jacobs critical mass flux, the oil retention was observed to be 16.87 g/m. The oil retention was also observed to increase with an increase in the OCR. At the mass flux of 83 kg/m^2-s, the oil retention increased by 31 % when the OCR was changed from 1 % to 3 %, while a 49 % increase in oil retention was observed when the OCR was varied from 1 % to 5 %. The pressure drop was found to decrease up to the point of flow reversal, after which it increased at the Jacobs critical limit. For instance at 3 % OCR, the pressure drop decreased from 2940 Pa/m to 2000 Pa/m when the mass flux was reduced from 165 kg/m^2-s to 125 kg/m^2-s. Further reduction in mass flux gave pressure drop values of 1410 Pa/m and 1330 Pa/m at mass fluxes of 83 kg/m^2-s and 62 kg/m^2-s respectively. This was followed by an increased pressure drop value of 2180 Pa/m at the Jacobs mass flux, due to an increase in the hydrostatic component of pressure drop. Though flow visualization showed liquid film reversal at the mass flux of 60 kg/m^2-s, all of the pressure drop data consistently seem to indicate a minimum pressure drop value located between 60 kg/m^2-s and 82.5 kg/m^2-s, leading to the conclusion that flow reversal had initiated at a mass flux higher than 60 kg/m^2-s, probably close to 70 kg/m^2-s.

3.2.4 Lubricant Retention and Pressure Drop for R410A/POE 32

Variation in oil retention and pressure drop with respect to mass flux is shown in Figure 3.16 and 3.17 respectively for the case of R410A/POE 32. The OCR was varied between 1-5 %, with both quantities being represented per meter length of the suction line. Similar to the case of R410A/POE 100, the mass flux was varied from 165 kg/m^2-s to 45 kg/m^2-s for all OCR values. The lower limit of 45 kg/m^2-s corresponds to the Jacobs critical mass flux limit for vertical suction risers. Visualization studies showed that the flow transitions from annular flow into churn flow at the Jacobs limit for vertical suction lines.

3.2.4.1 Horizontal Pipe

The trends of the results obtained were analogous to those obtained for the previous refrigerant-oil mixtures. At an OCR of 1 %, the horizontal oil retention dropped from 2.85 g/m to 2.32 g/m when the mass flux was changed from 164 kg/m^2-s to 125 kg/m^2-s. Again, this reduction in oil retention corresponded to a transition in the flow regime from annular flow regime at 164 kg/m^2-s to the stratified flow regime at 125 kg/m^2-s. Further reduction in the mass flux to 85 kg/m^2-s yields a similar oil retention of 2.51 g/m. Reducing the mass flux to values of 61 kg/m^2-s and 50 kg/m^2-s gave oil retention values of 3.00 g/m and 4.02 g/m respectively. Thus once can observe a high degree in similarity between the trends of the current results and the results obtained in the case of R410A/POE 100. An increase in OCR was characterized by an increase in oil retention. For instance, the oil retention increased by 82 % when the OCR was changed from 1 % to 3 % at a mass flux of 125 kg/m^2-s. On changing the OCR from 1 % to 5 % at the same mass flux, the oil retention more than doubled in quantity. For the horizontal suction line, the pressure drop reduced with drop in mass flux. For instance at 5 % OCR, the pressure drop reduced from 1750 Pa/m to 720 Pa/m when the mass flux is changed from 162 kg/m^2-s to 125 kg/m^2-s. The pressure drop gradually reduced to 10 Pa/m when the mass flux was reduced to 46 kg/m^2-s. Also, the pressure drop was found to increase with increase in OCR. At a mass flux of 125 kg/m^2-s, the horizontal pressure drop increased by 42 % and 75 %, when the OCR was change from 1 % to 3 % and from 1 % to 5 % respectively.

3.2.4.2 Vertical Pipe

The lubricant retention in the vertical suction line was observed to continuously increase with a decrease in mass flux. At an OCR of 3 %, the oil retention increased from 4.69 g/m to 5.80 g/m

when the mass flux was reduced from 164 kg/m^2-sto 124 kg/m^2-s. Further reduction of the mass flux to 84 kg/m^2-s and 61 kg/m^2-s yielded oil retention values of 7.13 g/m and 10.39 g/m respectively. On further reduction of the mass flux upto the Jacobs critical mass flux of 47 kg/m^2-s, a high oil retention of 16.34 g/m was observed. Also, the oil retention was observed to increase with increasing OCR values. At a mass flux of 125 kg/m^2-s, the oil retention was found to increase by 43 % when the OCR changed from 1 % to 3 %. Similarly, increasing the OCR from 1 % to 5 % yielded an oil retention increase of 56 %. The pressure drop in the vertical suction was initially observed to decrease until the point of flow reversal, beyond which it again increased towards the Jacobs critical limit. At 5 % OCR, the vertical pressure drop decreased from 2280 Pa/m to 1600 Pa/m when the mass flux was reduced from 165 kg/m^2-s to 125 kg/m^2-s. This was followed by a minimum pressure drop of 1000 Pa/m at a mass flux of 82.5 kg/m^2-s. Subsequent reduction of the mass flux to 60 kg/m^2-s and 45 kg/m^2-s yielded higher pressure drops of 1210 Pa/m and 1850 Pa/m respectively. Also, the pressure drop was found to increase with increase in OCR at the same mass flux. For instance at 125 kg/m^2-s, the vertical pressure drop increased by 39 % when the OCR was increased from 1 % to 3 %. Similarly, increasing the OCR from 1 % to 5 % yielded an increase in pressure drop by 70 %. Analogous to the results observed in the case of R410A/POE 100, the pressure drop data indicated that flow reversal initiated at a mass flux higher than 60 kg/m^2-s.

3.3 Effect of Lubricant Viscosity on Oil Retention and Pressure Drop

The effect of lubricant viscosity on the amount of oil retained as well as the pressure drop observed - for horizontal and vertical test sections – was studied in detail. For this purpose, comparisons were made with the experimental measurements obtained using two different viscosity lubricants, namely POE 100 and POE 32. Thus oil retention and pressure drop

measurements for R134a/POE 32 and R1234yf/POE 32 which were obtained by Sethi and Hrnjak (2011) were utilized, besides the experimental measurements made in the current study. The results are provided in an individual manner for each refrigerant, i.e., results are provided first for R134a, followed by those of R1234yf and R410A. Variation of oil retention and pressure drop with mass flux is both represented per unit length of the suction lines. All test data were measured at a saturation temperature of 13 °C along with a superheat of 15 °C.

3.3.1 Effect of Lubricant Viscosity in R134a

Figures 3.18 and 3.19 show the difference in oil retention and pressure drop for R134a, when POE 32 and POE 100 are employed. The data for R134a/POE 32 was obtained from Sethi and Hrnjak (2011). Each figure also shows the effect of the OCR on these parameters. As observed, similar conditions of mass flux were employed for the purpose of comparison. Both oil retention and pressure drop results were presented per unit length of the suction line.

3.3.1.1 Horizontal Pipe

The comparison of R134a in POE 32 and POE 100 in terms of oil retention in the horizontal suction line is represented in Figure 3.18. It was observed that in terms of oil retention, POE 100 gave rise to a marginally increased oil retention value in comparison to POE 32, when R134a was employed. When POE 100 is employed, the oil rich liquid film viscosity is greater than that in the case of POE 32. Thus when operating at the same mass flux, the R134a refrigerant vapor cannot carry away the liquid mixture in the case of POE 100 as much as it would in the case of POE 32, as increased vapor momentum would be required. In order to have similar retention values, one would theoretically have to increase the mass flux, thereby increase the superficial vapor velocity and consequently increase the momentum transfer between the refrigerant vapor and the liquid film. At an OCR of 5 %, it was observed that the horizontal oil retention nominally

increased between 5-14 %. In the case of 3 % OCR, the retention was found to nominally increase between 2-15 %. It was also observed for the case of 3 % OCR that at the Jacobs critical flux condition, there was approximately a 70 % increase in oil retention in POE 100, in comparison to POE 32. Similar trends were also observed in the case of 1 % OCR, with a maximum increase in oil retention of 34 % at the Jacobs critical limit. Figure 3.19 shows the variation of horizontal suction line pressure drop with the mass flux in R134a, for both POE 32 and POE 100. The horizontal suction line pressure drop slightly increased in the case of POE 100 in comparison to POE 32, at similar conditions of mass flux. This is again a consequence of the increase in liquid film viscosity, which leads to an increased liquid film thickness, at the same conditions of OCR and mass flux. Due to the increased film thickness, the annular film area will increase leading to a decrease in the vapor core area, thereby marginally increasing the vapor core velocity. This increased vapor velocity leads to a higher frictional pressure drop component, thereby leading to an increase in the overall pressure drop. At an OCR of 5 %, a maximum increase in pressure drop of 13 % was observed. Similar observations were also made in the case of 3 % and 1 % OCR.

3.3.1.2 Vertical Pipe

Figure 3.18 shows the variation in the vertical suction line oil retention for POE 32 and POE 100 in R134a. Similar to the horizontal suction line, POE 100 led to an increased oil retention due to the higher liquid film viscosity in comparison to that observed in the case of POE 32. At an OCR of 5 % for POE 100, the vertical suction line oil retention was found to have increased by a maximum of 11 % in comparison to that in POE 32. Oil retention at 3 % OCR also nominally increased by 2-11 % in the case of POE 100. A maximum oil retention increase of 47 % was observed at the Jacobs critical mass flux in the case of POE 100. For the case of 1 % OCR, the

oil retention for POE 100 increased by a maximum of 21 % in comparison to POE 32. The vertical suction line pressure drop for POE 100 exhibited the greatest percentage increase in comparison to that of POE 32. At an OCR of 5 %, the vertical suction line pressure drop for POE 100 increased by 4-55 % in comparison to POE 32, while at an OCR of 3 %, a maximum pressure drop increase of 41 % was observed. Similarly a maximum percentage increase of 41 % was observed for 1 % OCR, in POE 100. Thus based on the previous discussions, it may be concluded that the vertical suction line pressure drop is the most affected parameter, with variations as high as 55 % encountered. It was also observed that the suction line oil retention values are only marginally different for POE 100 in comparison to POE 32. This implies that the liquid-film mixture viscosity for both the lubricants are probably very close to each other, thereby giving similar retention values. This also brings out the importance of the mixture property over the pure lubricant property, since POE 100 - which is thrice more viscous that POE 32 – gives similar oil retention values.

3.3.2 Effect of Lubricant Viscosity in R1234yf

The suction line oil retention and pressure drop values for R1234yf in POE 32 and POE 100 are shown in Figures 3.20 and 3.21. The data for the mixture R1234yf/POE 32 was obtained from Sethi and Hrnjak (2011). Each figure also shows the effect of the OCR on these parameters. Similar conditions of mass flux were employed for the purpose of comparison. Both oil retention and pressure drop results were presented per unit length of the suction line.

3.3.2.1 Horizontal Pipe

Figure 3.20 shows the variation in horizontal oil retention for POE 100 with respect to POE 32 for R1234yf. Analogous to the results of R134a, POE 100 gave rise to a marginal increase in oil retention in comparison to POE 32. This again was a result of the larger liquid film mixture

viscosity in the case of POE 100 in comparison to POE 32. At an OCR of 5 %, the horizontal oil retention increased by 7-21 % for POE 100, while for an OCR of 3 % a maximum oil retention increase of 17 %. Similarly for an OCR of 1 %, the oil retention was found to increase by a maximum of 45 %. The horizontal suction line pressure drop is represented in Figure 3.21. Similar to the case of R134a, POE 100 gave rise to an increased horizontal suction line pressure drop in comparison to POE 32. For instance at an OCR of 5 %, a maximum increase of horizontal suction line pressure drop of 27 % was observed, while at a 3 % OCR, a 19 % increase in horizontal pressure drop was observed. Similarly at 1% OCR, a maximum pressure drop increase of 10 % was achieved.

3.3.2.2 Vertical Pipe

The variation of the vertical suction line oil retention and pressure drop for POE 100 and POE 32 in R1234yf is shown in Figure 3.20. The trends of the results obtained were similar to those obtained in the case of R134a. POE 100 always gave rise to a higher oil retention in R1234yf, in comparison to POE 32. The vertical suction line oil retention increased by 3-18 % in POE 100 in comparison to that of POE 32 at an OCR of 5 %. Similarly at an OCR of 3 %, the vertical oil retention increased by 2-20 % while at an OCR of 1 %, a maximum increase in vertical oil retention of 28 % was observed. The higher lubricant retention in POE 100 was again due to the higher liquid-film viscosity. The vertical suction line pressure drop showed trends similar to those seen in R134a. In general, the pressure drop increased substantially with POE 100 due to higher liquid film thickness, which leads to an increased vapor velocity. At an OCR of 5 %, maximum pressure drop increase of 31 % was observed for POE 100 in comparison to POE 32. Similarly at both 3 % and 1 % OCR, the vertical pressure drop increased by a maximum of 27 %.

3.3.3 Effect of Lubricant Viscosity in R410A

The suction line oil retention and pressure drop values for R410A in POE 32 and POE 100 are shown in Figures 3.22 and 3.23. The effect of OCR on oil retention and pressure drop is shown. Similar conditions of mass flux were employed for the purpose of comparison. Both oil retention and pressure drop results were presented per unit length of the suction line.

3.3.3.1 Horizontal Pipe

The difference in horizontal oil retention between POE 100 and POE 32 is shown in Figure 3.22. The oil retention was always greater in POE 100 due to the higher liquid film viscosity in comparison to POE 32. In the case of 5 % OCR, it was observed that the horizontal lubricant retention increased by 3-25 % in POE 100 in comparison to POE 32. Similarly at an OCR of 3 %, the horizontal retention for POE 100 increased by 8-31 % while at an OCR of 1 % the retention was increased by 10-42 %. The trends of the horizontal pressure drop were also similar to those seen in R134a and R1234yf. The horizontal suction line pressure drop in POE 100 was observed to be greater than that seen in POE 32. For an OCR of 5 %, the pressure drop in POE 100 was observed to increase as large as 48 % in comparison to POE 32. A maximum of 44 % increase of oil retention was observed in the case of POE 100 at an OCR of 3 % while at 1 % OCR, a maximum of 62 % increase in oil retention was observed for POE 100.

3.3.3.2 Vertical Pipe

Figure 3.23 represents the vertical suction line oil retention and pressure drop in POE 100 with comparison to POE 32, for R410A. Trends of the results were similar to those observed in R134a and R1234yf. The vertical suction line oil retention and pressure drop were increased in the case of POE 100 in comparison to POE 32. At an OCR of 5 %, the vertical oil retention increased by

0-11 % in POE 100 in comparison to POE 32. Similarly for an OCR of 3 % an increase of retention of 2-15 % was observed in POE 100, while at an OCR of 1 % the oil retention increased by 4-12 %. The vertical pressure drop was found to increase in POE 100 in comparison to POE 32. At an OCR of 5 %, the vertical pressure drop was found to increase 19-56 % in POE 100 in comparison to POE 32. Similarly at an OCR of 3 %, the vertical pressure drop increased by 38-56 % for POE 100 while at an OCR of 1 %, the vertical pressure drop increased by 14-64 %.

3.4 Comparison of Oil Retention and Pressure Drop in Different Refrigerants

This section represents the differences in oil retention and pressure drop for the same oil in different refrigerants, namely R134a, R1234yf and R410A. At a given OCR, comparisons are made at similar conditions of mass flux, superficial vapor velocity and system cooling capacity. The system cooling capacity was calculated assuming a 40 °C condenser temperature without subcooling, with an evaporator temperature of 10 °C and a degree of superheat of 10 °C. These conditions were similar to those assumed by Sethi and Hrnjak (2011). Figures 3.24 to 3.29 show comparisons for POE 32 lubricant in terms of suction line oil retention and pressure drop. Oil retention and pressure drop values are represented per unit length of the suction line. Similarly, Figures 3.30 to 3.35 show comparisons in oil retention and pressure drop for POE 100. As mentioned previously, the operating conditions were a saturation temperature of 13 °C and a superheat of 15 °C. Also, the oil retention and pressure drop results for R134a/POE 32 and R1234yf/POE 100 were obtained from Sethi and Hrnjak (2011).

3.4.1 Comparisons in POE ISO 32

The change in oil retention in POE 32 for R134a, R1234yf and R410A is shown in Figures 3.24, 3.26 and 3.28. Similarly the variation of suction line pressure drop is depicted in Figures 3.25, 3.27 and 3.29. Each plot shows variations corresponding to a particular OCR.

3.4.1.1 Comparisons in Oil Retention

For an OCR of 5 %, Figure 3.24 shows the oil retention variation. At the same superficial vapor velocity, it was observed that R410A had much lower oil retention in comparison to R134a and R1234yf. At the same conditions of operation, R410A had a higher refrigerant vapor density in comparison to R134a and R1234yf. Thus for the same refrigerant superficial vapor velocity, R410A vapor has greater momentum in comparison to R134a and R1234yf. As a result of this higher momentum, the vapor is able to transport more lubricant out of the test sections, thus leading to a lower amount of oil retention in the suction lines. It was observed that the oil retention of R134a and R1234yf in POE 32 were very similar to each other under similar conditions of superficial vapor velocity. At the same mass flux condition, R410A had the largest oil retention due to its high refrigerant vapor density. As a result of this high density, R410A has lower superficial vapor velocity in comparison to R134a and R1234yf, as a consequence of which it has lower momentum available to transport the oil-rich mixture. Similarly, R1234yf possesses a marginally higher refrigerant vapor density in comparison to R134a, as a result of which it has higher oil retention in comparison to R134a at the same mass flux. Comparisons were also made at the same cooling capacity conditions. At the same evaporator conditions, R410A has a higher enthalpy of vaporization compared to R134a and R1234yf. Thus in order to match the capacity, the mass flow rate of R410A should be reduced, which consequently leads to a reduction in vapor momentum, which translates into an increased oil retention compared to

R134a and R1234yf. In a similar manner, the enthalpy of vaporization of R1234yf is lower than that of R134a at similar conditions. In order to match the system cooling capacity, the mass flow rate of R1234yf is increased, thereby increasing its superficial vapor velocity. This increase leads to the situation where both R1234yf and R134a have similar vapor velocities, thereby leading to similar oil retentions. These results were observed for both horizontal suction lines as well as vertical suction lines. Figures 3.26 and 3.28 show similar trends for 3 % and 1 % OCR respectively.

In a quantitative sense, the following observations were made in POE 32 lubricant. At a superficial vapor velocity of 1 m/s, R410A has horizontal oil retention of 5.67 g/m, as opposed to the 9.6 g/m and 9.29 g/m of oil retention observed in R134a and R1234yf respectively. This translates into a 70 % increase in oil retention in R134a, in comparison to R410A. The oil retention in R134a is only 3 % more than that observed in R1234yf, which for all practical purposes may be assumed the same. Similarly in the vertical test section, it was observed that at a superficial vapor velocity of 1 m/s, R410A had an oil retention of 11.9 g/m as opposed to the values of 16.32 g/m and 16.34 g/m observed in R134a and R1234yf respectively. This translates into 37 % higher oil retention in R134a in comparison to R410A. Interestingly at a vapor velocity of 4 m/s, R134a is found to have an oil retention that is just 4 % more than that in R410A, showing that the percentage difference in oil retention decreases with an increase in superficial vapor velocity. In terms of the same mass flux, it was observed that R1234yf has more oil retention that R134a. At a mass flux of 100 kg/m^2-s for 5 % OCR, R1234yf has 12 % more oil retention than R134a in the horizontal pipe. This percentage increases to 19 % and 30 % when the mass flux decreases to 80 kg/m^2-s and 60 kg/m^2-s respectively. It was also observed that at the same system cooling capacity of about 0.65 kW, the vertical suction line oil retention

was 16.98 g/m for the case of R410A in comparison to 9.63 g/m and 8.92 g/m observed in R1234yf and R134a respectively. It was observed that oil retention values of R1234yf and R134a were very similar at the same conditions of cooling capacity.

3.4.1.2 Comparisons in Pressure Drop

Figure 3.25 shows the comparison in pressure drop for both horizontal and vertical suction lines in R1234yf, R134a an R410A in POE 32, for an OCR of 5 %. In general, it can be observed that for the same superficial vapor velocity, R410A had a larger horizontal suction line pressure drop in comparison to R134a and R1234yf. This is because of the larger momentum associated with R410A refrigerant vapor due to its larger vapor density. This leads to a higher exchange of momentum between the vapor and the liquid mixture at the interface, which is characterized by the formation of interfacial waves. This ultimately leads to an increased pressure drop for R410A, in comparison to R134a and R1234yf. Similarly, it was observed that R1234yf had a higher pressure drop in comparison to R134a, due to its higher refrigerant vapor density. Similar trends were seen in the vertical suction line for high vapor velocities. For instance at a vapor velocity of 3 m/s, R410A has the highest pressure drop. But at a lower velocity of 1.5 m/s, it is interesting to observe that R410A has a lower pressure drop in comparison to R134a and R1234yf. This is because a velocity of 1.5 m/s corresponds to a mass flux for R410A where flow reversal of the annular liquid film has initiated. This flow reversal point is associated with the minimum pressure drop condition in vertical suction lines. On the other hand, this vapor velocity also corresponds to the Jacobs critical mass flux condition for R134a and R1234yf, where the pressure drop increases due to the hydrostatic pressure drop component. For similar conditions of mass flux, R410A had the lowest pressure drop value, again due to its high refrigerant vapor density. This was true for all mass fluxes in the case of the horizontal suction line. Similar trends

were observed for high mass flux conditions in the vertical suction line. At a lower mass flux of about 60 kg/m^2-s, R410A had the largest pressure drop over R134a and R1234yf. This was again because of the fact that flow reversal had initiated in R410A at a mass flux higher than 60 kg/m^2-s, as a result of which the pressure drop increases due to the hydrostatic pressure drop component. But at the same mass flux of 60 kg/m^2-s, R134a and R1234yf are still in the annular flow regime, thereby possessing a lower overall pressure drop. For a similar system cooling capacity, R410A was observed to possess the largest pressure drop in comparison to R134a and R1234yf, for all mass fluxes in both horizontal and vertical test sections. It was also observed that R1234yf had an increase in pressure drop in comparison to R134a, due to its larger refrigerant vapor density.

Quantitatively, at an OCR of 5 % and at a superficial vapor velocity of 3 m/s, R410A possessed an 82 % greater horizontal suction line pressure drop in comparison to R134a, while a 41 % increase in pressure drop was observed in the vertical suction line. At the same condition of operation, R134a and R1234yf varied in pressure drop by 5 % in both the suction lines. Also, it was observed that at the same conditions of mass flux, R134a had 10-15 % greater pressure drop in comparison to R1234yf, due to the higher vapor velocity it possesses. Similarly, R410A possessed the least pressure drop due to its high vapor density. For instance, at a mass flux close to 122 kg/m^2-s, R134a possessed a 72 % higher pressure drop in comparison to R410A. At a similar system cooling capacity, R1234yf possesses about 20-30 % higher pressure drop over that observed in R134a, in both horizontal and vertical test sections. Thus these results are significant in terms of employing R1234yf as a drop-in replacement for R134a. Similar results for 3 % and 1 % OCR are shown in Figures 3.27 and 3.29 respectively.

3.4.2 Comparisons in POE 100

The change in oil retention in POE 100 for R134a, R1234yf and R410A is shown in Figures 3.30, 3.32 and 3.34. Similarly the variation of suction line pressure drop is depicted in Figures 3.31, 3.33 and 3.35. Each plot shows variations corresponding to a particular OCR.

3.4.2.1 Comparisons in Oil Retention

Comparisons in oil retention among various refrigerants in POE 100 possessed trends that were similar to those observed in POE 32. At an OCR of 5 %, Figure 3.30 shows the variation of oil retention with the superficial vapor velocity. As observed in POE 32, R410A always had the least oil retention due to the greater momentum it possessed. At a superficial vapor velocity of 1.5 m/s, it was observed that R1234yf possessed 68 % more oil retention in the horizontal suction line with respect to R410A, while a 54 % oil retention increase was observed in the vertical suction line. Similarly at a vapor velocity of 3 m/s, the vertical retention is 30 % greater in R1234yf in comparison to R410A, while a 5 % increase in horizontal oil retention was observed. In general for a 5 % OCR, it was observed that R1234yf had a 10-30 % increase in oil retention in comparison to R134a in both horizontal and vertical test sections. This is an interesting result, in comparison to that observed in POE 32 where R1234yf and R134a had similar oil retention values. Theoretically, one would expect R1234yf to possess lower oil retention in comparison to R134a at the same superficial vapor velocity, due to its marginally higher vapor density in comparison to R134a.These results indicate that refrigerant vapor density and consequently the vapor momentum are not perhaps the dominant criterion on which oil retention depends. It may depend on other parameters namely the liquid film viscosity and the void factor variation as well. Measurements did show that R1234yf/POE 100 mixture possessed a marginally higher liquid film viscosity in comparison to R134a/POE 100 at the same

conditions of operations. Also, the nature of the liquid-vapor interface may be different for R134a and R1234yf, thereby influencing different waves or ripples on the liquid film surface, thus influencing the void factor variation. At the same mass flux conditions, R410A had the highest oil retention in comparison to R134a and R1234yf due to its higher vapor density. At a mass flux of about 50 kg/m^2-s, R410A had almost double the oil retention in both horizontal and vertical suction lines, in comparison to R134a. At a higher mass flux of 60 kg/m^2-s, R410A had 32 % greater oil retention in the horizontal suction line in comparison to R134a, while a 50 % increase was observed in the vertical test section. At a mass flux of 80 kg/m^2-s, R410A only had a 39 % increase in vertical suction line oil retention in comparison to R134a. Thus one may observe that the importance of vapor density in oil retention seems to decrease with increasing mass flux. R1234yf also possessed greater oil retention in comparison to R134a, again due to its higher vapor density. For an OCR of 5 %, it was observed that R1234yf possessed 18-28 % more horizontal oil retention in comparison to R134a, while a 20-27 % increase in vertical oil retention was observed in R1234yf. For the same system cooling capacity, R410A had the largest oil retention due to the higher enthalpy of vaporization it possesses. For a system capacity of 0.65 kW, R410A had 91 % more horizontal oil retention in comparison to R134a, while the vertical oil retention almost doubled in comparison to that in R134a. Similarly at a capacity of 0.8 kW, R410A had a 32 % increase in horizontal oil retention in comparison to R134a while in the vertical suction line, the oil retention in R410A increased by 50 % in comparison to R134a in POE 100 lubricant. It was also noticed that for the same system capacity, R1234yf had larger oil retention in comparison to R134a in POE 100. This observation is of importance particularly in the aspect of using R1234yf as a drop-in replacement for R134a. It was observed that the vertical oil retention in R1234yf increased by 1-10 % over R134a. Similarly at a capacity of 0.65 kW,

R1234yf had 10 % more horizontal oil retention in comparison to R134a, while at a capacity of 1 kW, this percentage was 9 %. Similar trends for 1 % and 3 % OCR are shown in Figures 3.32 and 3.34 respectively.

3.4.2.2 Comparisons in Pressure Drop

Figures 3.31, 3.33 and 3.35 show comparisons in pressure drop between R134a, R1234yf and R410A in POE 100 lubricant. The observed trends in the horizontal and vertical suction line pressure drop were similar to those seen in POE 32. For an OCR of 5 %, and a superficial vapor velocity of 3 m/s, the horizontal pressure drop in R410A almost tripled in comparison to that observed in R134a, while the vertical pressure drop was 67 % greater in R410A. When the vapor velocity increased to 4 m/s, similar percentage increases were observed in R410 with respect to R134a. It was observed that for the same superficial vapor velocity, the horizontal pressure drop in R1234f increased by an average of 50 % over that observed in R134a, while in the vertical suction line a 15-30 % increase was observed in R1234yf. For the same mass flux, R134a had a suction line pressure drop that was 5-20 % greater than that observed in R1234yf. For higher cooling capacity values, R410A has the lowest pressure drop due to its high enthalpy of vaporization, which requires the reduction in the vapor mass flow rate for matching cooling capacity with R134a and R1234yf. It was observed that for the same system cooling capacity, R1234yf had a larger pressure drop than R134a, with the percentage of variation increasing with increase in capacity. It was observed that at a 5 % OCR, the average horizontal suction line pressure drop in R1234yf was about 50 % greater than that observed in R134a, while in the vertical suction line, the variation was 15-30 %. These observations have severe implications in employing R1234yf as a drop-in replacement for R134a. Similar results were seen in 1 % and 3 % OCR, as shown in Figures 3.33 and 3.35 respectively.

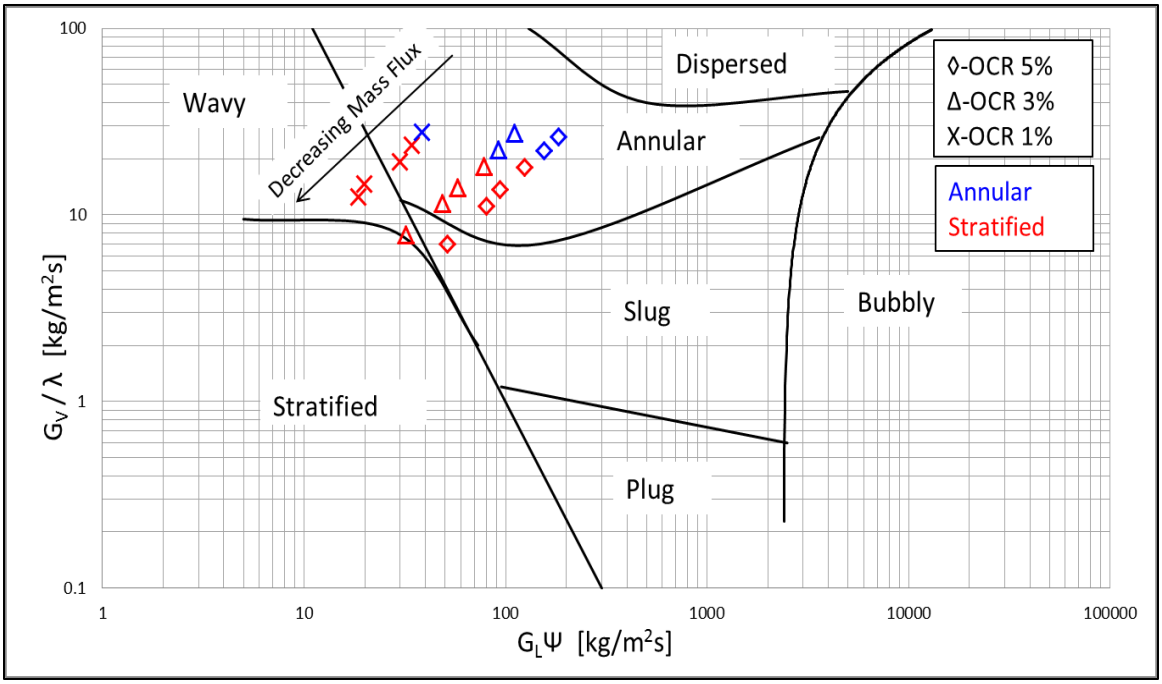

Figure 3.1 Modified Bakers (1954) flow map for R134a/POE 100 in a 10.2 mm internal diameter horizontal suction line

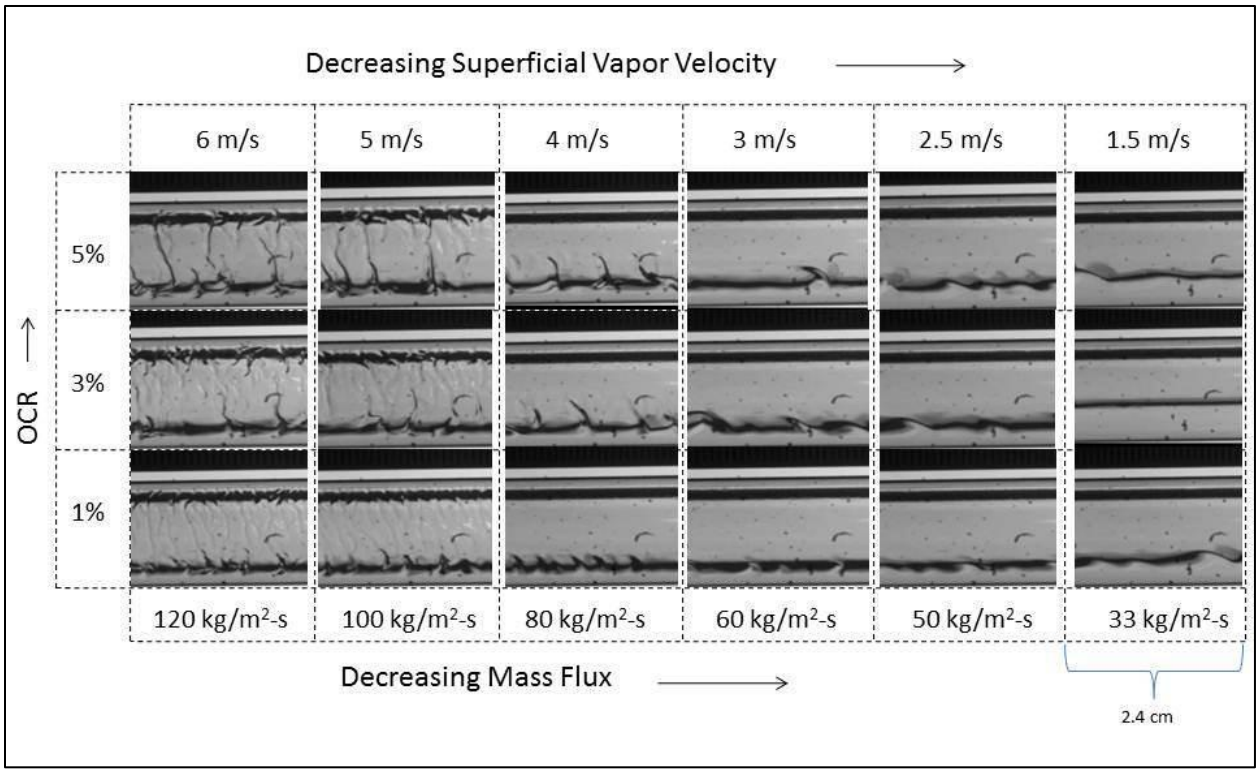

Figure 3.2 Horizontal suction line flow visualization for R134a/POE 100

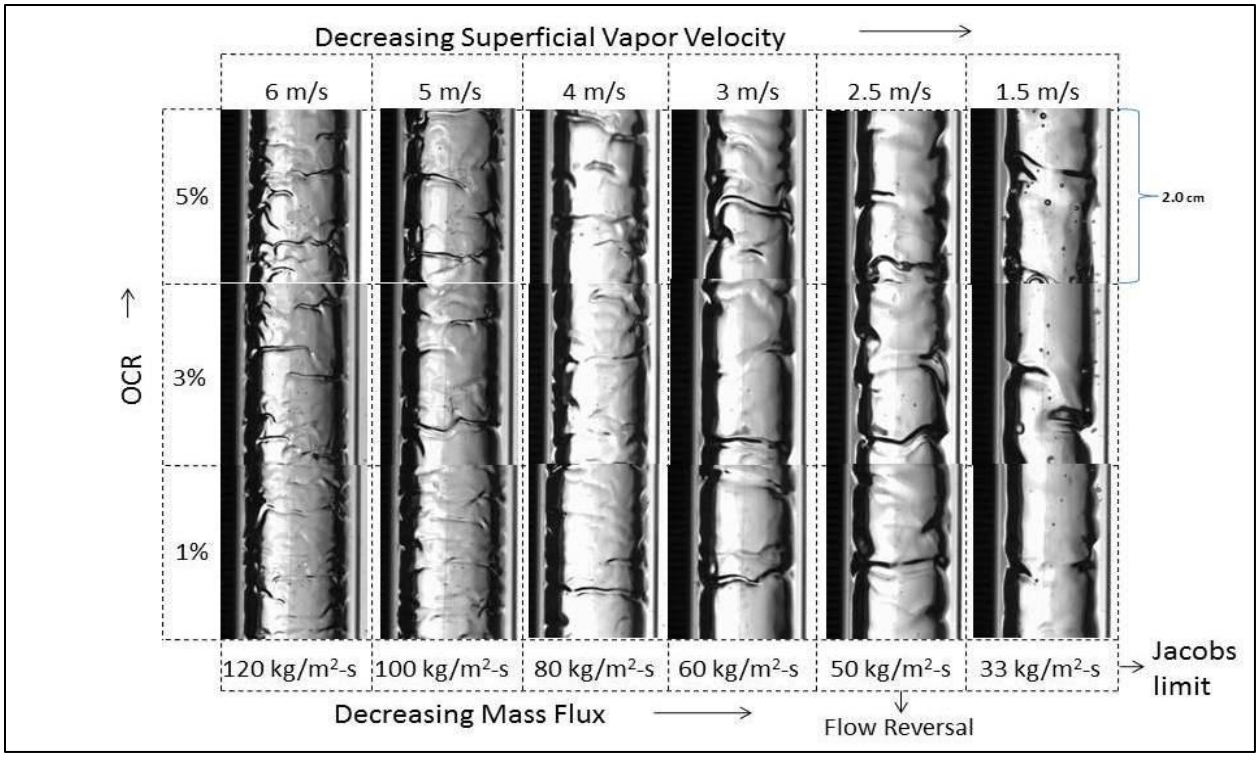

Figure 3.3 Vertical suction line flow visualization for R134a/POE 100

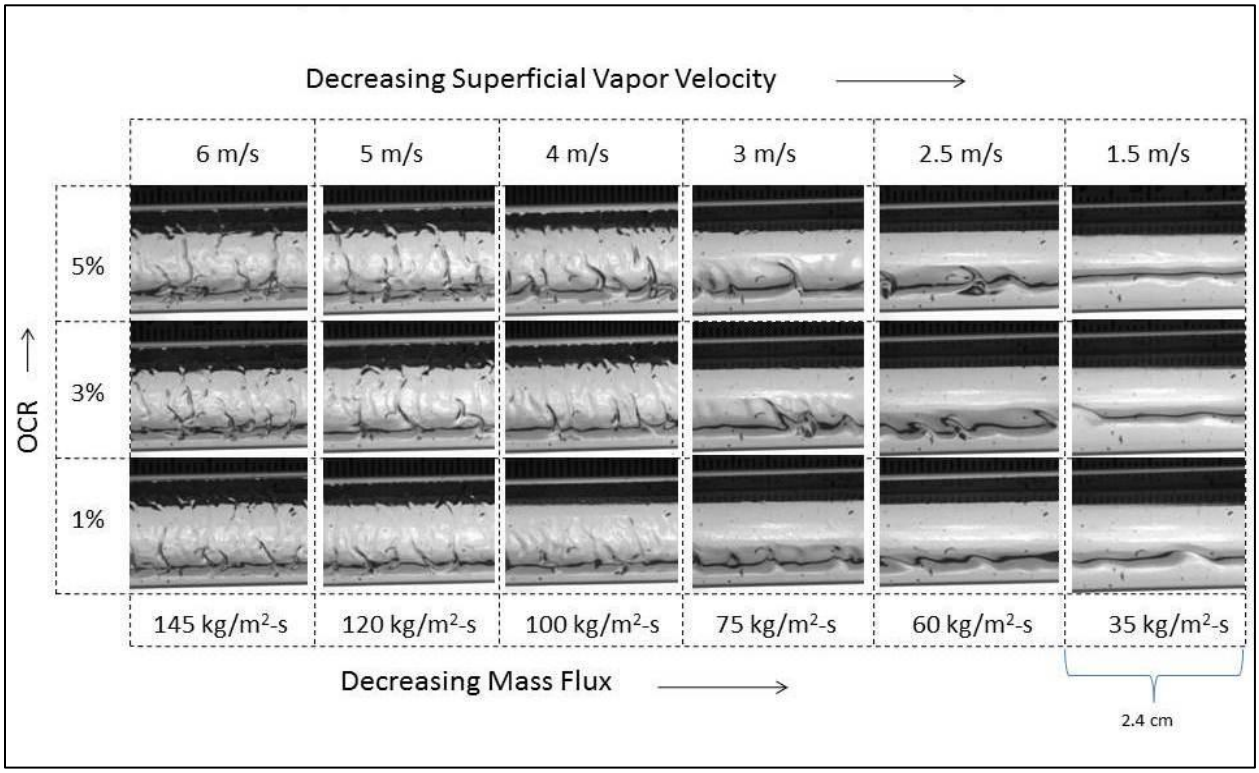

Figure 3.4 Horizontal suction line flow visualization for R1234yf/POE 100

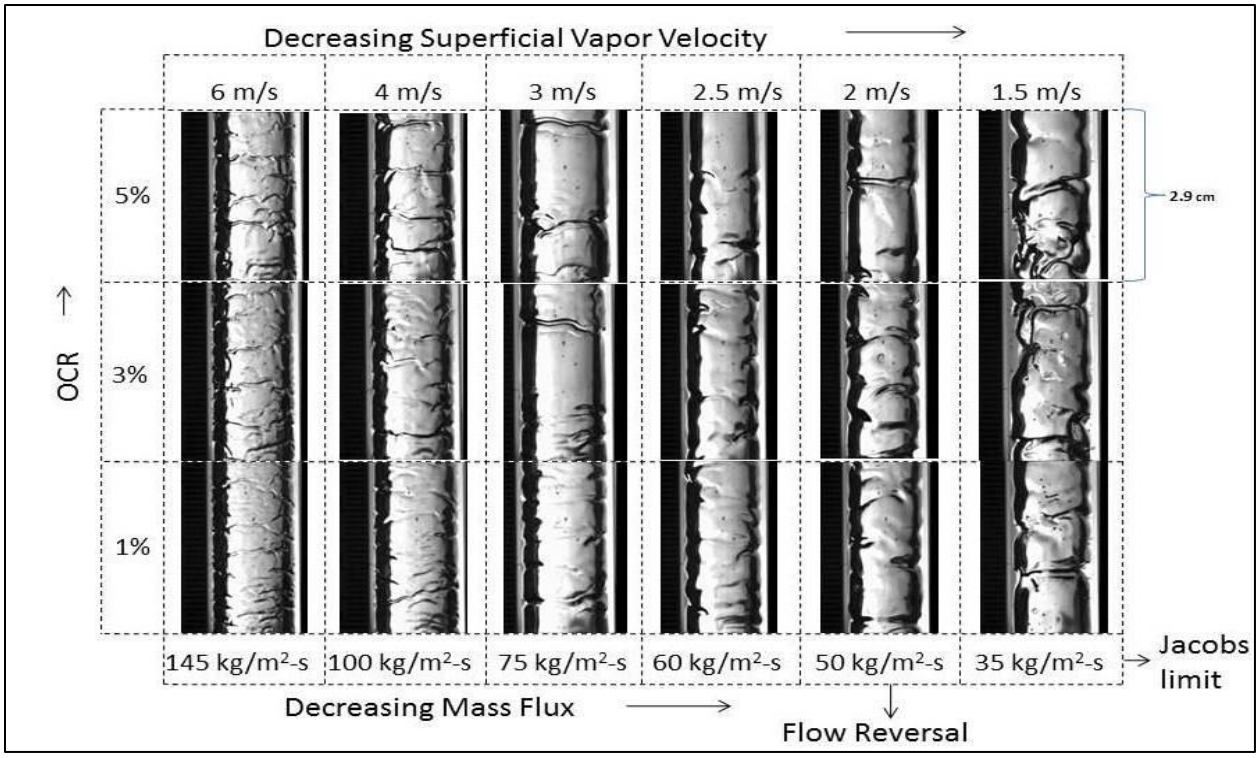

Figure 3.5 Vertical suction line flow visualization for R1234yf/POE 100

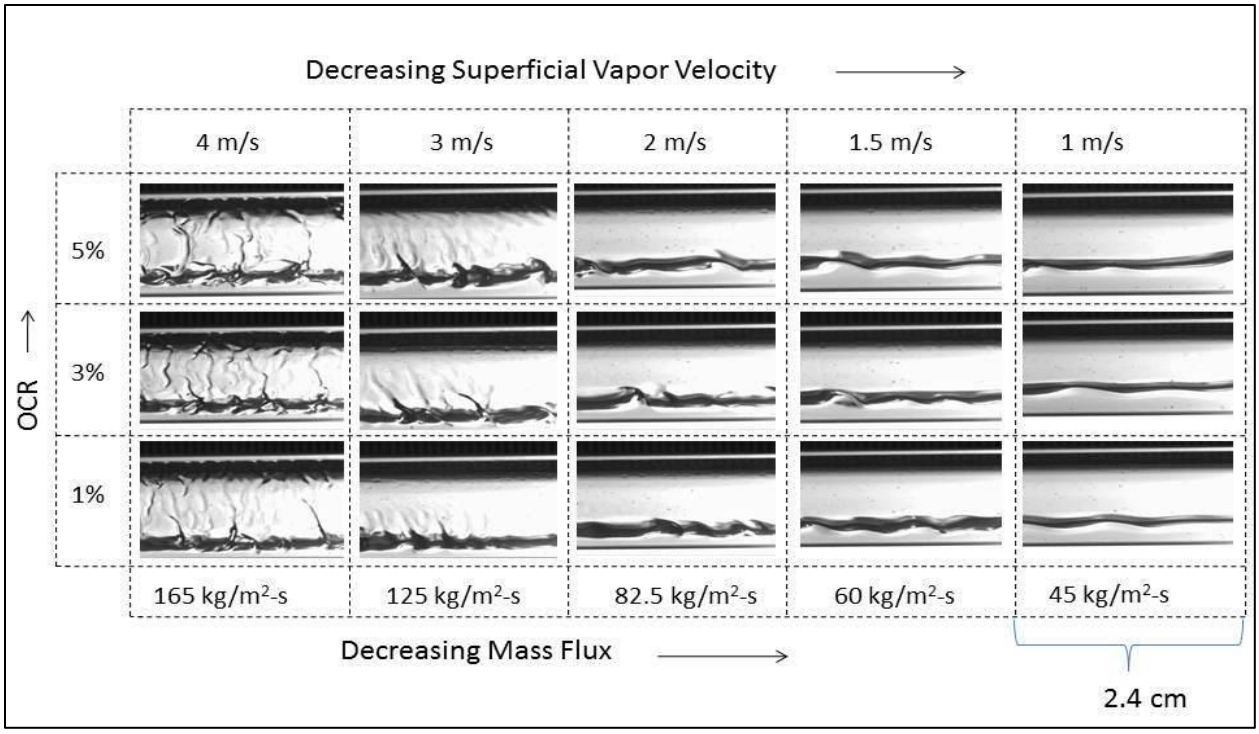

Figure 3.6 Horizontal suction line flow visualization for R410A/POE 100

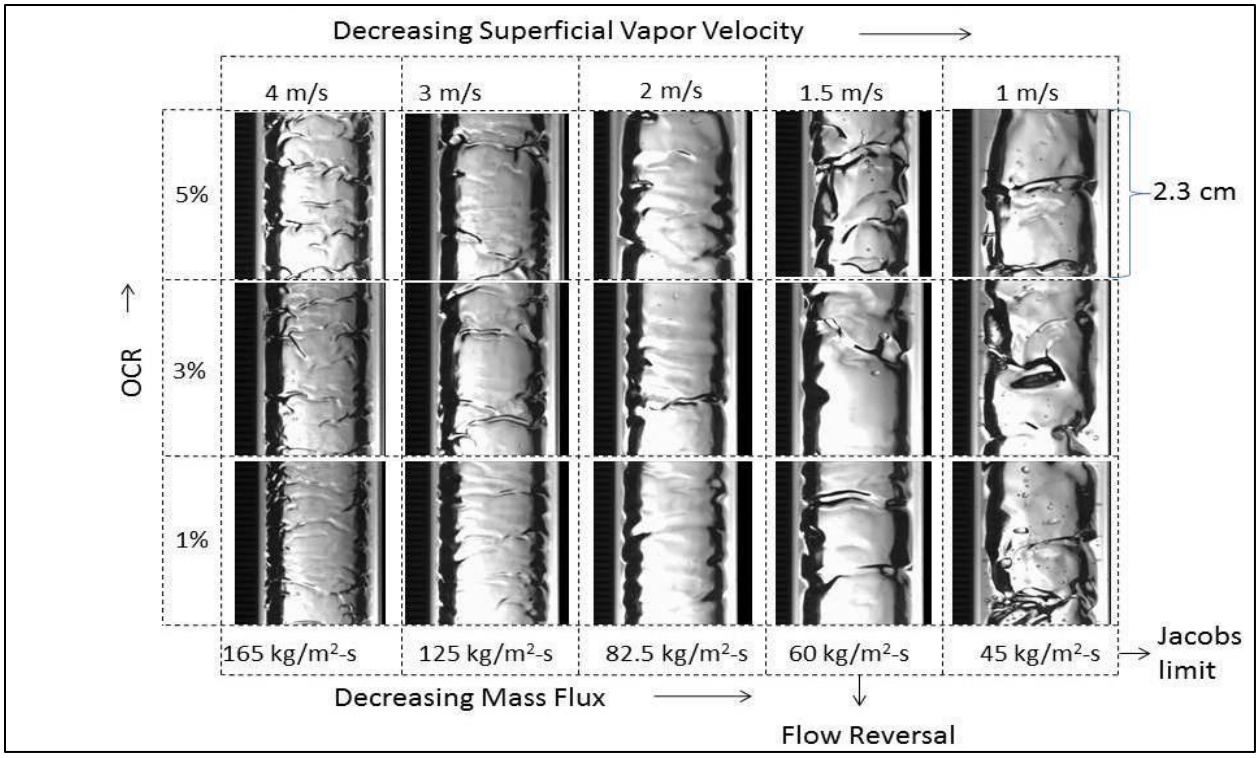

Figure 3.7 Vertical suction line flow visualization for R410A/POE 100

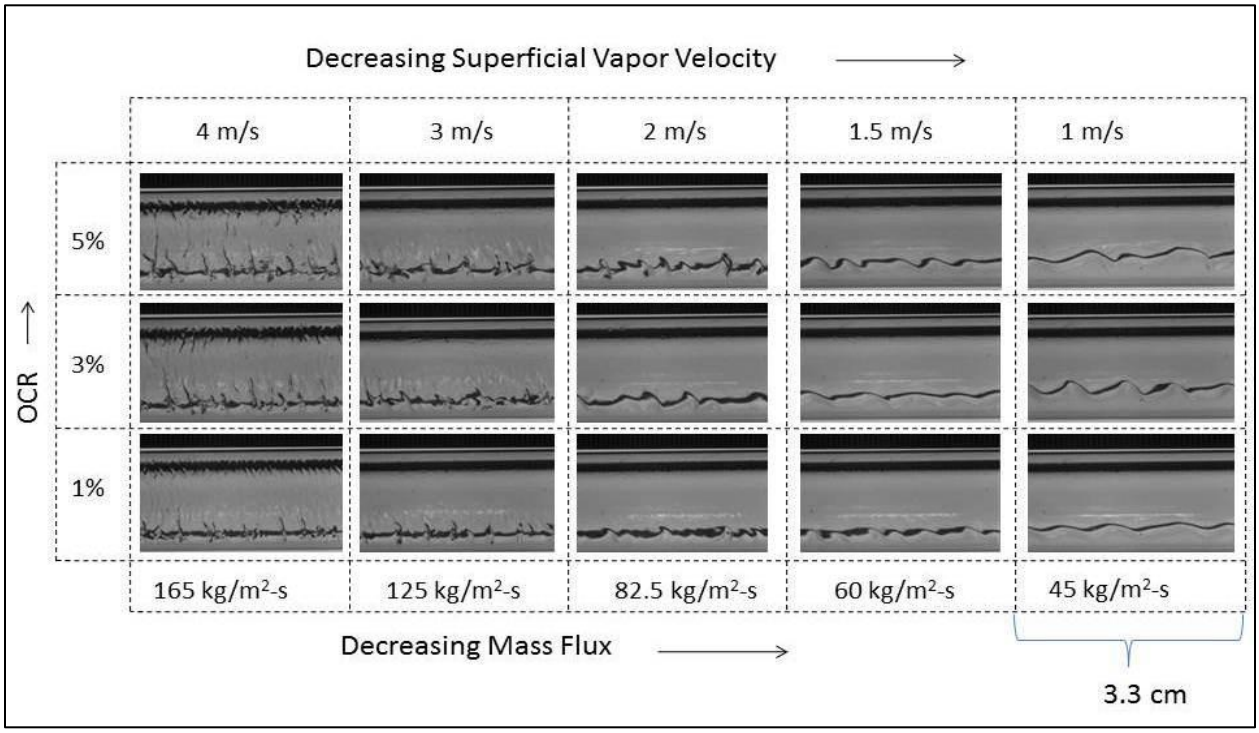

Figure 3.8 Horizontal suction line flow visualization for R410A/POE 32

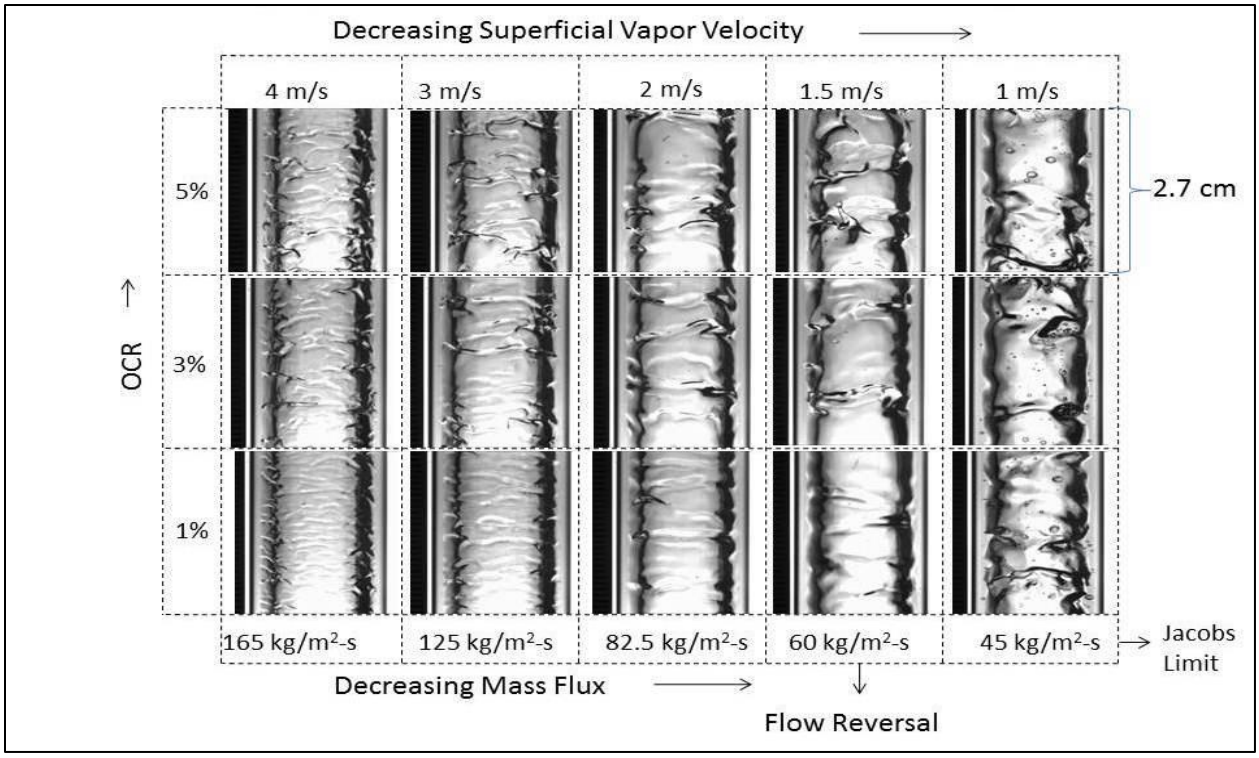

Figure 3.9 Vertical suction line flow visualization for R410A/POE 32

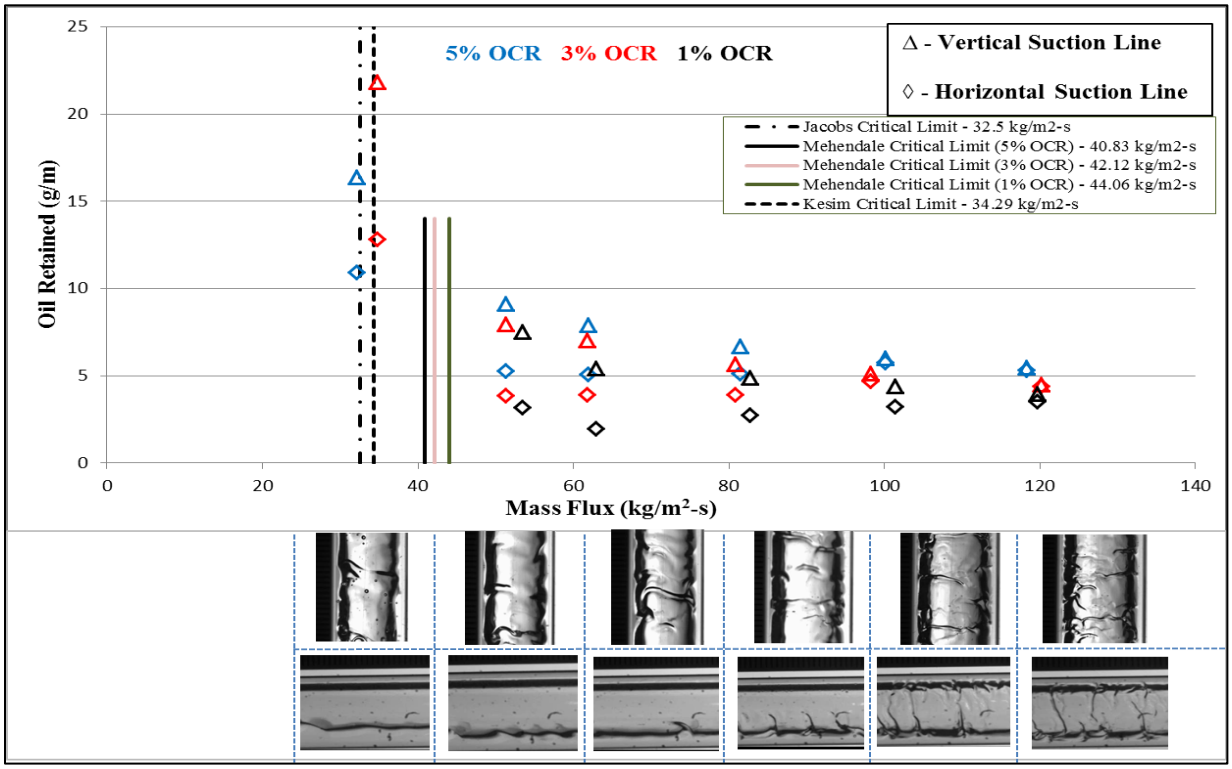

Figure 3.10 Variation of Oil Retention with Mass Flux for R134a/POE 100

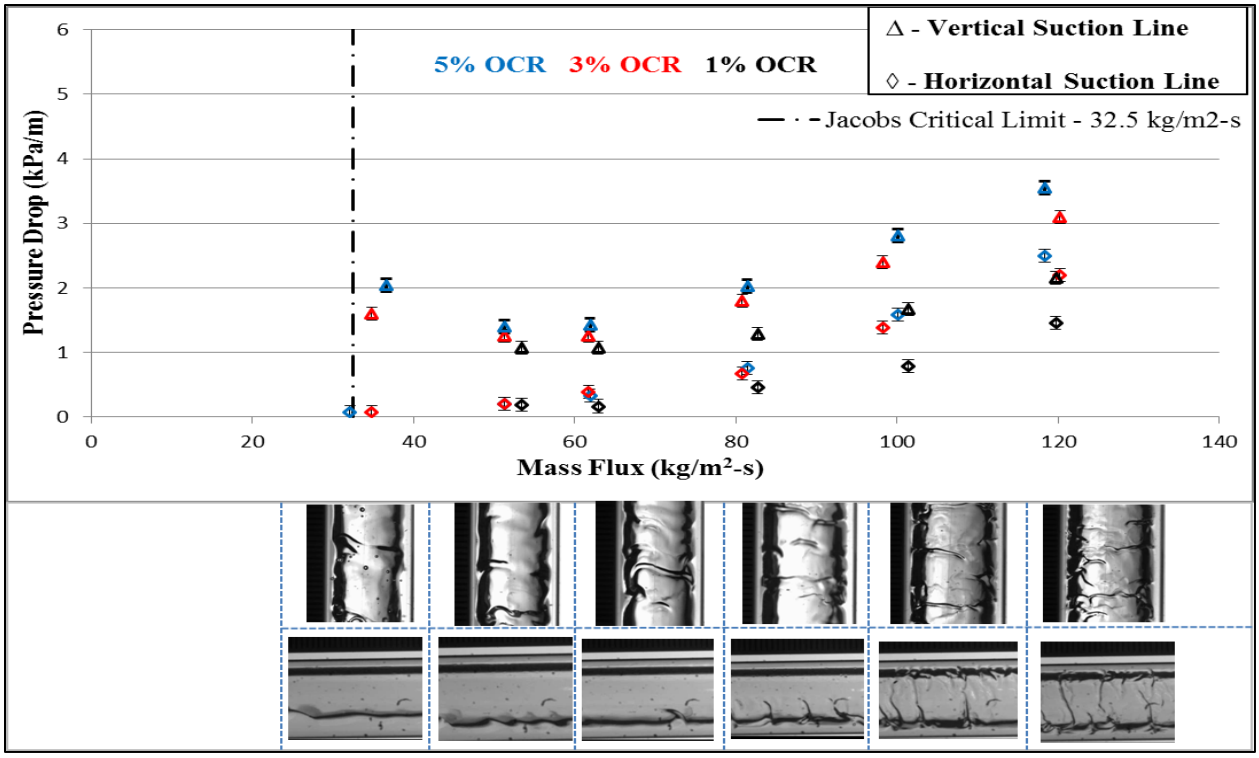

Figure 3.11 Variation of Pressure Drop with Mass Flux for R134a/POE 100

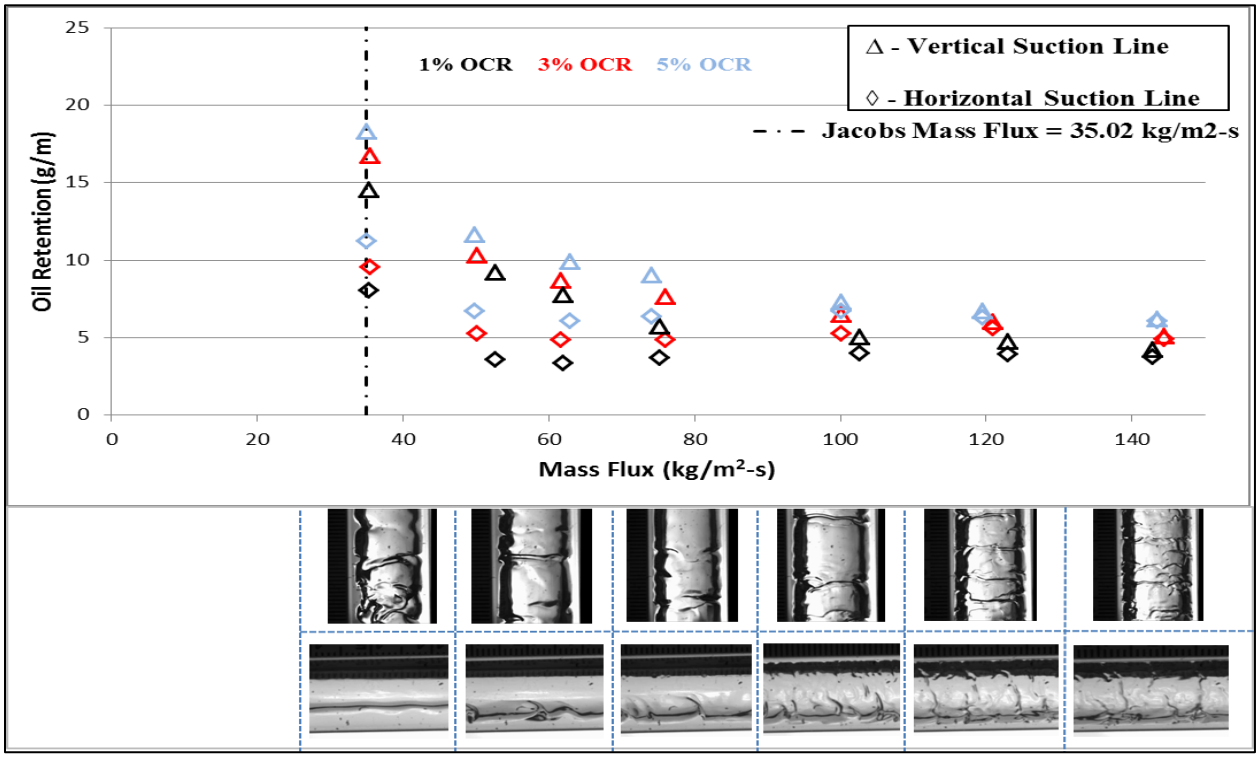

Figure 3.12 Variation of Oil Retention with Mass Flux for R1234yf/POE 100

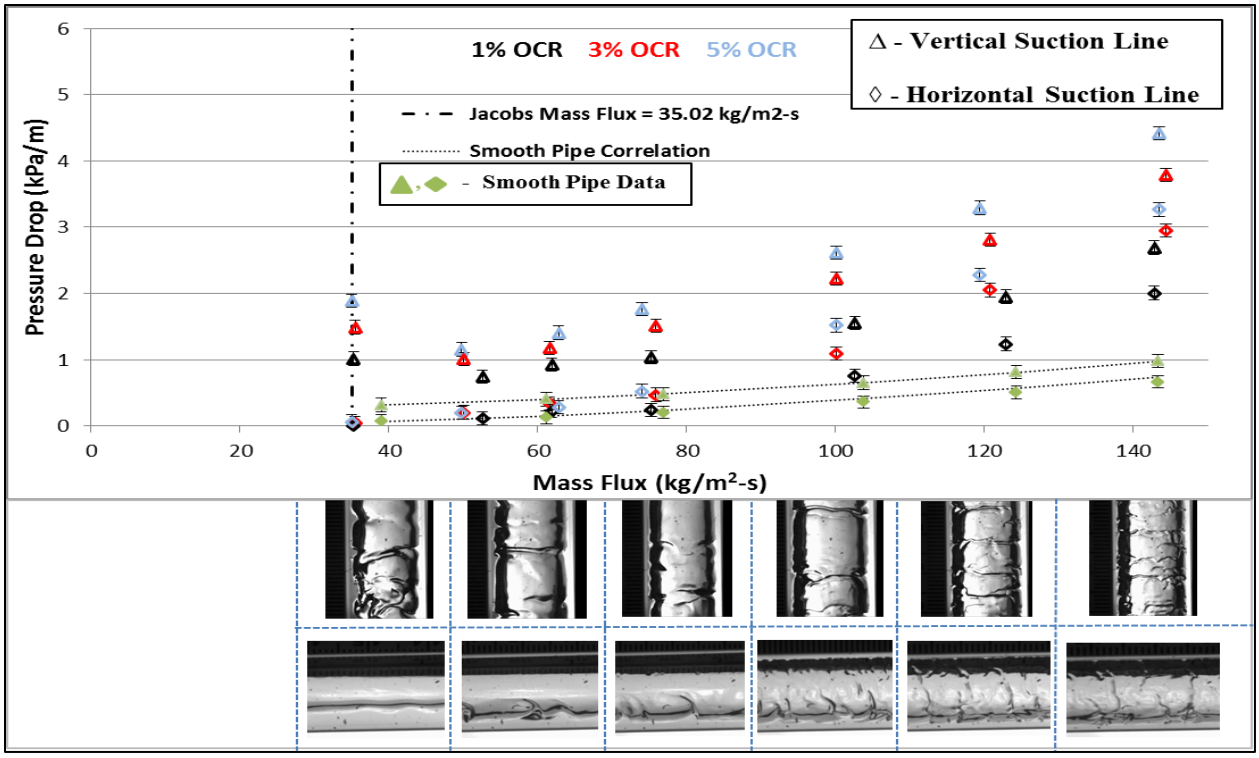

Figure 3.13 Variation of Pressure Drop with Mass Flux for R1234yf/POE 100

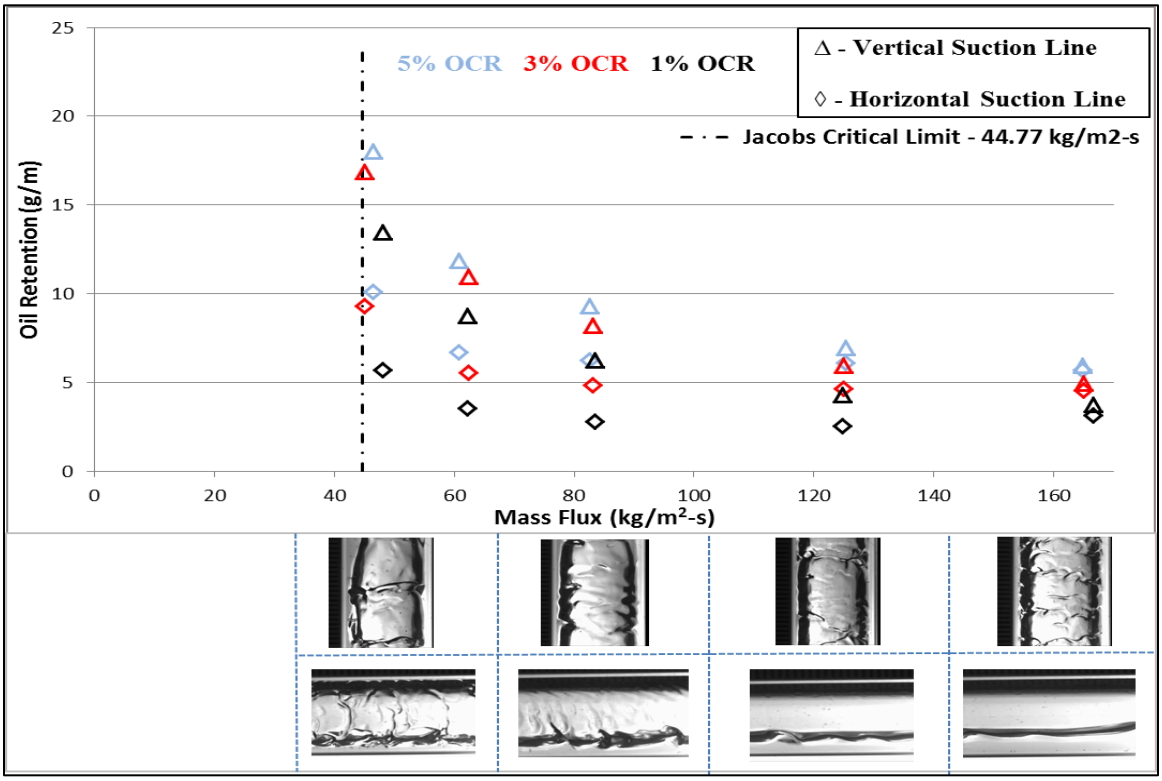

Figure 3.14 Variation of Oil Retention with Mass Flux for R410A/POE 100

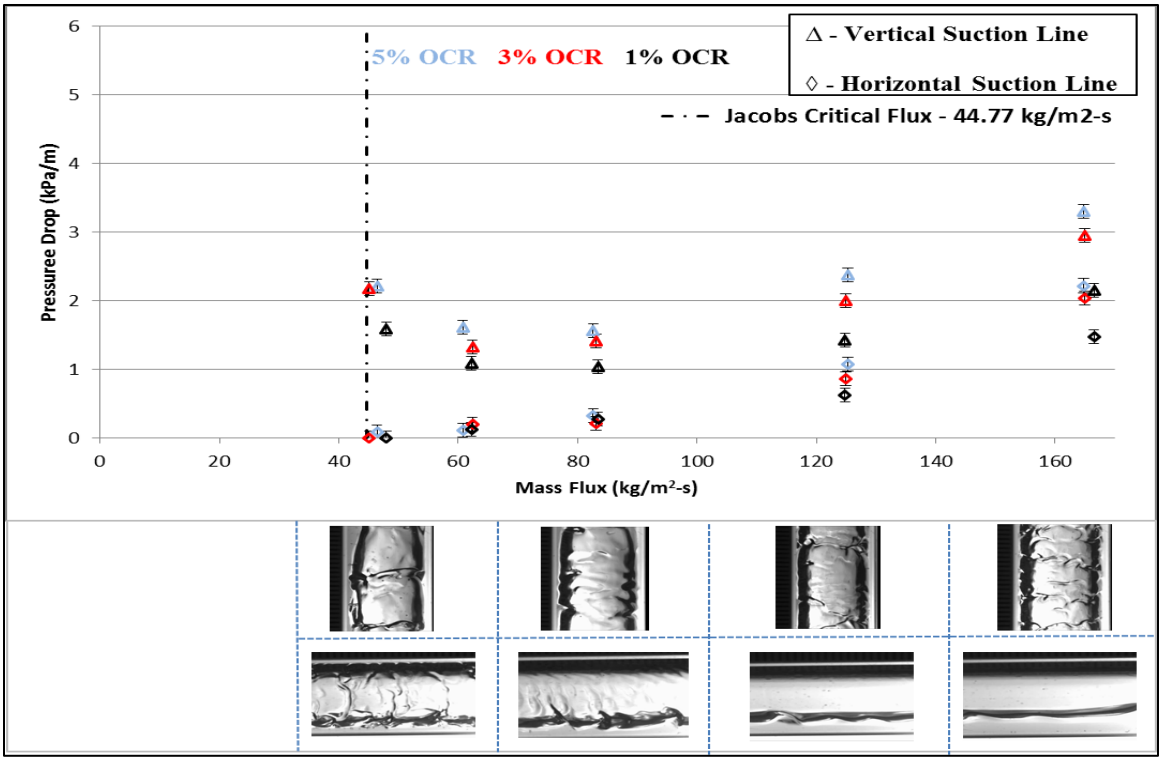

Figure 3.15 Variation of Pressure Drop with Mass Flux for R410A/POE 100

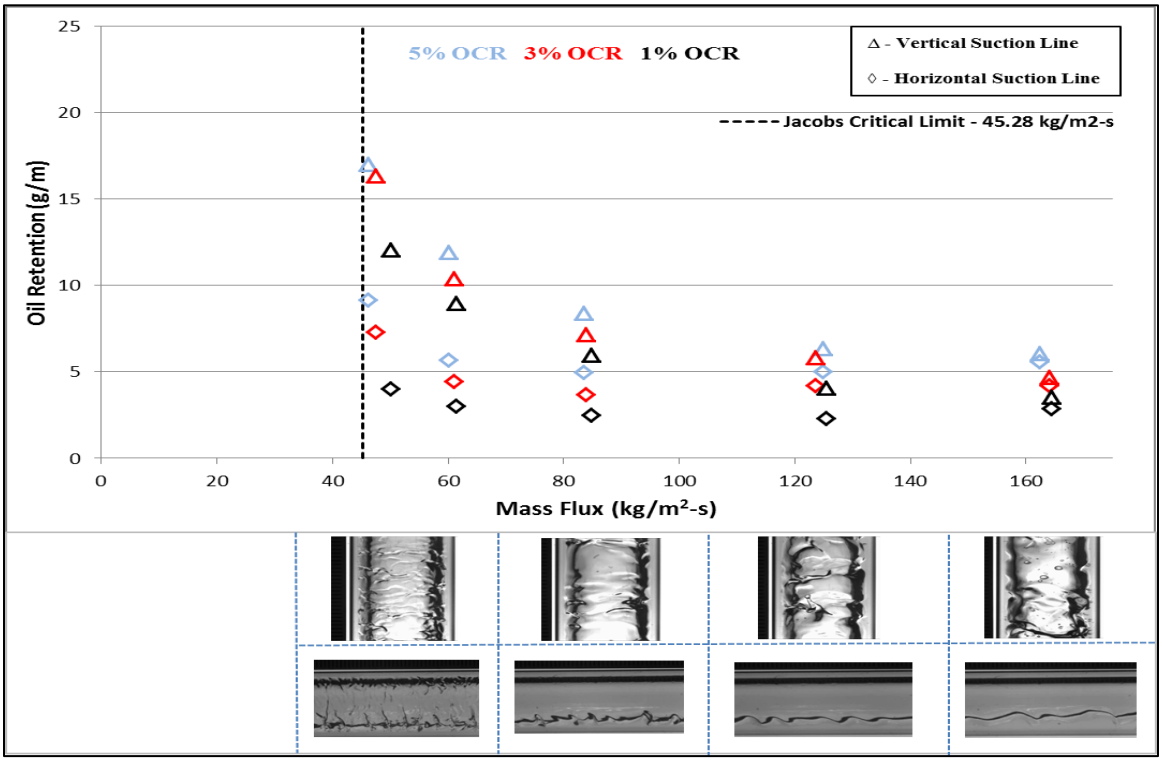

Figure 3.16 Variation of Oil Retention with Mass Flux for R410A/POE 32

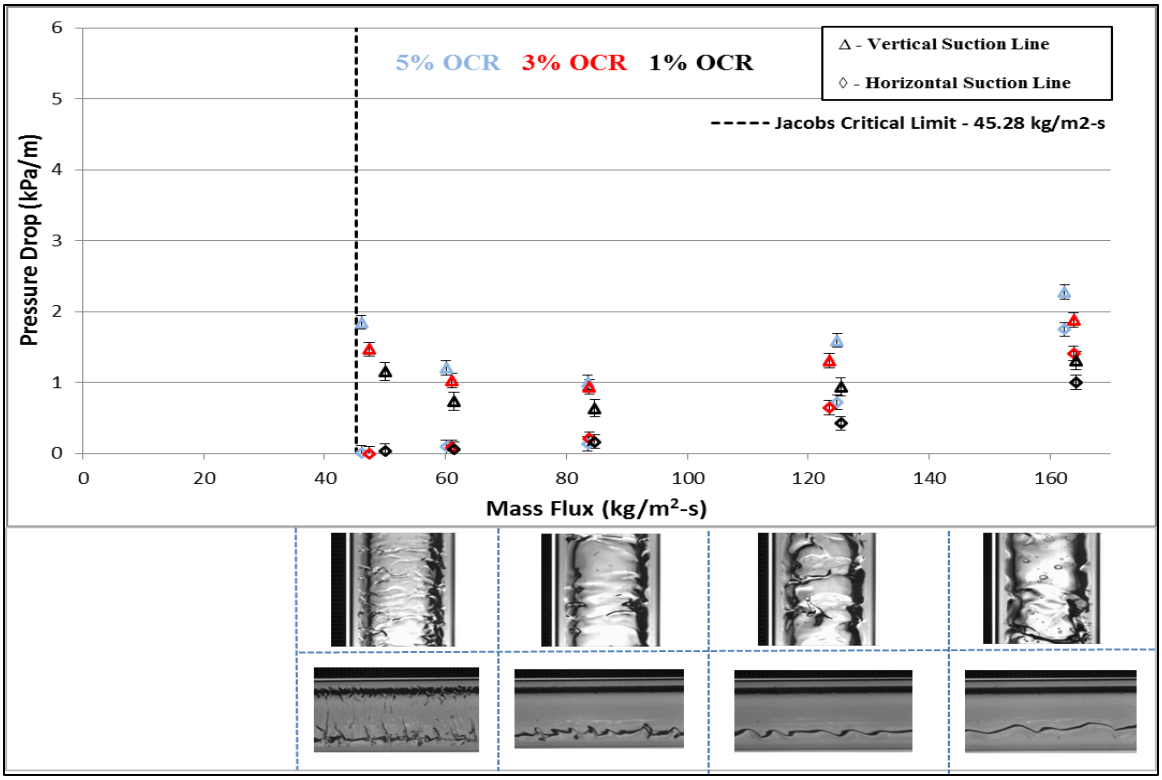

Figure 3.17 Variation of Pressure Drop with Mass Flux for R410A/POE 32

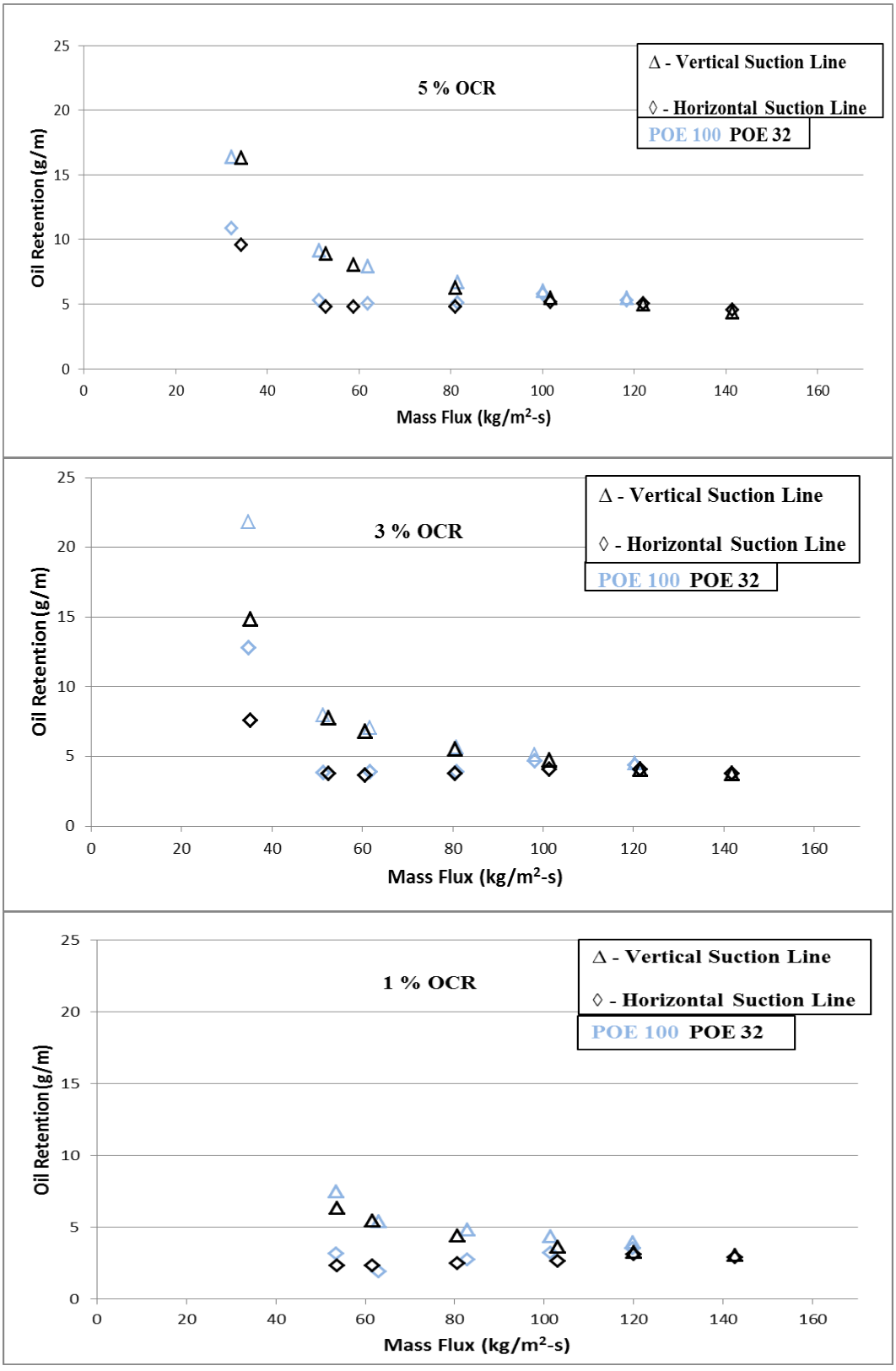

Figure 3.18 Effect of lubricant viscosity on oil retention for R134a at 3 OCR values

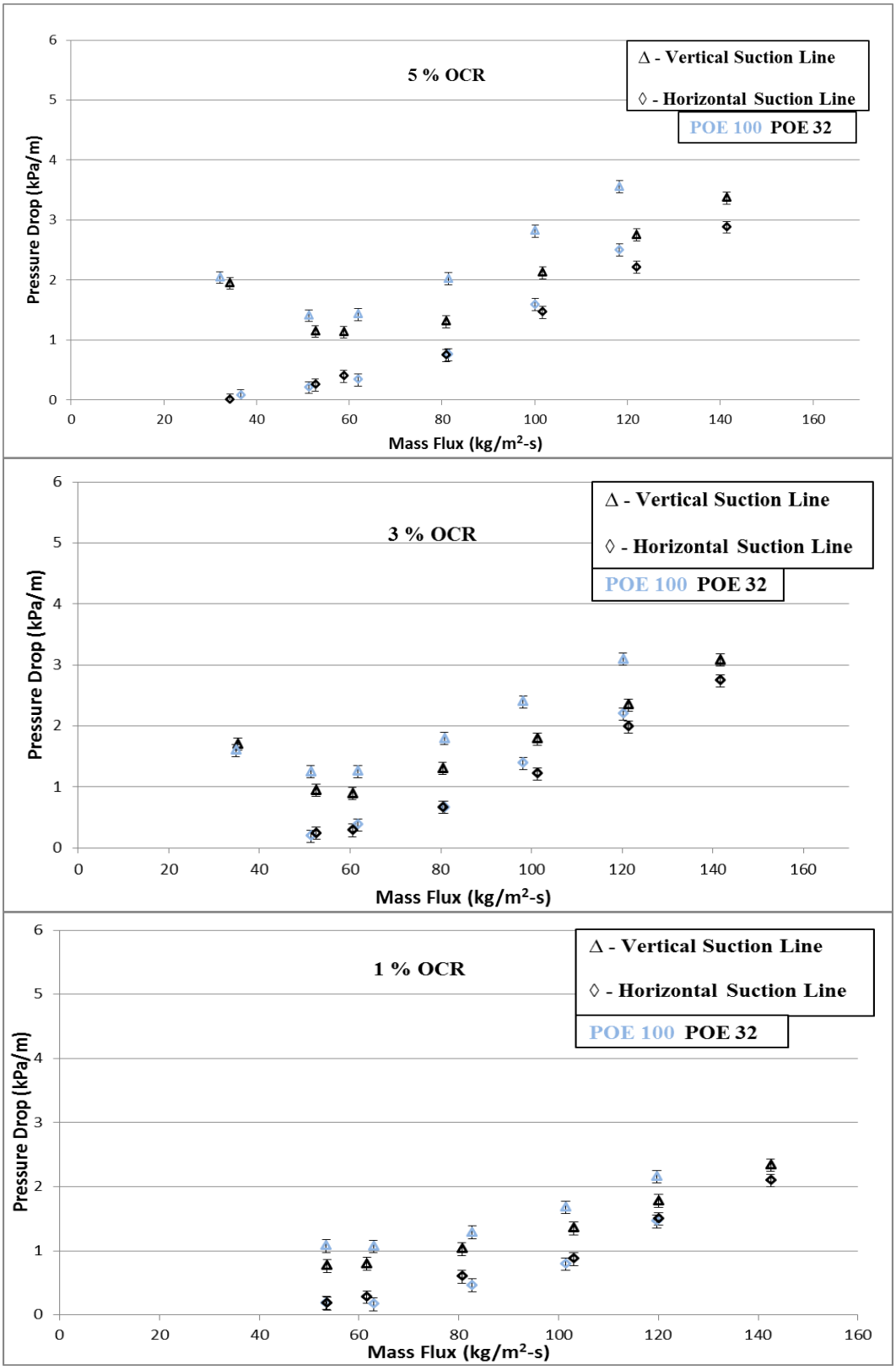

Figure 3.19 Effect of lubricant viscosity on pressure for R134a at 3 OCR values

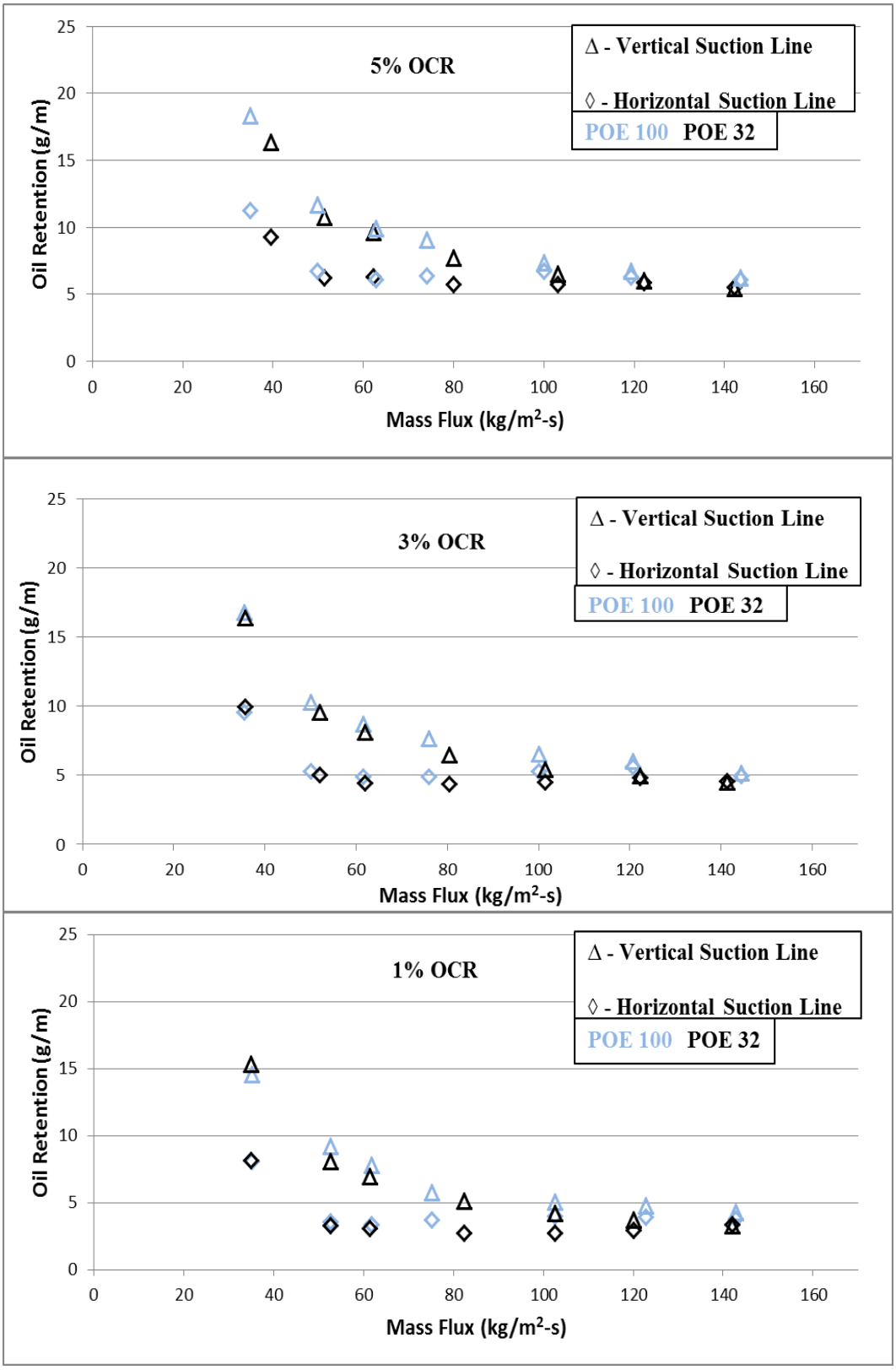

Figure 3.20 Effect of lubricant viscosity on oil retention for R1234yf at 3 OCR values

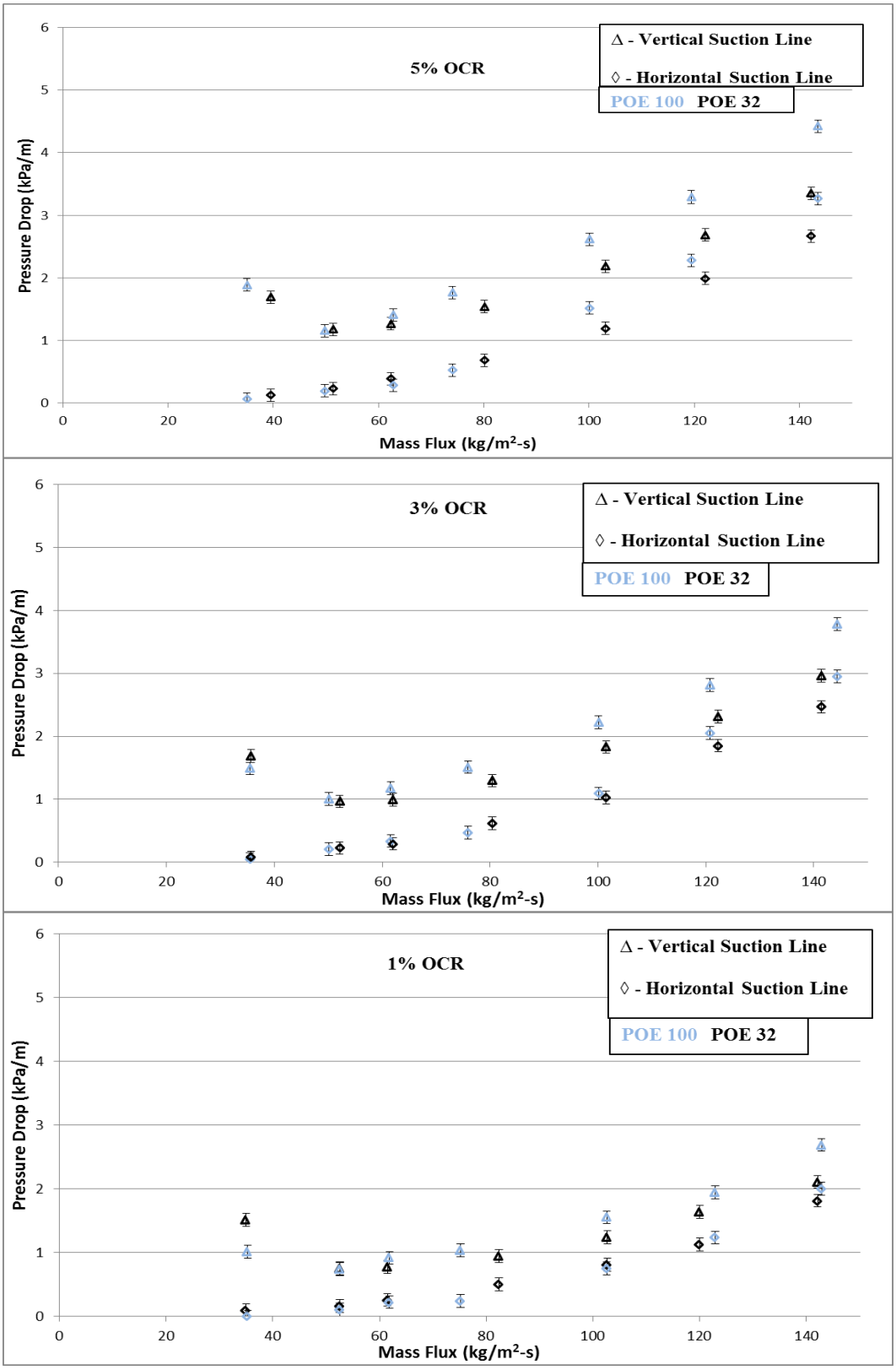

Figure 3.21 Effect of lubricant viscosity on pressure drop for R1234yf at 3 OCR values

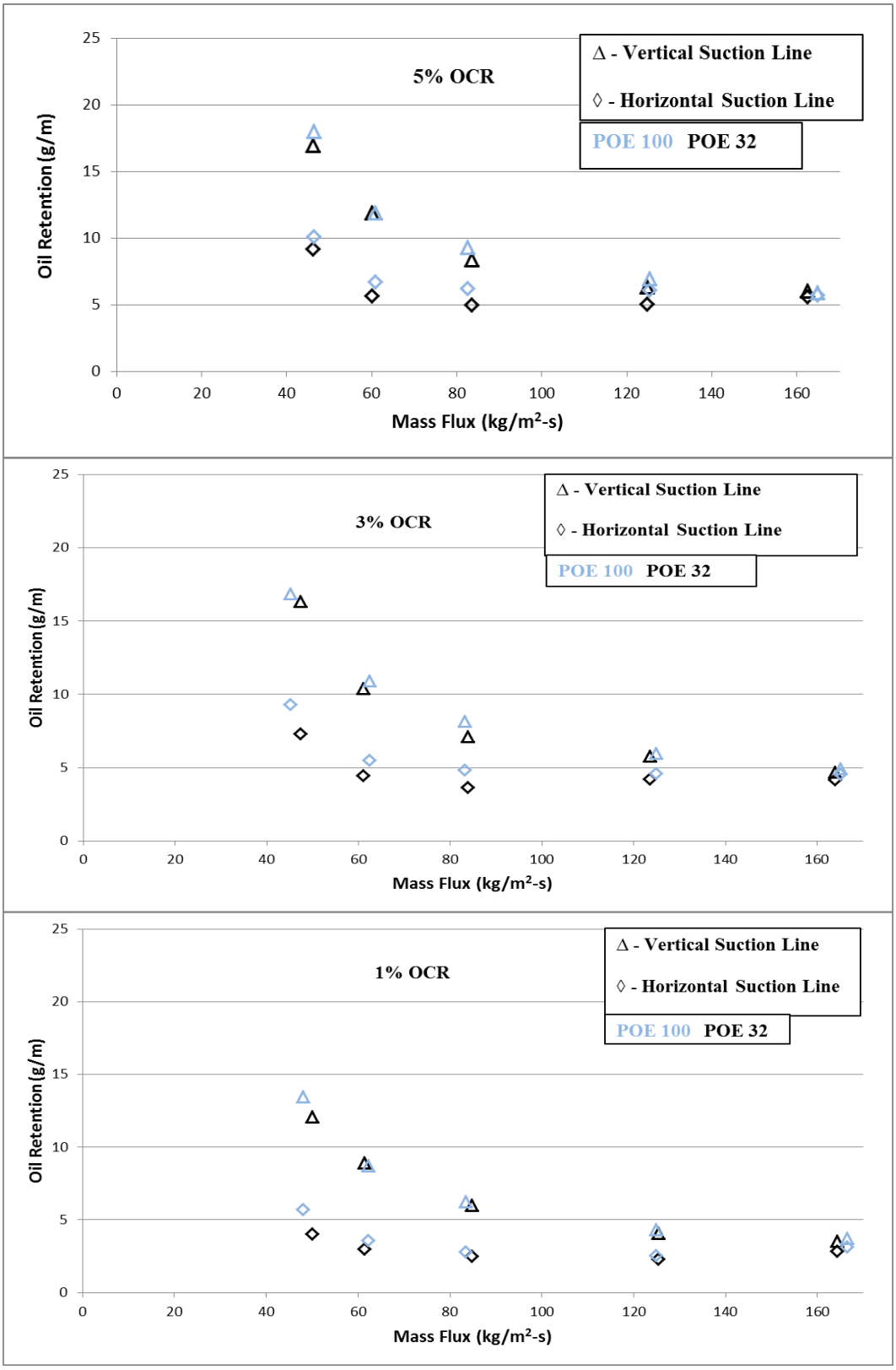

Figure 3.22 Effect of lubricant viscosity on oil retention for R410A at 3 OCR values

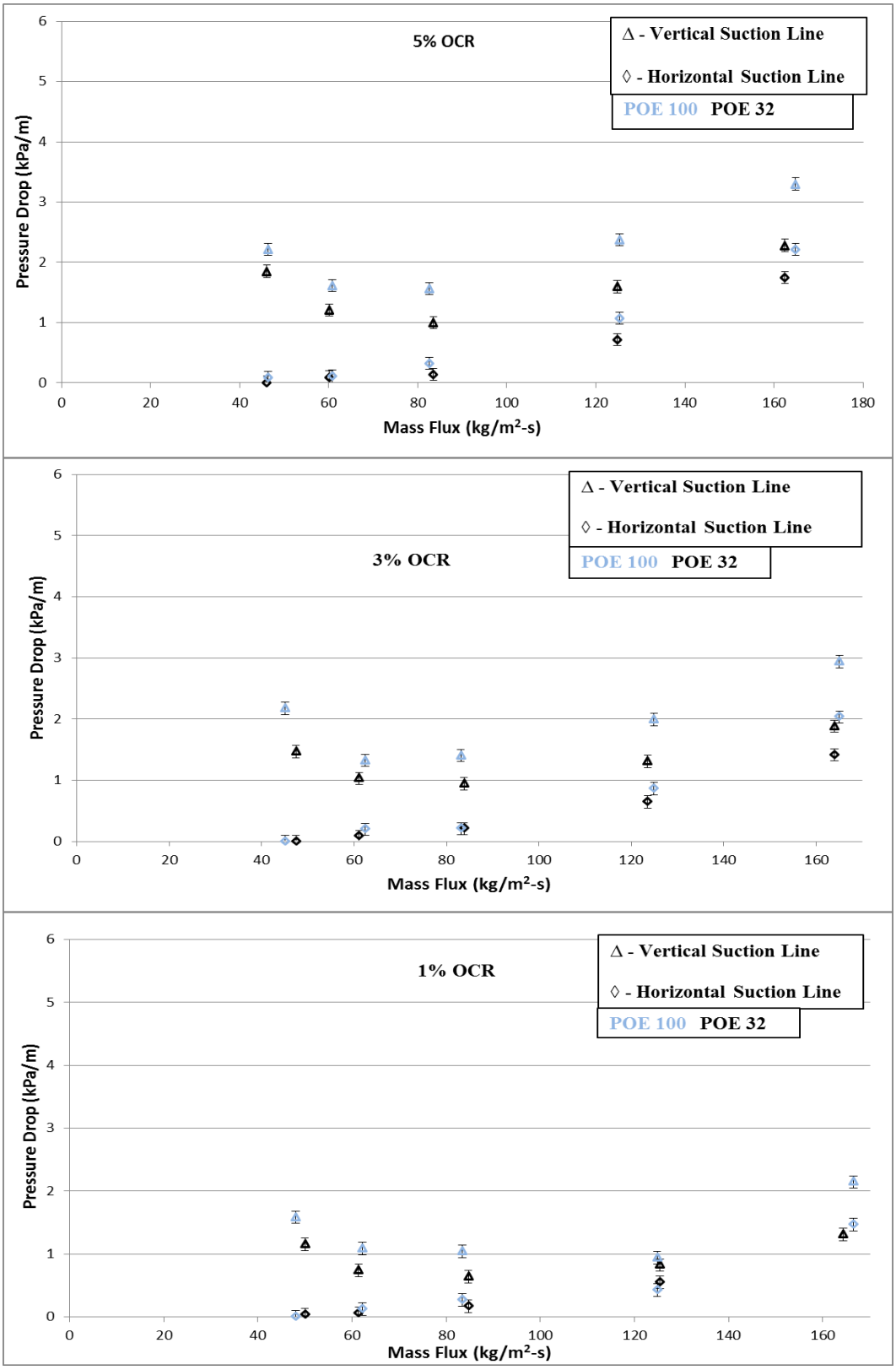

Figure 3.23 Effect of lubricant viscosity on pressure drop for R410A at 3 OCR values

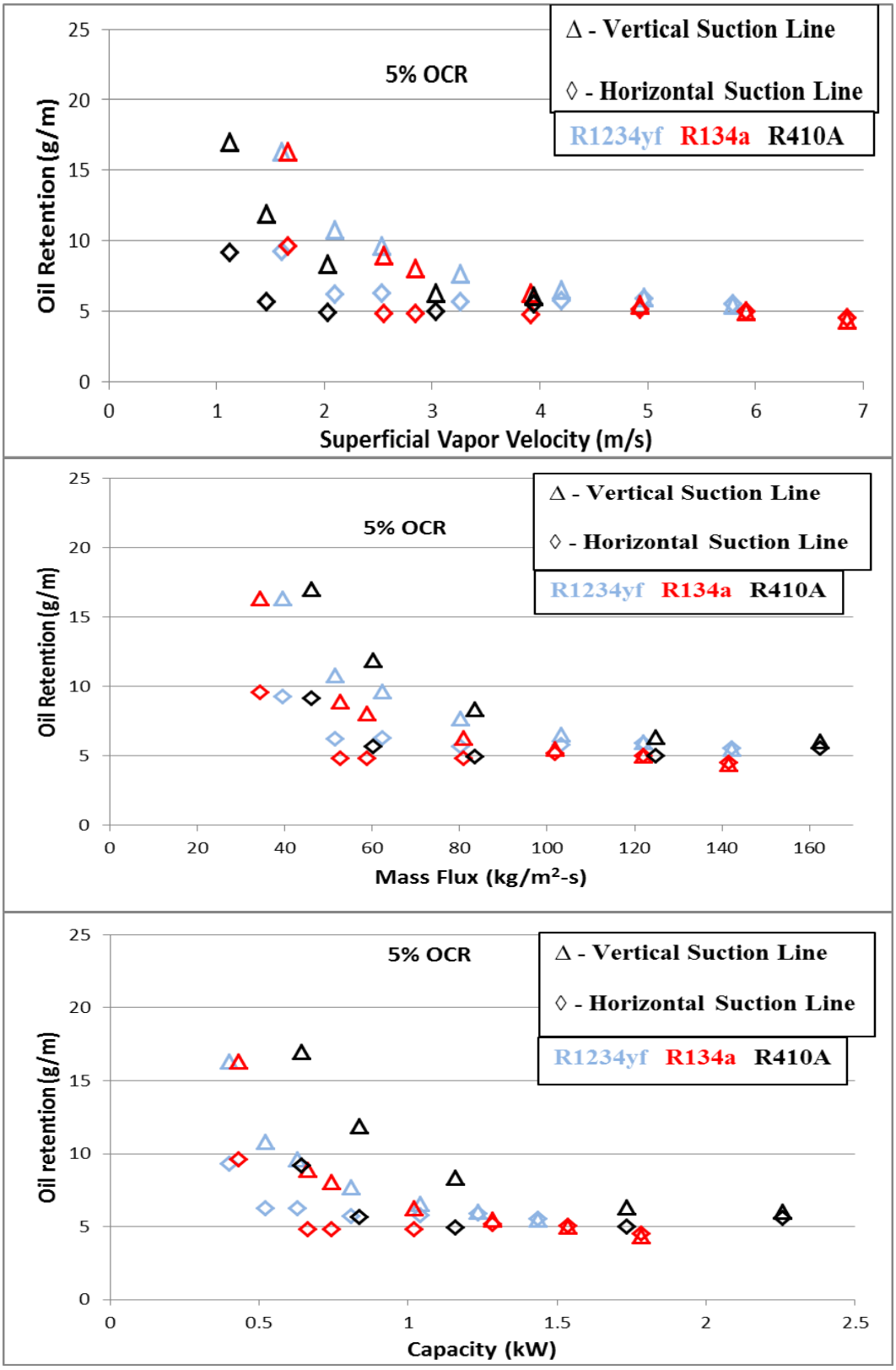

Figure 3.24 Comparison of Oil Retention in R1234yf, R134a and R410A with POE 32 at 5 % OCR

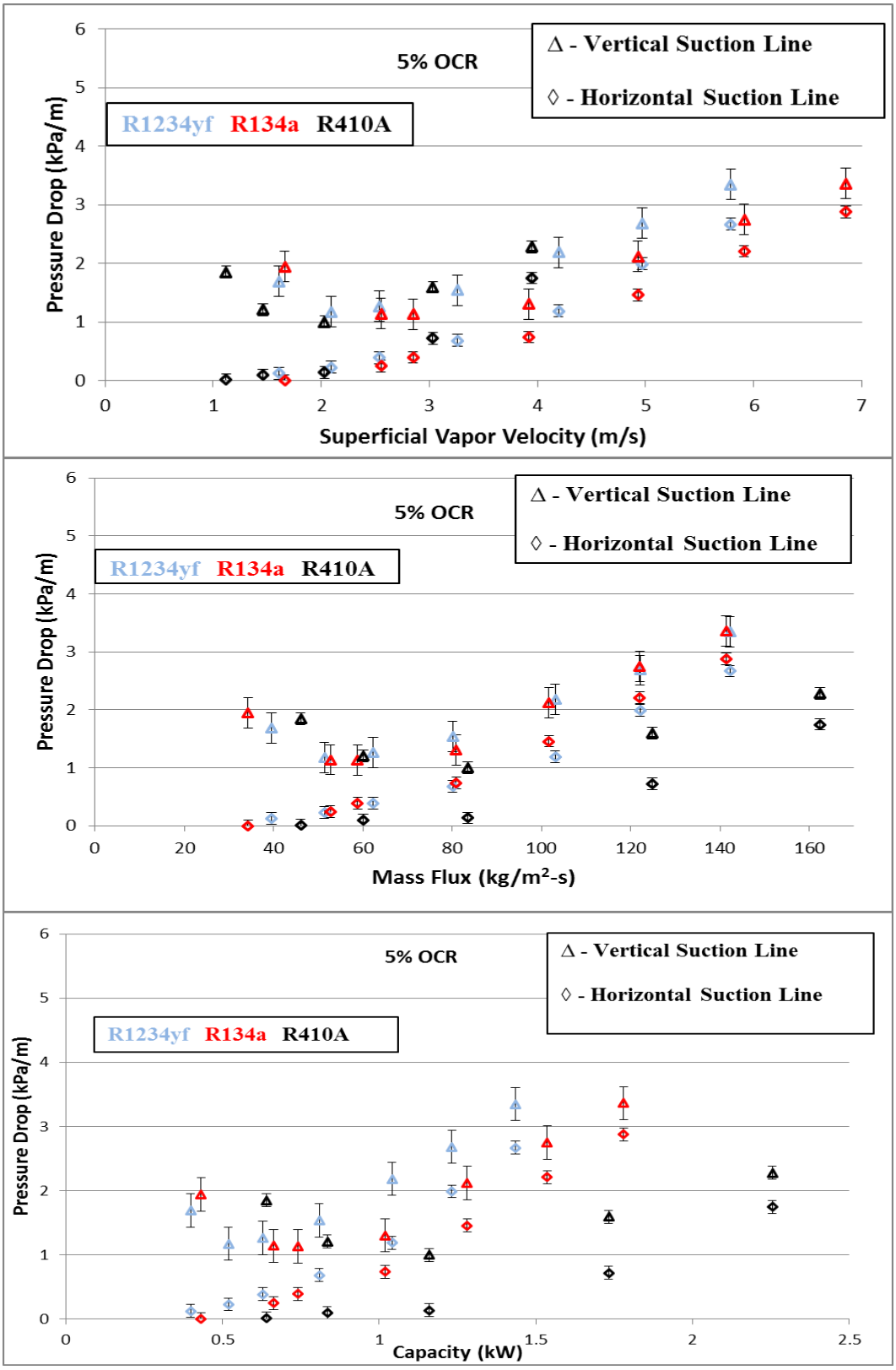

Figure 3.25 Comparison of Pressure Drop in R1234yf, R134a and R410A with POE 32 at 5 % OCR

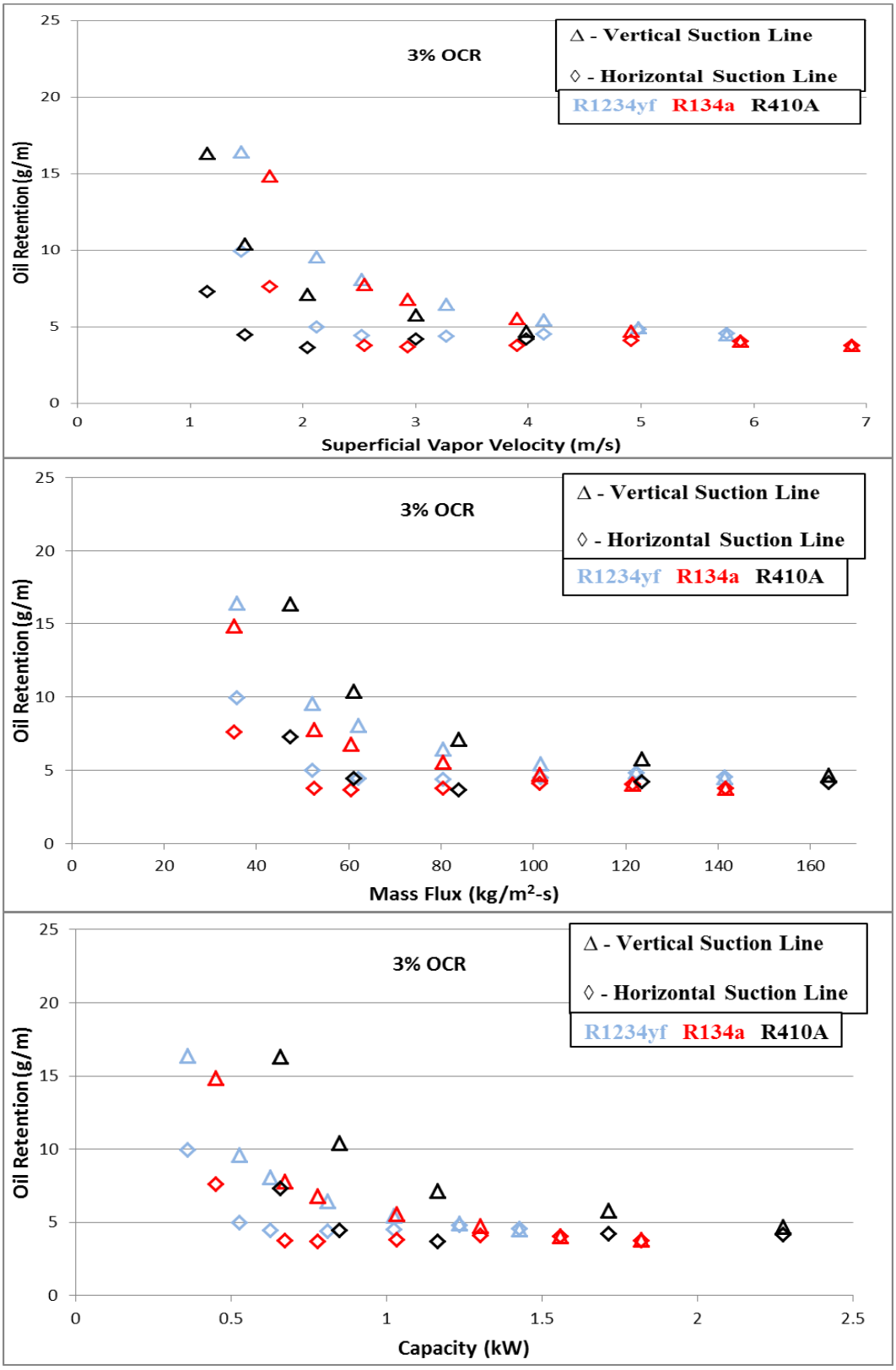

Figure 3.26 Comparison of Oil Retention in R1234yf, R134a and R410A with POE 32 at 3 % OCR

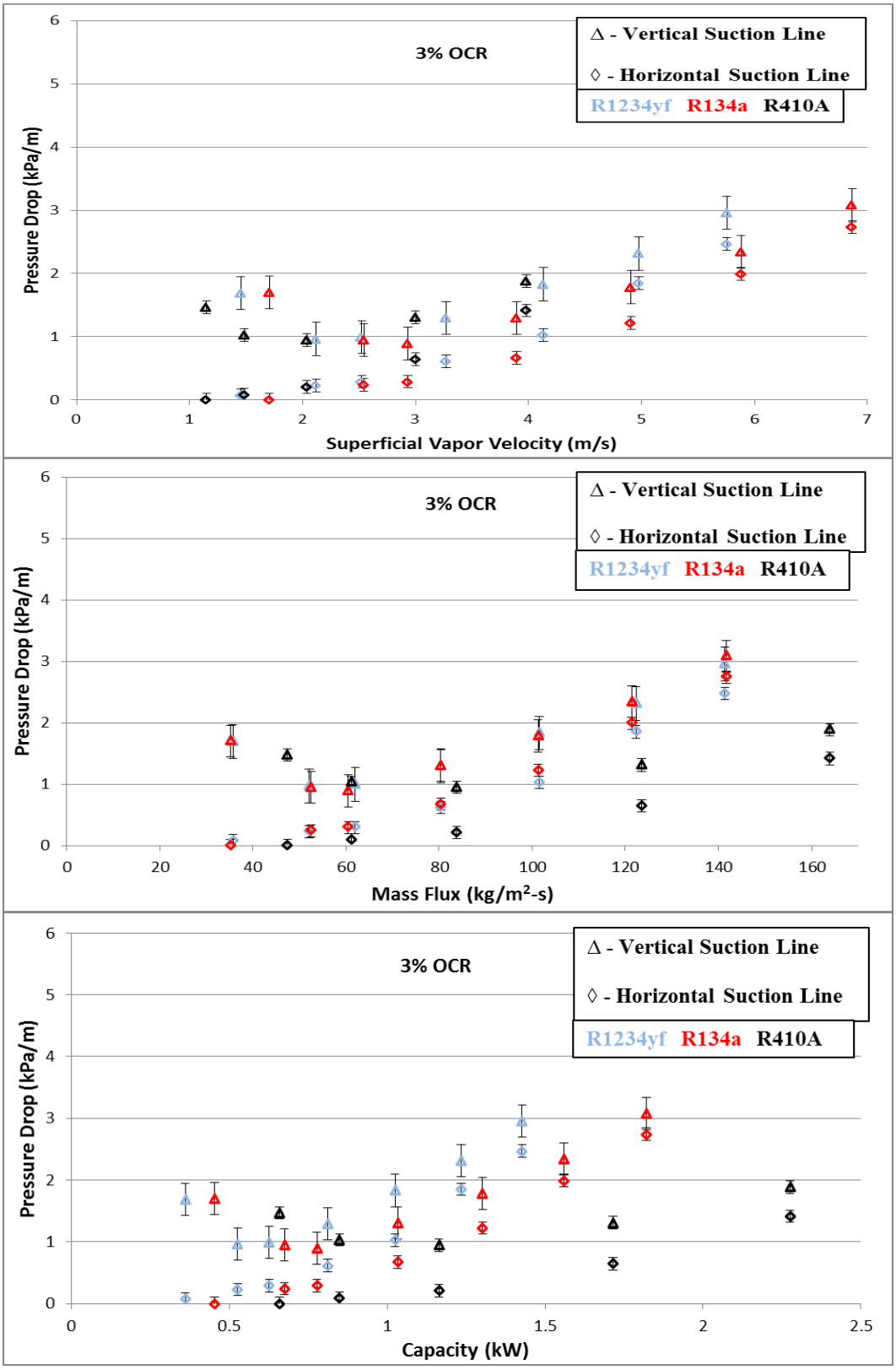

Figure 3.27 Comparison of Pressure Drop in R1234yf, R134a and R410A with POE 32 at 3 % OCR

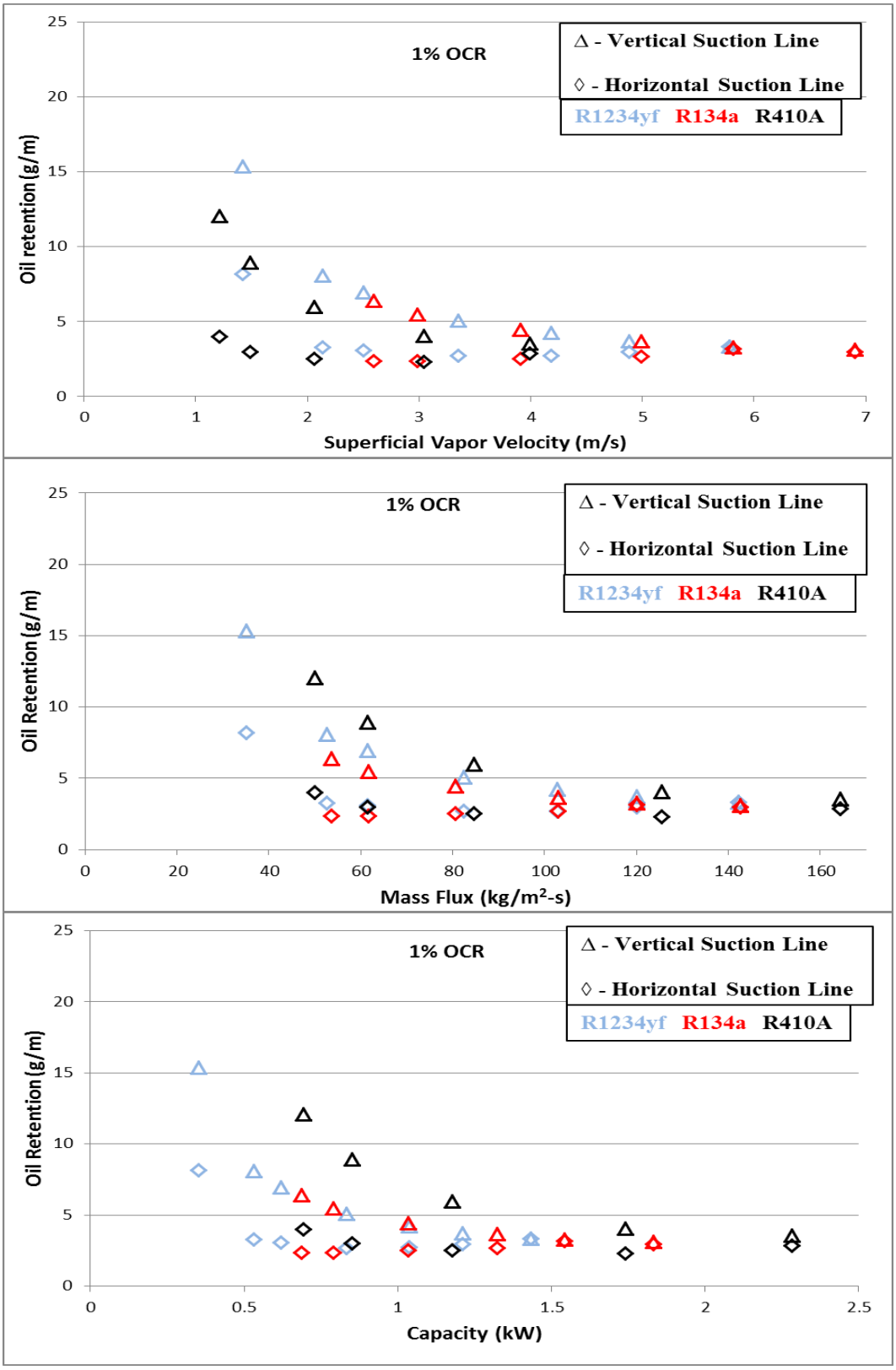

Figure 3.28 Comparison of Oil Retention in R1234yf, R134a and R410A with POE 32 at 1 % OCR

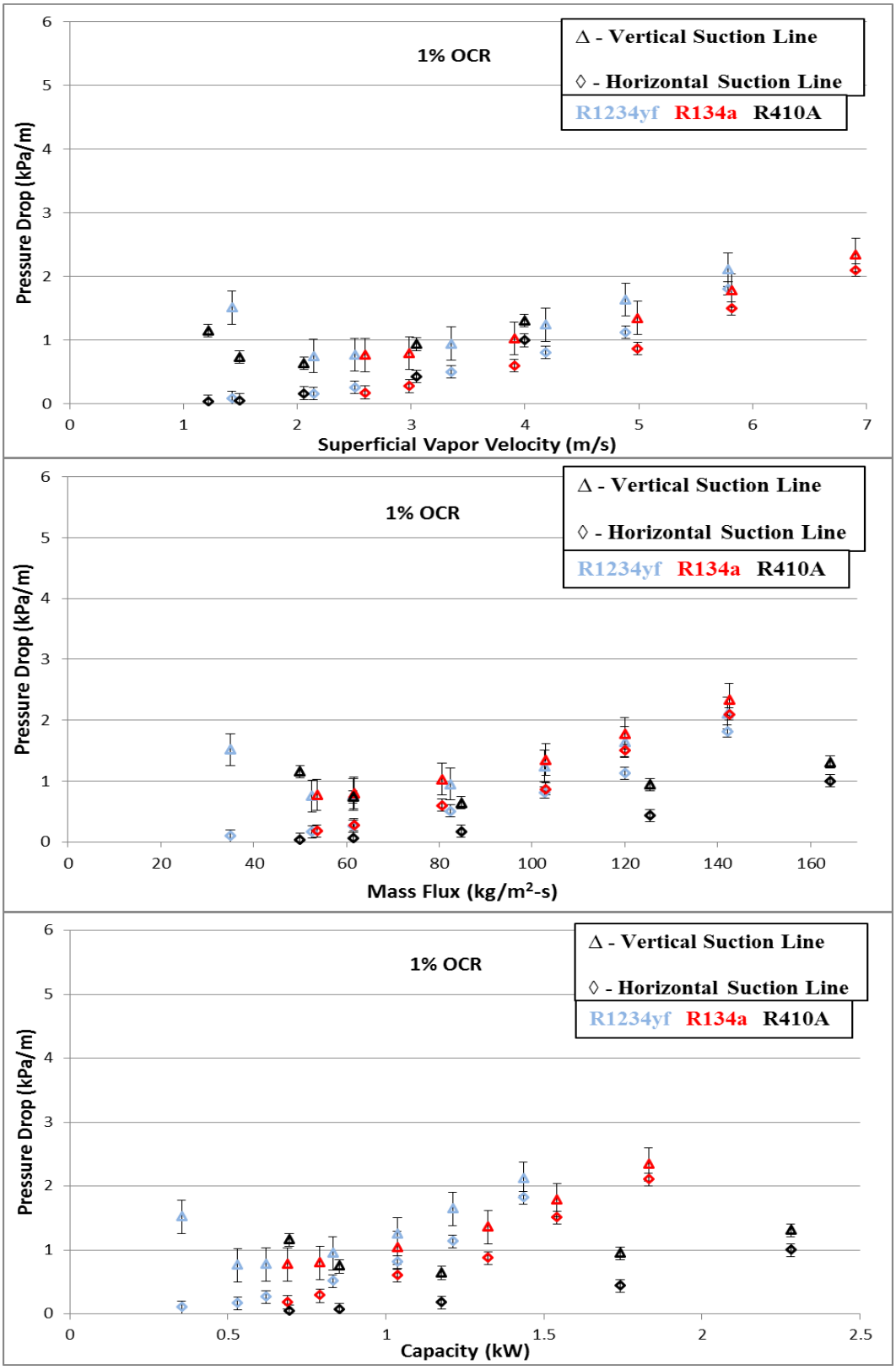

Figure 3.29 Comparison of Pressure Drop in R1234yf, R134a and R410A with POE 32 at 1 % OCR

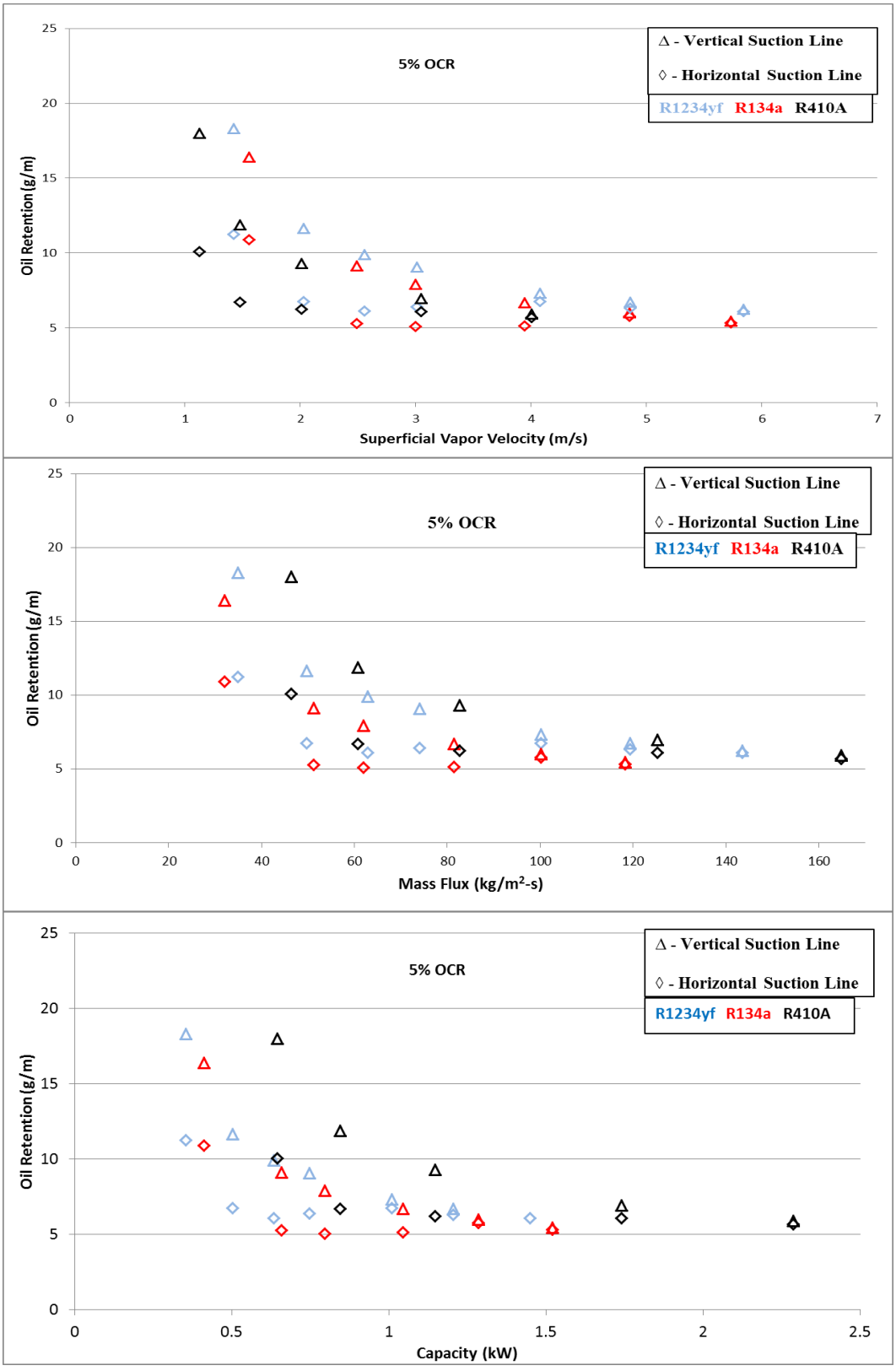

Figure 3.30 Comparison of Oil Retention in R1234yf, R134a and R410A with POE 100 at 5 % OCR

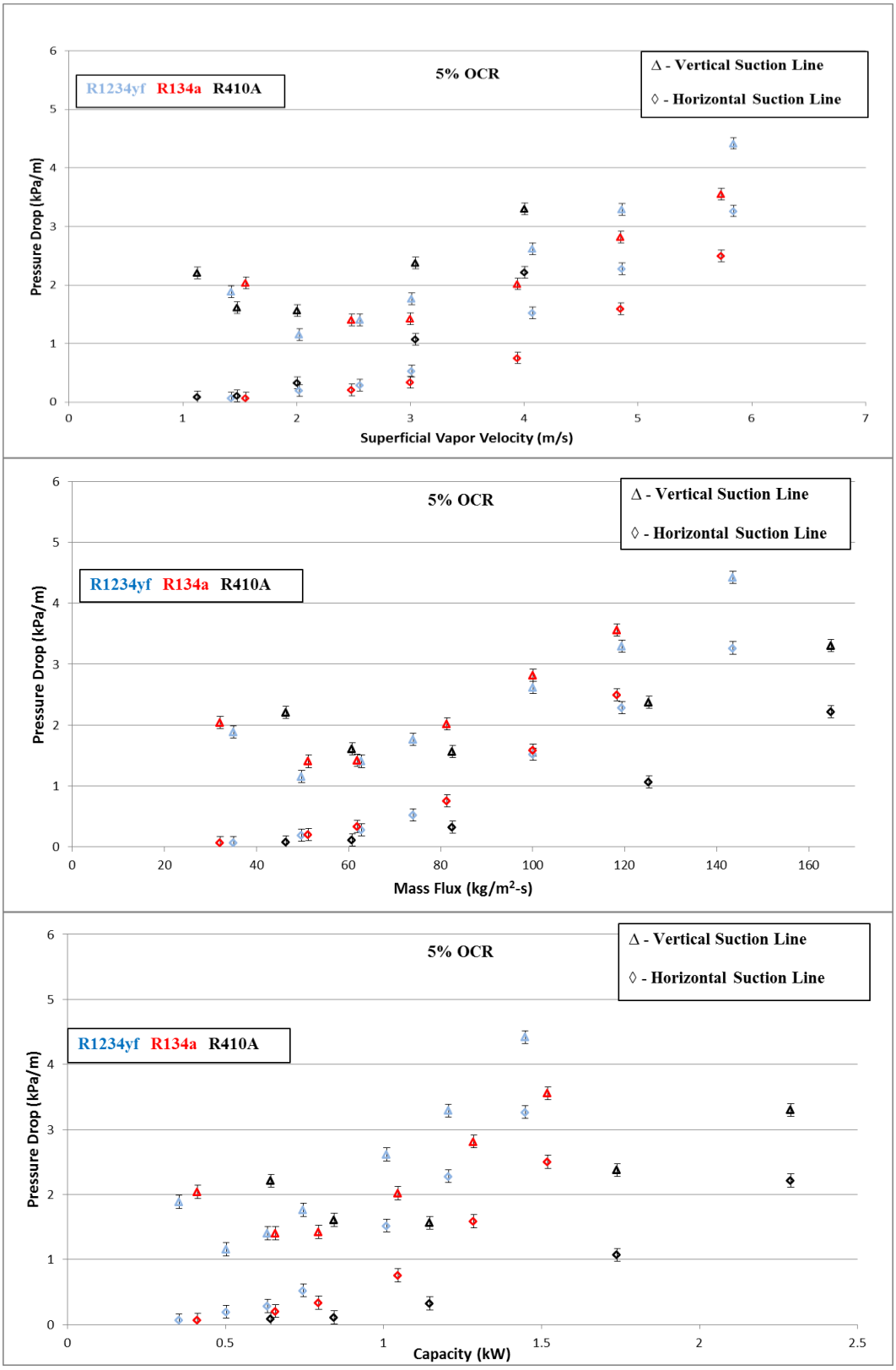

Figure 3.31 Comparison of Pressure Drop in R1234yf, R134a and R410A with POE 100 at 5 % OCR

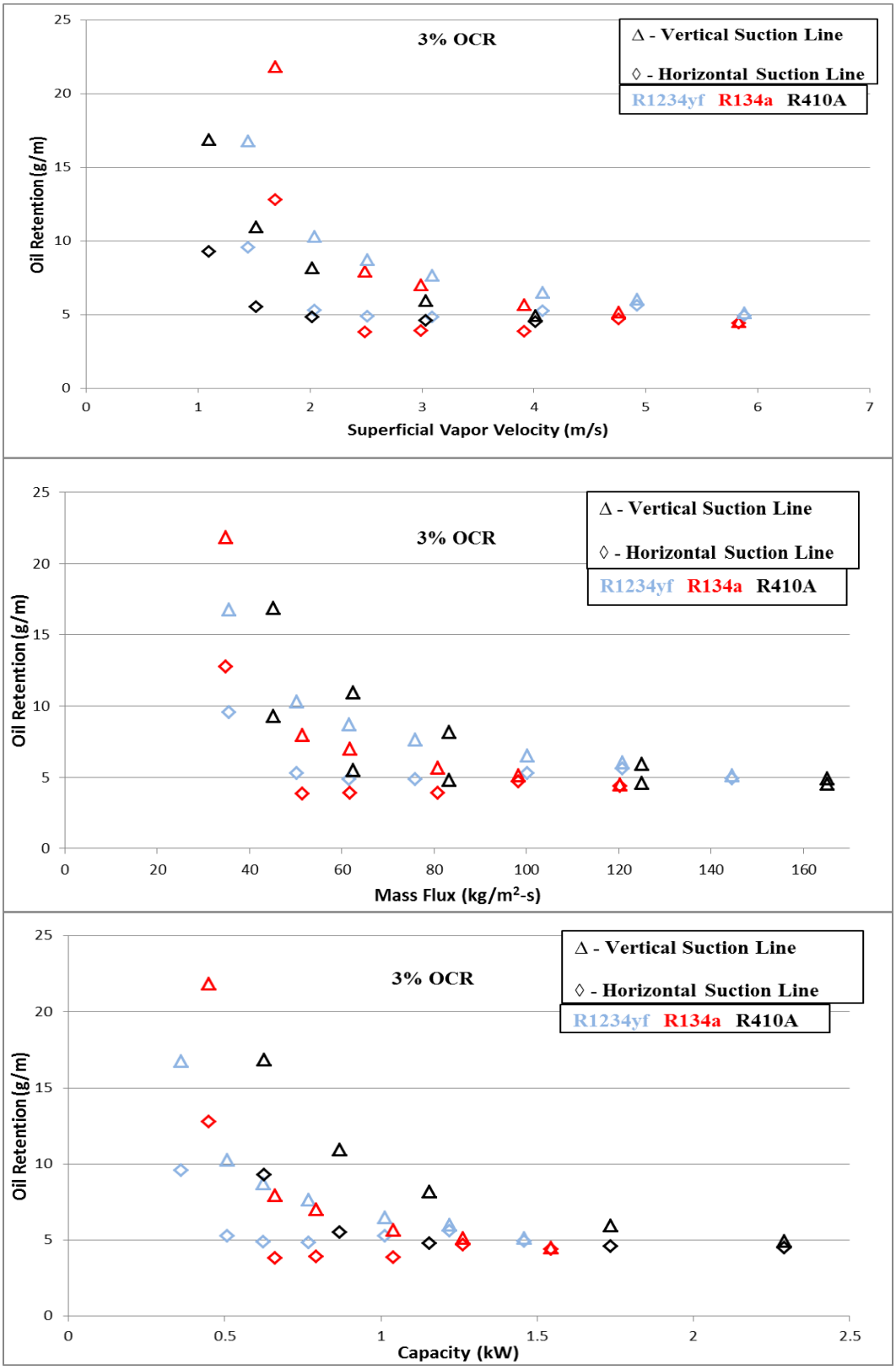

Figure 3.32 Comparison of Oil Retention in R1234yf, R134a and R410A with POE 100 at 3 % OCR

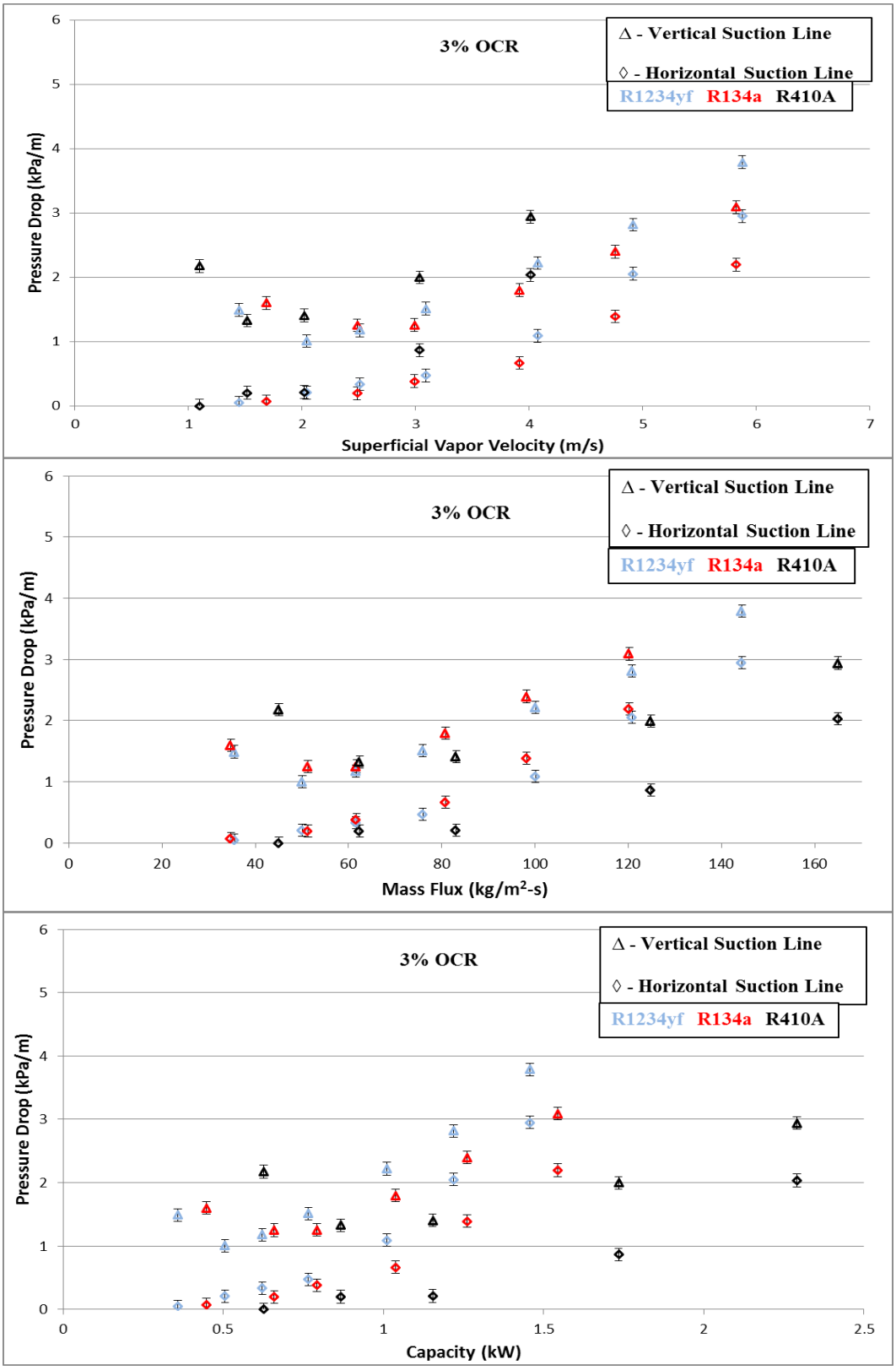

Figure 3.33 Comparison of Pressure Drop in R1234yf, R134a and R410A with POE 100 at 3 % OCR

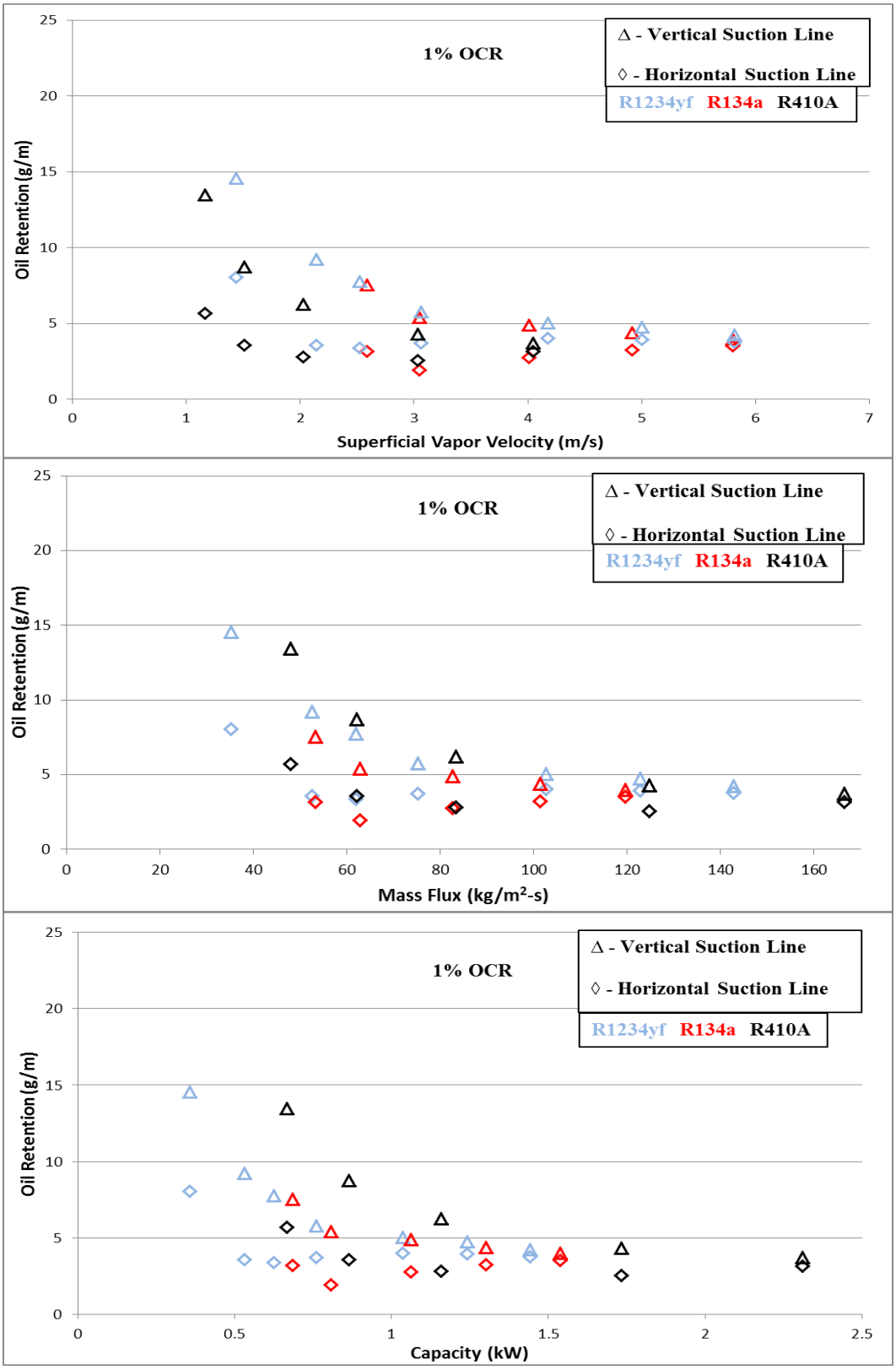

Figure 3.34 Comparison of Oil Retention in R1234yf, R134a and R410A with POE 100 at 1 % OCR

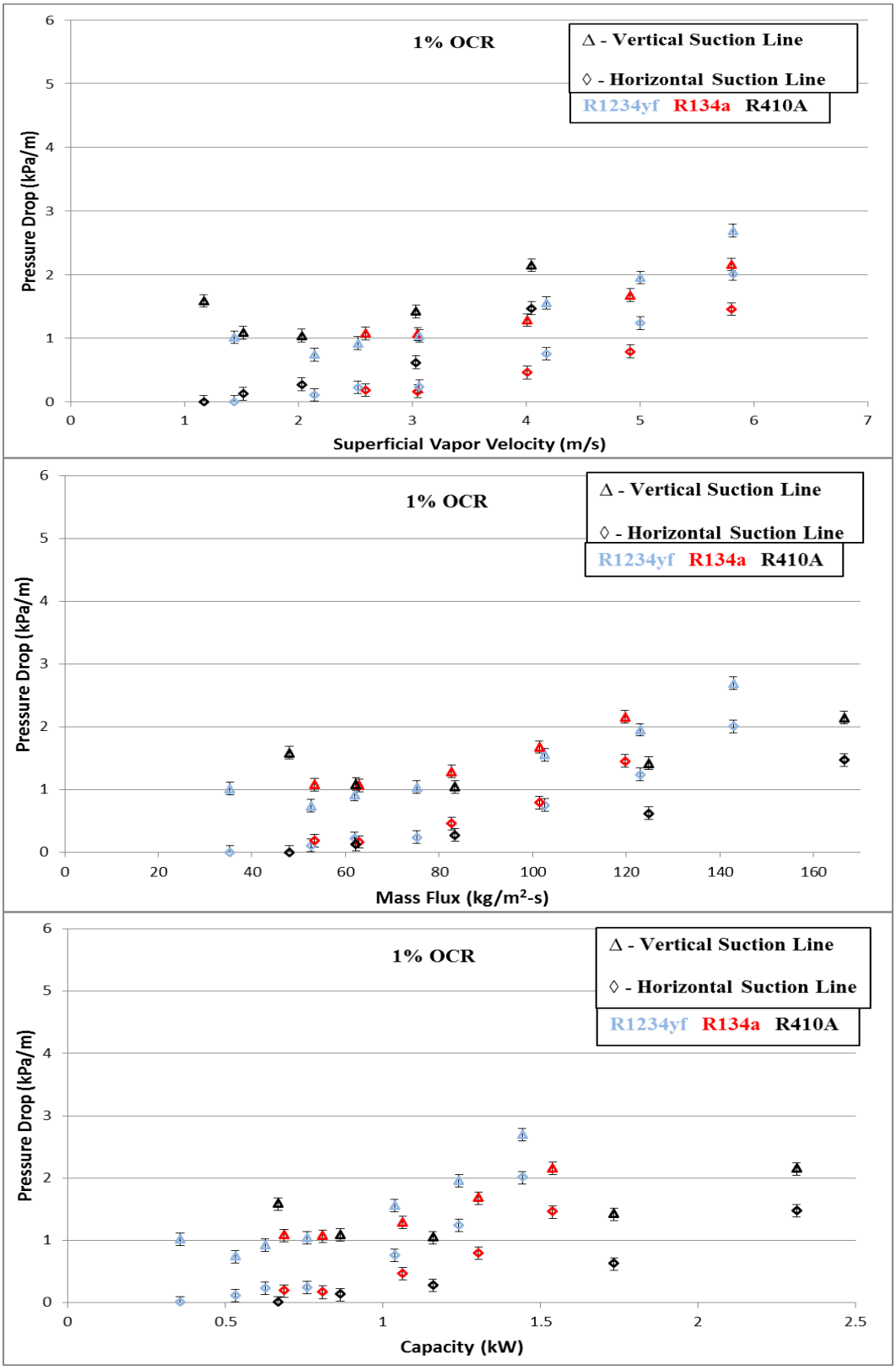

Figure 3.35 Comparison of Pressure Drop in R1234yf, R134a and R410A with POE 100 at 1 % OCR

CHAPTER 4- PREDICTION OF OIL RETENTION AND PRESSURE DROP IN VERTICAL SUCTION LINES

Predicting oil retention and pressure drop in suction lines for annular flows is very crucial, so that one may have prior knowledge of these parameters. On knowing oil retention and pressure drop, the goal of any system designer would be to minimize them, thereby improving system performance and efficiency. In almost all modeling studies, the suction line under consideration is the vertical line, since it possesses a higher oil retention and pressure drop in comparison to the horizontal suction line. In the scope of the current study, system performance improvement may be achieved by designing or sizing the suction lines in a better manner based on an optimal refrigerant mass flux, where oil retention and pressure drop are minimal. This chapter seeks to present such a model in which the effect of refrigerant mass flux, OCR, lubricant viscosity and superheat are included. The flow regime under consideration is annular, since that is the regime of operation that is preferred due to the lower oil retention and pressure drop observed in comparison to the churn flow regime.

4.1 Model Background

A semi-empirical mathematical model was developed in order to predict oil retention and pressure drop in vertical suction lines. The basic principle of the model has been employed in many previous works. Lee (2001) presented the approach that will be employed in the current work. The cylindrical Navier-Stokes equation was applied for the annular liquid film, from which the liquid film mass flow rate was obtained by means of integrating over the annular area as well as by applying boundary conditions. This mass flow rate was implicitly related to the pressure drop, the liquid-vapor interfacial shear stress and the annular liquid film thickness. The pressure drop was related to the interfacial shear stress by means of a momentum balance

performed on the vapor core. Finally the interfacial shear stress was related to the liquid film thickness by means of an interfacial friction factor correlation. It is this friction factor correlation that varies in different research works. The current work presents a new interfacial friction factor correlation that has incorporated data for mixtures including refrigerants R134a, R1234yf and R410A refrigerants, while POE 32 and POE 100 lubricants have been employed. The set of equations obtained were implicit in nature and were solved by employing the Engineering Equation Solver (EES), which has property databases for all refrigerants employed (F-Chart 2010). In general, refrigerant-oil mixture properties were taken from the ASHRAE 2002 Refrigeration Handbook.

4.1.1 Model Assumptions

The current model required certain assumptions that had to be made in order to simplify it, without compromising the underlying physical phenomenon that takes place in the multiphase flow.

- The annular liquid film was assumed to be of a constant thickness over the entire tube length as well as over the entire duration of data measurement. Thus the film thickness that is found in the model is essentially a time and space averaged value. As a consequence of this assumption, the void fraction of the flow is assumed to be constant.
- The flow was assumed to be steady, fully developed and adiabatic in nature. Tests were carried out in such a manner that nominally steady state conditions were achieved before recording data. Sufficient development pipe length was also provided so that the flow was both hydrodynamically as well as thermally developed before entering the suction lines.
- Oil droplet entrainment into the vapor core was also neglected.

- The flow was assumed to be axisymmetric.
- Flow is also considered to be incompressible in nature.

4.2 Model Derivation

This section describes in detail the various equations in the proposed mathematical model. Governing equations are presented with appropriate boundary conditions applied when required. Figure 4.1 represents the realistic depiction of annular flow in a vertical suction line. On applying the assumption of a constant annular film thickness, the flow problem may be represented diagrammatically as in Figure 4.2. The upward flow direction is represented by the z co-ordinate while the radial direction is represented by the r co-ordinate. Due to the assumed symmetry of the flow, the θ co-ordinate is not of relevance in the current analysis.

4.2.1 Application of Navier-Stokes Equation to the Annular Liquid Film

The continuity equation in cylindrical co-ordinates is represented as

$$\frac{\partial \rho}{\partial t} + \frac{1}{r}\frac{\partial}{\partial r}(\rho r v_r) + \frac{1}{r}\frac{\partial}{\partial \theta}(\rho v_\theta) + \frac{\partial}{\partial z}(\rho v_z) = 0 \tag{4.1}$$

For a flow that is axisymmetric, steady and incompressible and fully developed in the direction of flow, equation (4.1) reduces into

$$\frac{\partial}{\partial r}(r v_r) = 0 \tag{4.2}$$

Equation (4.2) on integration yields

$$r v_r = C \tag{4.3}$$

C is the constant of integration, which is evaluated by means of the no slip condition, such that the radial velocity of the liquid film is zero at the tube wall.

$$(rv_r)|_{r=R} = R \times (v_r)|_{r=R} = 0 \tag{4.4}$$

This implies that the radial velocity is zero in the entire annular film thickness.

$$v_r = 0, \forall R - \delta \le r \le R \tag{4.5}$$

On applying the momentum equation in the z direction, which is the direction of flow for the liquid film, we have

$$\rho\left(\frac{\partial v_z}{\partial t} + v_r \frac{\partial v_z}{\partial r} + \frac{v_\theta}{r}\frac{\partial v_z}{\partial \theta} + v_z \frac{\partial v_z}{\partial z}\right) = \frac{\partial p}{\partial z} - \left[\frac{1}{r}\frac{\partial}{\partial r}(r\tau_{rz}) + \frac{1}{r}\frac{\partial}{\partial \theta}\tau_{\theta z} + \frac{\partial}{\partial z}\tau_{zz}\right] + \rho_l g_z \tag{4.6}$$

On expanding the shear stress term and applying the necessary boundary conditions equation (4.6) reduces into

$$\frac{\mu_l}{r}\frac{d}{dr}\left(r\frac{dv}{dr}\right) = \frac{dP}{dz} + \rho_l g_z \tag{4.7}$$

This on integration over r yields

$$\mu_l r\left(\frac{dv}{dr}\right) = \left(\frac{dP}{dz} + \rho_l g_z\right)\frac{r^2}{2} + A \tag{4.8}$$

A is the constant of integration.

From Newton's Law of viscosity, we have

$$\tau_{rz} = \tau = -\mu_l\left(\frac{\partial v_r}{\partial z} + \frac{\partial v_z}{\partial r}\right) = -\mu_l \frac{\partial v}{\partial r} \tag{4.9}$$

Plugging equation (4.9) into equation (4.8), we get

$$-\tau.r = \left(\frac{dP}{dz} + \rho_l g_z\right)\frac{r^2}{2} + A \tag{4.10}$$

The primary boundary condition that has to be applied here is to designate the shear stress at the vapor core – liquid film interface to be the interfacial shear stress, τ_i. Thus we have the boundary condition that at $r = R - \delta$, $\tau = \tau_i$. Equation (4.10) thus becomes

$$-\tau_i.(R-\delta) = \left(\frac{dP}{dz} + \rho_l g_z\right)\frac{(R-\delta)^2}{2} + A \tag{4.11}$$

The constant of integration A may be eliminated by subtracting equation (4.10) from equation (4.11), which after rearrangement gives

$$\tau = \tau_i \frac{(R-\delta)}{r} - \frac{1}{2}\left(\frac{dP}{dz} + \rho_l g_z\right)\left(\frac{r^2 - (R-\delta)^2}{r}\right) \tag{4.12}$$

Substituting equation (4.9) in equation (4.12) for the shear stress to give

$$-\mu_l \frac{dv}{dr} = \tau_i \frac{(R-\delta)}{r} - \frac{1}{2}\left(\frac{dP}{dz} + \rho_l g_z\right)\left(\frac{r^2 - (R-\delta)^2}{r}\right) \tag{4.13}$$

In order to get an expression for the velocity profile across the annular film thickness, we integrate equation (4.13) with respect to r in order to get

$$-\mu_l v = \tau_i (R-\delta)\ln r - \frac{1}{2}\left(\frac{dP}{dz} + \rho_l g_z\right)\left(\frac{r^2}{2} - (R-\delta)^2 \ln r\right) + B \tag{4.14}$$

The constant of integration B was again eliminated by applying the no slip condition $v\ (r=R) = 0$ to give

$$B = -\tau_i (R-\delta)\ln R + \frac{1}{2}\left(\frac{dP}{dz} + \rho_l g_z\right)\left(\frac{R^2}{2} - (R-\delta)^2 \ln R\right) \tag{4.15}$$

Substituting for B in equation (4.14), we get on rearrangement the liquid film velocity profile as

$$v = \frac{1}{\mu_l}\left[\left(\tau_i (R-\delta) + \left(\frac{(R-\delta)^2}{2}\left(\frac{dP}{dz} + \rho_l g_z\right)\right)\right)\ln\frac{R}{r} - \frac{1}{4}\left(\frac{dP}{dz} + \rho_l g_z\right)(R^2 - r^2)\right] \tag{4.16}$$

The annular liquid film mass flow rate was obtained by integrating the velocity profile over the annular film cross-sectional area as follows

$$\dot{m}_l = \int_{R-\delta}^{R}\int_{0}^{2\pi} \rho_l v r dr = \int_{R-\delta}^{R} 2\pi\rho_l v r dr \tag{4.17}$$

Substituting the velocity profile into equation (4.17), the following expression was obtained

$$\dot{m}_l = \frac{2\pi\rho_l}{\mu_l}\left[\left(\tau_i (R-\delta) + \left(\frac{(R-\delta)^2}{2}\left(\frac{dP}{dz} + \rho_l g_z\right)\right)\right)\times\left(\frac{(R^2 - (R-\delta)^2)}{4} - \frac{(R-\delta)^2}{2}\ln\frac{R}{R-\delta}\right)\right] - \frac{\pi\rho_l}{8\mu_l}\left(\frac{dP}{dz} + \rho_l g_z\right)(R^2 - (R-\delta)^2)^2 \tag{4.18}$$

This expression is a function of three unknown components, namely the interfacial shear stress (τ_i), the suction line pressure drop (dp/dz) and annular liquid film thickness (δ). In order to solve for this equation, two more relations which interrelate the mentioned terms are required.

4.2.2 Momentum Balance on the Refrigerant Vapor Core

The momentum balance on the refrigerant core gives rise to the following equation

$$\frac{dP}{dz} + \rho_v g_z + \frac{\tau_i \pi D_c}{A_c} = 0 \tag{4.19}$$

The components of this momentum balance are represented in Figure 4.2. The introduction of the void fraction α yields

$$\frac{dP}{dz} + \rho_v g_z + \frac{4\tau_i}{D\sqrt{\alpha}} = 0 \tag{4.20}$$

where

$$\alpha = \frac{A_c}{A} = \left(\frac{D_c}{D}\right)^2 = \left(\frac{D - 2\delta}{D}\right)^2 \tag{4.21}$$

Equation (4.20) thus relates the pressure drop with the interfacial shear stress. For completing the set of equations, a closure equation is required which relates the interfacial shear stress with the annular liquid film thickness. This is achieved by means of the interfacial friction factor correlation.

4.2.3 Interfacial Friction Factor Correlation

The interfacial friction factor correlation serves as the closure equation for the equations mentioned in the previous sections. There have been many friction factor correlations proposed for annular flow problems that are available in literature. The correlation proposed by Wongwises and Kongkiatwanitch (2001) has been a popular one, having been used in many studies. It relates the smooth pipe friction factor, f_i, with the refrigerant vapor Reynolds number and the dimensionless liquid film thickness. The authors found that the proposed correlation was able to predict their experimental f_i values within ± 25 %. Also, the data employed for this correlation made use of experimental data from air/water mixture flow tests. It has been determined (Lee, 2001) that this correlation was unsuitable for refrigerant/oil mixtures as well as being specifically suitable for flow conditions where liquid film thickness is large and the vapor

Reynolds number is small (Cremaschi, 2004). The Wallis (1969) friction factor correlation has also been found numerous studies, where f_i is expressed as a function of the annular film thickness non-dimensionalized with the pipe diameter, D. As pointed out by Sethi and Hrnjak (2011), it has been ascertained that the Wallis correlation under-predicts f_i for non-dimensional film thicknesses, $\delta/D \geq 0.02$ and over-predicts it for $\delta/D \leq 0.005$ (Belt *et al*., 2009). The current work relates the interfacial friction factor with the vapor core Reynolds number, the liquid film Reynolds number, the non-dimensional film thickness and the mixture Weber number. The form of the correlation is similar to the one described in Asali *et al.* (1985), where the interfacial friction factor is divided by the smooth pipe friction factor (f_s) correlation. Thus when the liquid film thickness goes to zero, f_i will become f_s as expected. Thus the friction factor correlation was of the following form.

$$\frac{f_i}{f_s} = 1 + K\,\mathrm{Re}_{lf}^{a}\,\mathrm{Re}_{v}^{b}\,\delta_{v}^{+c}\,We_{mix}^{d} \tag{4.22}$$

The non-dimensional parameters are defined as follows.

$$f_s = 0.046\,\mathrm{Re}_{v}^{-0.2} \tag{4.23}$$

The smooth pipe friction factor was chosen from Abdolahi *et al.* (2007), which is the Blasius form of the friction factor, following the modified $1/9^{th}$ power law. Also we have

$$\mathrm{Re}_{lf} = \frac{G(1-x)D}{4\mu_l} \tag{4.24}$$

$$\mathrm{Re}_{v} = \frac{GxD}{\mu_v} \tag{4.25}$$

The non-dimensional film thickness is defined similar to that in Sethi and Hrnjak (2011), with the film thickness being normalized by the vapor kinematic viscosity and the friction velocity, v^*.

Thus we have for the non-dimensional film thickness, the following form.

$$\delta_v^+ = \frac{\delta}{\upsilon_v} v^* \tag{4.26}$$

Where we have

$$v^* = \sqrt{\frac{\tau_i}{\rho_v}} \tag{4.27}$$

The mixture Weber number was defined as

$$We_{mix} = \frac{G^2 D}{\sigma_{mix} \rho_l} \tag{4.28}$$

Where σ_{mix} is the mixture surface tension and was computed based on the formulation available in Cremaschi (2004).

$$\sigma_{mix} = \sigma_{ref,liq} + (\sigma_{oil} - \sigma_{ref,liq})\sqrt{w_{local}} \tag{4.29}$$

The pure liquid refrigerant surface tension, $\sigma_{ref,liq}$, is calculated in EES. The pure oil surface tension values, σ_{oil}, are chosen to be the same as described in Cremaschi (2004). The surface tension of pure mineral oil was taken to be 33 mN/m, while POE was assumed to possess a surface tension of 46 mN/m. Thus f_i is related to the interfacial shear τ_i stress by means of the following expression.

$$\tau_i = \frac{1}{2} f_i \rho_v (v_v - v_l)^2 \tag{4.30}$$

Realistically, the liquid film velocity is much smaller than the superficial vapor velocity. Thus in the above expression v_l may be dropped to give

$$\tau_i = \frac{1}{2} f_i \rho_v v_v^2 \tag{4.31}$$

Where

$$v_v = \frac{Gx}{\rho_v \alpha} \tag{4.32}$$

The mixture Weber number was specifically considered in this work to account for the effects of liquid film surface tension on the oil retention and pressure drop. The coefficients in Equation (4.22) were obtained by performing a least square regression analysis fit on the collected experimental data. The data employed for this purpose involved R134a/POE 32, R134a/POE 100, R1234yf/POE 100 and R410A/POE 32. The final correlation that was achieved as a result of modeling was as follows

$$\frac{f_i}{f_s} = 1 + 137240835.2\,\mathrm{Re}_{lf}^{-0.0539}\,\mathrm{Re}_v^{-2.08}\,\delta_v^{+1.0112}\,We_{mix}^{0.864} \tag{4.33}$$

This friction factor model is valid only for upward flow in vertical suction lines, where an annular flow regime is observed. An important aspect of this modeling is the coefficients of the non-dimensional variables that are obtained. Regression analysis software like MS Excel is generally used for this purpose. It is of utmost importance to note that this software does not consider the physics of the problem when it gives output coefficients. Rather these coefficients are presented because they lead to the best R-squared value, thereby giving the best fit for the

data provided. It is the duty of the modeler to make sure that these coefficients make sense physically.

For instance, depending on the data input, the regression analysis occasionally provided coefficients for the liquid film Reynolds number (Re_{lf}) which were positive. Now consider a situation where Re_{lf} is reduced, in a manner that does not change the other non-dimensional variables. From Equation (4.24), the easiest way to decrease Re_{lf} is to increase μ_l. This is similar to switching the lubricant from POE 32 to POE 100, thereby increasing the liquid film viscosity. Experimental results from Chapter 3 have indicated that POE 100 has a larger pressure drop in comparison to POE 32. From Equation (4.20), a larger pressure drop leads to a larger τ_i, which in turn leads to a larger f_i. For a friction factor correlation that is chosen in the form of Equation (4.22), the only possible way for f_i to increase with decreasing Re_{lf} is for the coefficient 'a' to be negative. Though the regression analysis may give an output for 'a' that is positive and has a good fit to the data, it does not make physical sense.

4.3 Model Calculations

The presented model requires certain input parameters in order to compute oil retention and pressure drop in the vertical suction line for annular flow. Conditions of operation like the saturation pressure, superheated evaporator outlet temperature, total mass flux of operation and oil in circulation ratio (OCR) have to be input into the model. Also required are the thermophysical properties of the refrigerant liquid and vapor, the liquid oil as well as the oil-rich liquid mixture at appropriate conditions. Physical dimensions namely the length of the suction line and its diameter should also be defined. The OCR was calculated as described in Zoellick and Hrnjak (2010), with ideal mixing between refrigerant and oil assumed in the oil tank.

The model also required the calculation of the local oil concentration as well as the bulk vapor quality at the evaporator exit. It should be noted that even though superheated conditions are employed, there will always be some refrigerant vapor dissolved in the liquid film, thereby leading to a bulk vapor quality less than one. The local oil concentration was calculated by the methodology that was initially proposed by Takaishi and Oguchi (1987) for R22/AB oil, which was further extended to different refrigerant/oil mixtures by Thome (1995). The main equations employed in calculating the local oil concentration are

$$T_{bub} = \frac{A(w_{local})}{\ln(P_{sat}) - B(w_{local})} \tag{4.34}$$

$$A(w_{local}) = a_0 + a_1 w_{local} + a_2 w_{local}^3 + a_3 w_{local}^5 + a_4 w_{local}^7 \tag{4.35}$$

$$B(w_{local}) = b_0 + b_1 w_{local} + b_2 w_{local}^3 + b_3 w_{local}^5 + b_4 w_{local}^7 \tag{4.36}$$

a_1 = 182.52 b_1 = -0.72212

a_2 = -724.21 b_2 = 2.3914

a_3 = 3868 b_3 = -13.779

a_4 = -5268.9 b_4 = 17.066

The values of a_0 and b_0 are computed by using Equation (4.34) along with a pure refrigerant vapor pressure equation for the system pressure. Consequently the vapor quality was calculated by using the following equation

$$w_{local} = \frac{OCR}{1 - x} \tag{4.37}$$

The equations described in Sections 4.1 and 4.2 are sets of implicit equations, which yield the vertical suction line pressure drop and the annular liquid film thickness. The mass of oil retained in the vertical suction line is computed based on the liquid film thickness.

$$m_{oil} = w_{local}.2\pi R\delta L\rho_l \tag{4.38}$$

4.4 Model Validation

The proposed model was validated by means of various experimental data for both oil retention and pressure drop, as shown in Figures 4.3 and 4.4 respectively. Experimental data from Sethi and Hrnjak (2011) for R134a/POE 32 in a 10.2 mm diameter suction line was employed. Similarly data from Zoellick and Hrnjak (2010) for R410A/POE 32 in a 7.1 mm suction line was used. Data from the current experimental work, namely R134a/POE 100 and R1234yf/POE 100 is also shown. More than 90 % of the oil retention data was predicted within a limit of ± 35 % from the experimental values, while more than 90% of the pressure drop data was predicted within a limit of ± 40 % from experimental data. Data from Cremaschi (2004) is also represented in the same validation. It can be observed that this data is not well predicted by the model. A possible explanation for this may the difference in methodology by which the experiments were performed. The current work, along with that of Sethi and Hrnjak (2011) and Zoellick and Hrnjak (2010) employed direct measurement technique, while Cremaschi (2004) used injection-separation method.

Figure 4.5 shows the variation of oil retention with respect to mass flux for both experimental data and model predictions for R134a/POE 32. The effect of OCR is included as well. Figure 4.6 shows the variation of pressure drop with mass flux in R134a/POE 32, including the effects of OCR. Figure 4.7 shows the variation of oil retention with OCR at different mass flux conditions

for R134a/POE 32. The conditions of operation were a saturation temperature of 13 °C with a superheat of 15 °C. In general, the current model captures the trend of oil retention and pressure drop variation with mass flux, especially at high mass flux values where the flow regime is annular in nature. It can be seen that the model over-predicts the oil retention at non-annular flow conditions. Similar plots are shown for R410A/POE 32 in Figures 4.8 to 4.10, where a saturation temperature of 12 °C and a superheat of 15 °C were maintained in a suction line of an internal diameter of 7.1 mm. Plots for R1234yf/POE 100 are shown in Figures 4.11 and 4.13.

This model was validated in the following limits for the vertical suction line:

- $0.01 \leq \delta/D \leq 0.08$
- $0.25 \leq Re_{lf} \leq 7$
- $35{,}000 \leq Re_{v} \leq 140{,}000$
- $0.2 \leq We_{mix} \leq 11.2$

4.5 Parametric Study

4.5.1 Effect of Vertical Suction Line Diameter

The effect of the vertical suction line diameter on oil retention and pressure drop is observed in Figure 4.14. Calculations were made for R134a/POE 100 mixture, with a condensing temperature of 40 °C and a sub-cooling of 5 °C, while the evaporator temperature was 10 °C with a superheat of 10 °C. These conditions were chosen to replicate similar conditions that are observed in mini-split air-conditioning systems. Similarly, an OCR of 0.2 % was chosen for a system condensing capacity of 3 Tons (10.6 kW). The suction line inner diameter was varied from 10 to 50 mm. The model shows that the optimum suction line diameter is between 20-30 mm. Below a diameter of 20 mm, the pressure drop increases enormously while above 30 mm

diameter, the oil retention value becomes very high. At a given OCR value, the pressure drop increases with decrease in suction line diameter due to increase in superficial vapor velocity, which in turn increases the frictional component of pressure drop. Also, as the suction line diameter increases, the vapor velocity reduces which in turn leads to an increase in the amount of oil retained.

4.5.2 Effect of Degree of Superheat

Figure 4.15 shows the effect of the degree of superheat on oil retention and pressure drop. Results are shown for a mass flux of 300 kg/m^2-s, while the other parameters remained the same as described in the previous section. The degree of superheat was varied between 5-35 °C, while the suction line diameter was maintained at a standard dimension of 5/8 inches (16 mm). It can be observed that both the oil retention and pressure drop increase with an increase in superheated temperature. This is because an increase in superheat leads to an increase in the mixture viscosity of the annular liquid film, since more refrigerant is driven out of the liquid mixture. Higher viscosity of the liquid film leads to an increased liquid film thickness. This consequently leads to an increase in oil retention as well as pressure drop.

4.5.3 Effect of Cooling Capacity

Figure 4.16 shows the effect of system cooling capacity on oil retention and pressure drop. Similar conditions are employed for the variation, with a superheat of 10 °C used. The cooling capacity was varied from 0.3 Tons upto 3 Tons capacity, which translated into 1-10.6 kW capacity. The oil retention can be seen to increase with a decrease in system cooling capacity, due to a reduction in mass flux. For a capacity less than 2.92 kW, the oil retention increases by a very large amount, indicating the onset of flow reversal in the annular liquid film. The pressure drop is also seen to increase when the capacity is reduced below 2.92 kW, due to increase in

hydrostatic component of pressure drop. At the Jacobs critical mass flux limit, both the oil retention and pressure drop have extremely large values. This clearly illustrates that the Jacobs mass flux is unsuitable for designing vertical suction lines.

4.6 Critical Refrigerant Mass Flux Prediction

It has been established from Zoellick and Hrnjak (2010) that the Jacobs critical refrigerant mass flux is highly unsuitable for designing vertical suction lines. The Jacobs critical flux limit is characterized by high oil retention, since the annular liquid film has transitioned into a churn flow regime. Also, the vertical pressure drop at this region is high due to the increase in hydrostatic pressure drop component. Thus a suitable critical mass flux limit would ideally be higher than the Jacobs value, preferably at a value where both oil retention and pressure drop are optimally minimized. An ideal value of the critical mass flux should that at which the annular liquid film starts reversing. This point is characterized by a minimum pressure drop while the oil retention is significantly lower compared to that at the churn flow regime, as can be observed in experimental results presented in Chapter 3.

4.6.1 Model Development

This model is similar to the approach adopted by Sethi and Hrnjak (2011). The critical mass flux is taken to be that value at which the upward flowing annular liquid film starts reversing its flow direction. At this condition at which the liquid film near the tube wall just starts falling downwards, the shear stress at the wall should go to zero. The wall shear stress (τ_w) is obtained at the tube wall ($r = R$) from Equation (4.12) as follows

$$\tau_w = \tau_i \frac{(R-\delta)}{R} - \frac{1}{2}\left(\frac{dP}{dz} + \rho_l g_z\right)\left(\frac{R^2 - (R-\delta)^2}{R}\right) \tag{4.39}$$

When τ_w goes to zero and assuming δ^2 is negligible, we get the following relation

$$\tau_i \frac{(R-\delta)}{R} = \frac{1}{2}\left(\frac{dP}{dz} + \rho_l g_z\right)(2R-\delta) \tag{4.40}$$

Thus in order to calculate the critical mass flux, certain input parameters are required. The OCR, saturation pressure, the superheated suction line inlet temperature, the diameter and length of the suction line and the thermophysical properties of the liquid and vapor components need to be specified. As before, the suction line inlet quality and the local oil concentration are calculated in accordance with Thome (1995). Equation (4.40) is solved in conjunction with Equations (4.18), (4.20), (4.33) and the following two equations.

$$\dot{m}_v = \pi\alpha\rho_v \frac{D^2}{4} v_v \tag{4.41}$$

$$x = \frac{\dot{m}_v}{\dot{m}_v + \dot{m}_l} \tag{4.42}$$

Where x is the inlet vapor quality, m_v and m_l are the vapor core and the liquid film mass flow rates respectively. The critical refrigerant mass flux is thus calculated as follows.

$$G_{Critical} = \left(\frac{\dot{m}_v + \dot{m}_l(1-w_{local})}{\frac{\pi}{4}D^2}\right) \tag{4.43}$$

This critical mass flux should ideally be used to design vertical suction lines.

4.6.2 Comparison with Other Critical Mass Flux Limits

From Figures 4.17 and 4.18, the vertical suction line oil retention and pressure drop data are shown, along with various critical mass flux limits. The mass flux proposed by Jacobs *et al.* (1976) was observed to be the lowest mass flux value, where both oil retention and pressure drop are high and clearly this is unsuitable. The critical mass flux proposed by Kesim *et al.* (2000) assumed the volumetric flow rate of the oil to be zero as the limiting condition. It can be observed that this flux is only slightly higher than the Jacobs critical flux. The minimum mass flux proposed by Mehendale and Radermacher (2000) assumes the mass flux at which the annular liquid film starts reversing its direction to be the critical limit. This study also considered the effect of OCR on flow reversal, with lower OCR values having larger critical mass flux values. These critical mass flux values are larger than the Jacobs and Kesim's critical flux values. But flow visualization studies have indicated that film reversal occurs at a higher mass flux of around 50 kg/m^2-s, which is not accurately predicted by the this model. The use of the Wallis (1969) friction factor correlation maybe a possible reason for this discrepancy. The current model predicts higher critical mass flux values, in comparison to that predicted by Mehendale and Radermacher (2000). The effect of OCR is again accounted for in this correlation. Tables 4.1, 4.2 and 4.3 show the critical system capacity of operation for R134a/POE 100 mixture, with an OCR value of 0.1 %, 0.2 % and 0.3 % respectively. These capacities are achieved by converting the system critical mass flux at appropriate conditions of operation. A condensing temperature of 40 °C was employed, while the derived correlation has been applied for smooth copper tube, assuming negligible effect of surface roughness. These tables also capture the effect of saturation temperature and suction line inlet temperature on capacity. Correction multipliers are also provided for other liquid saturation temperatures.

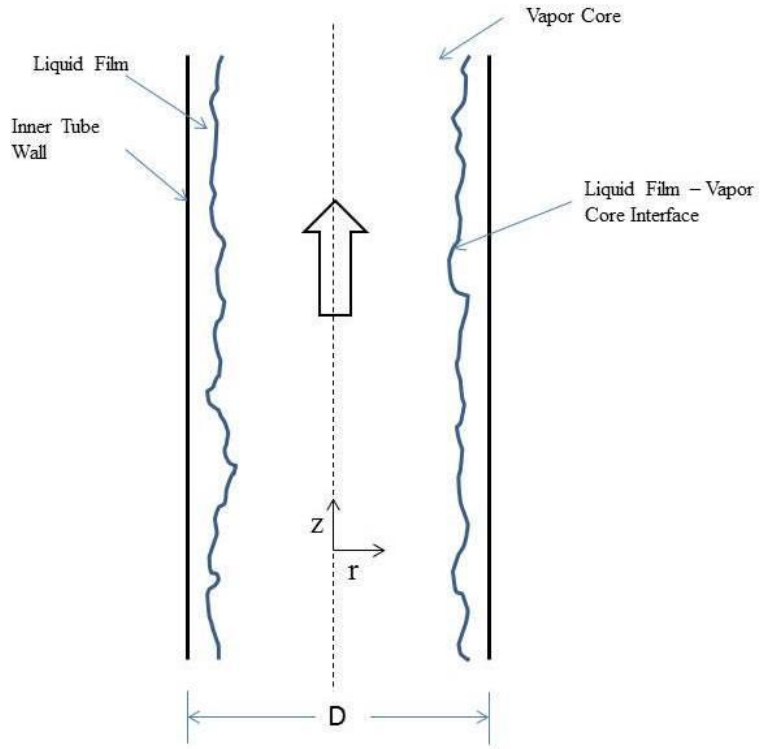

Figure 4.1 Realistic representation of annular flow in vertical suction line

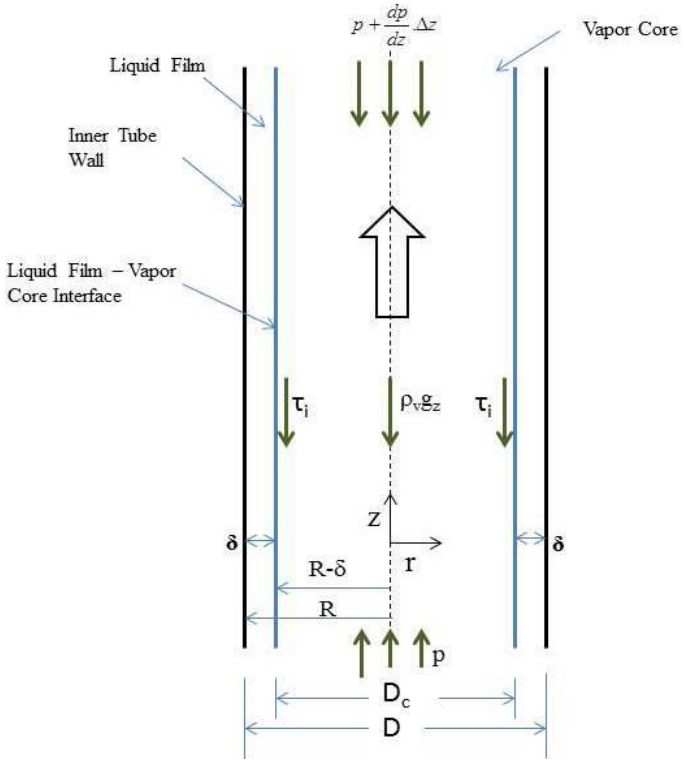

Figure 4.2 Simplified annular flow profile with momentum balance on the vapor core

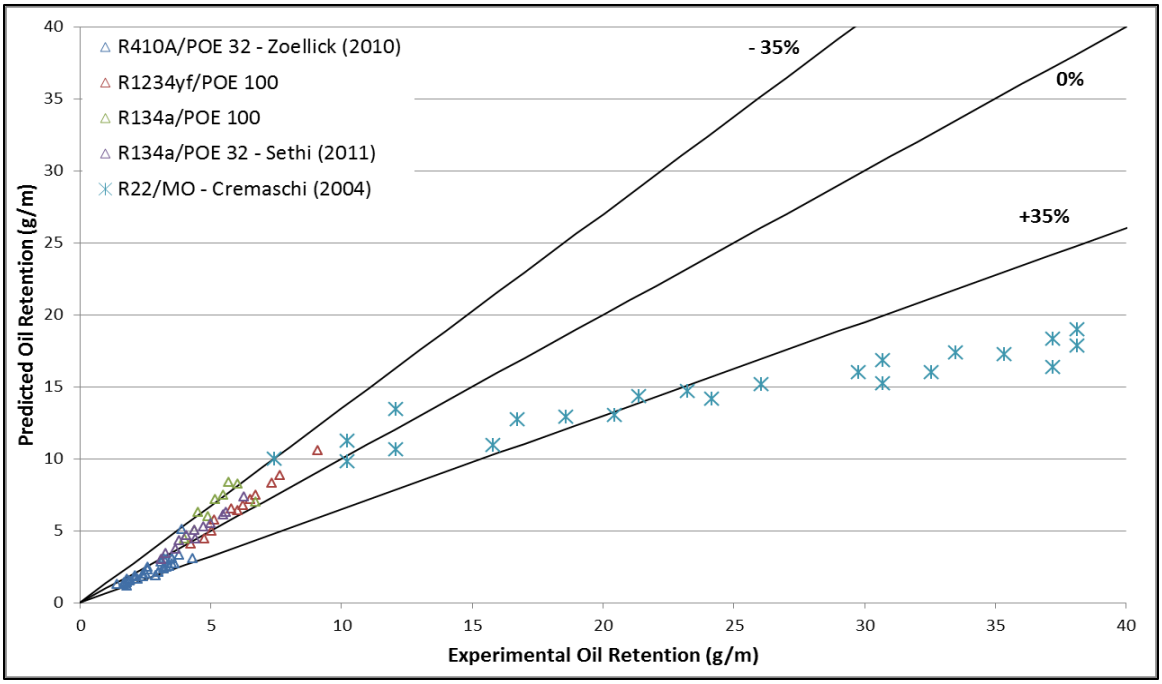

Figure 4.3 Validation of the proposed model for oil retention in vertical suction lines

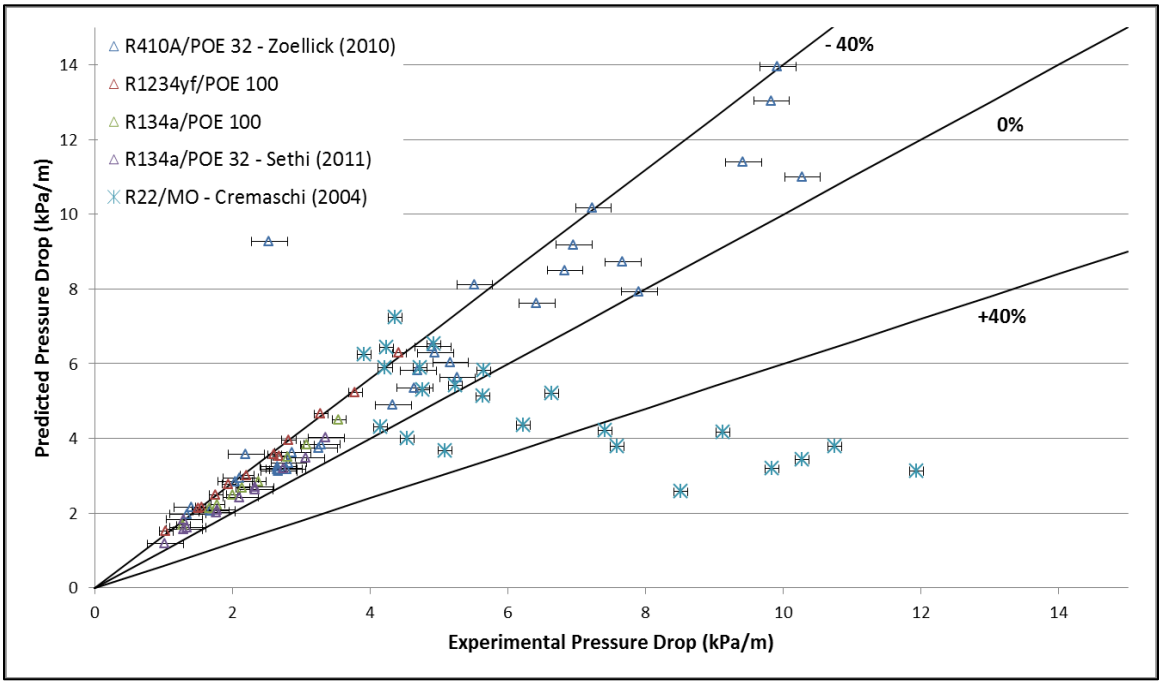

Figure 4.4 Validation of the proposed model for pressure drop in vertical suction lines

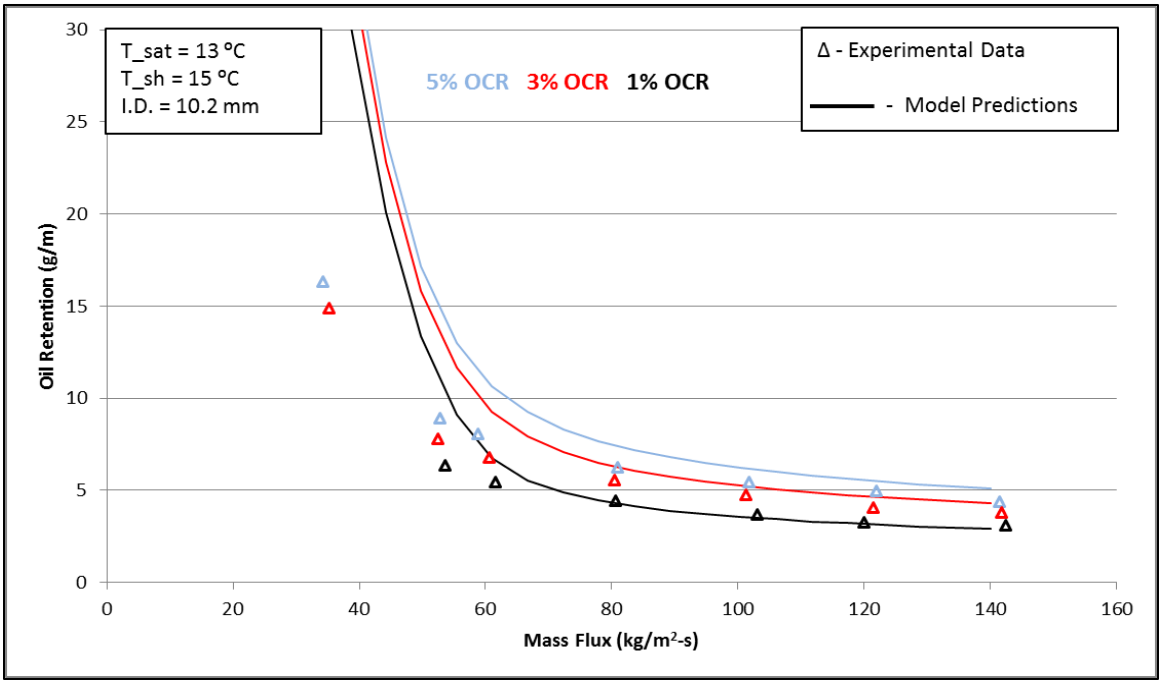

Figure 4.5 Experimental data and model predictions for variation of oil retention with mass flux in R134a/ POE 32

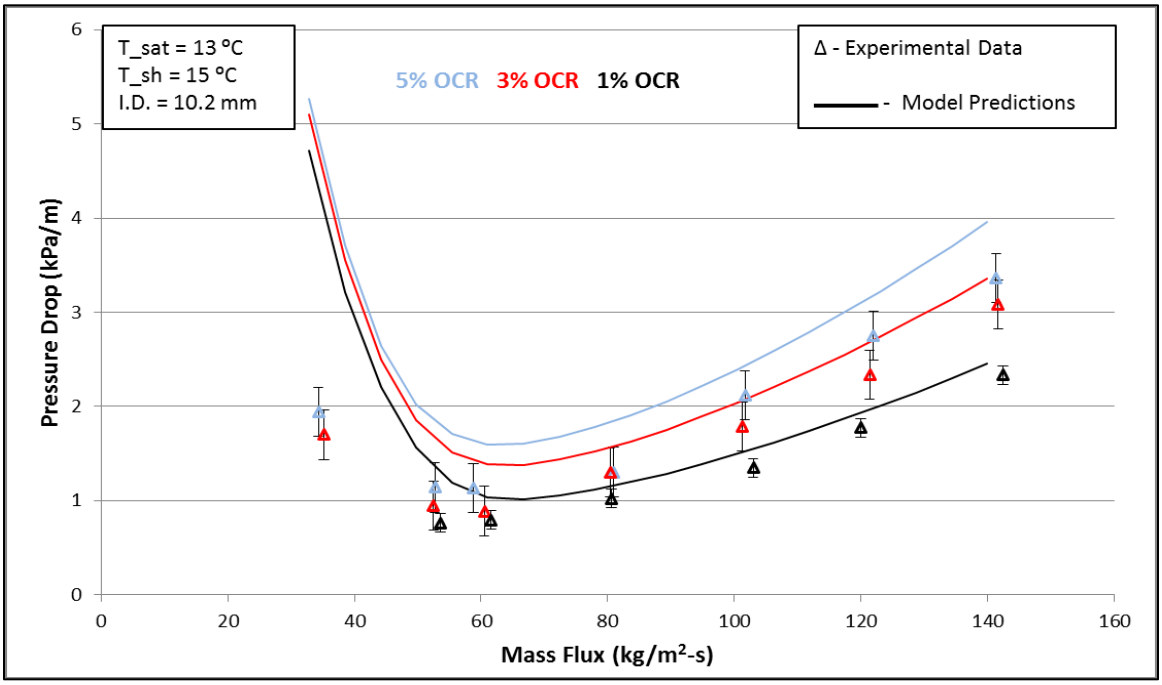

Figure 4.6 Experimental data and model predictions for variation of pressure drop with mass flux in R134a/POE 32

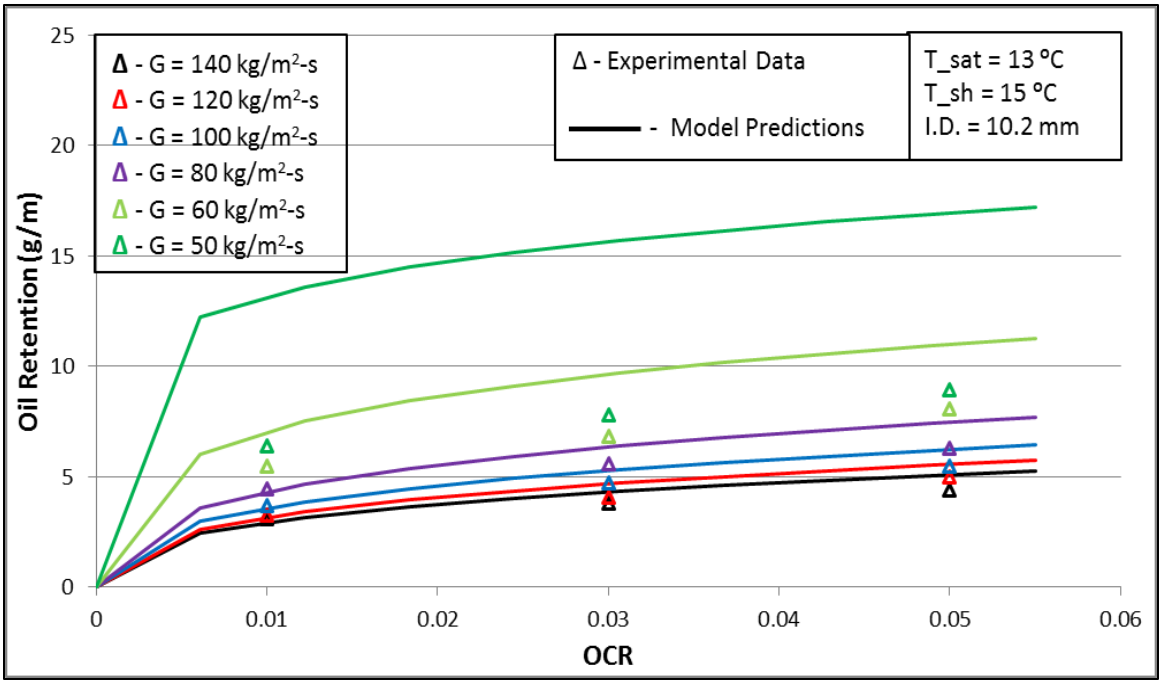

Figure 4.7 Experimental data and model predictions for variation of oil retention with OCR in R134a/POE 32

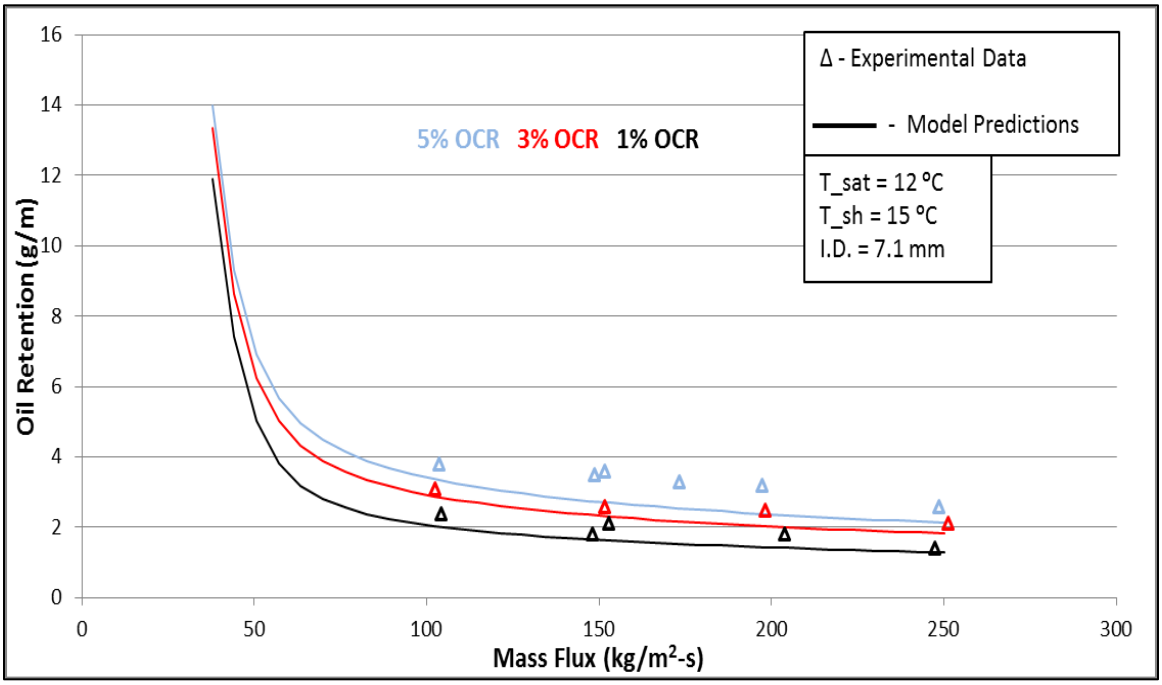

Figure 4.8 Experimental data and model predictions for variation of oil retention with mass flux in R410A/ POE 32

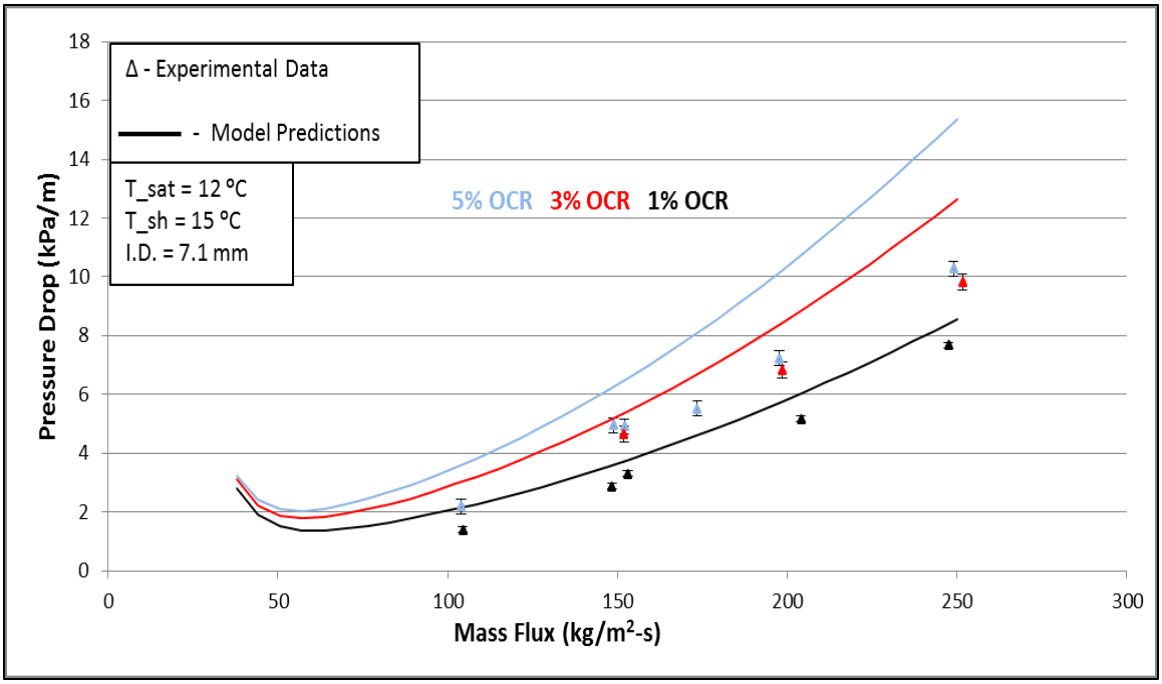

Figure 4.9 Experimental data and model predictions for variation of pressure drop with mass flux in R410A/POE 32

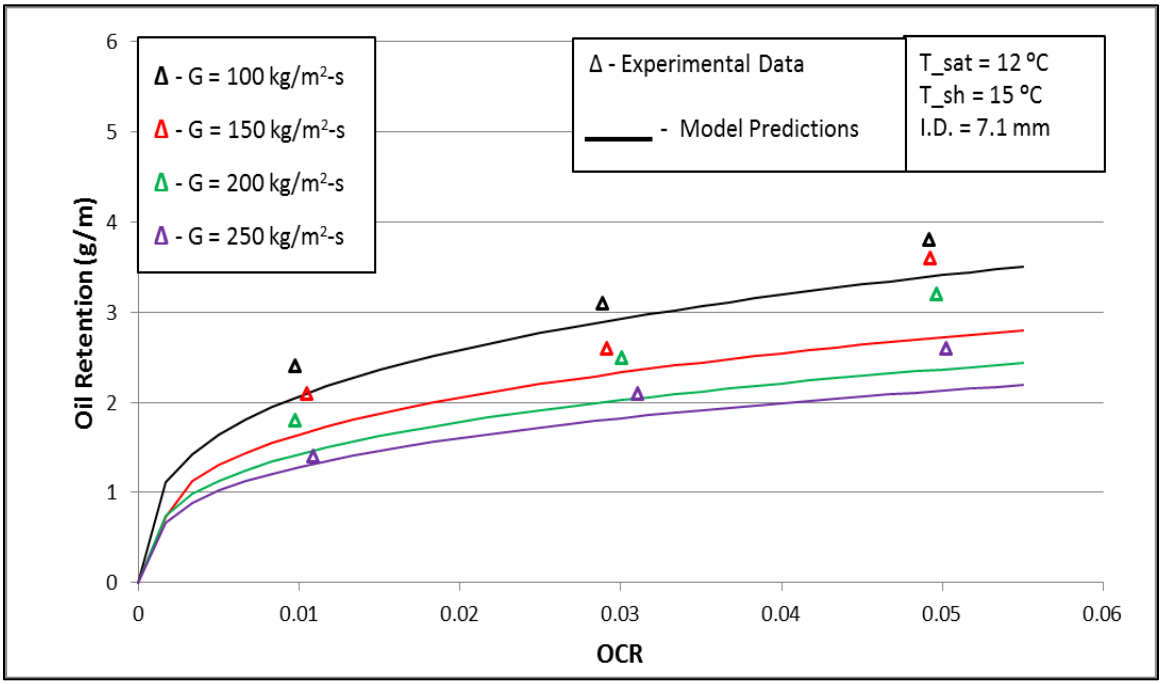

Figure 4.10 Experimental data and model predictions for variation of oil retention with OCR in R410A/POE 32

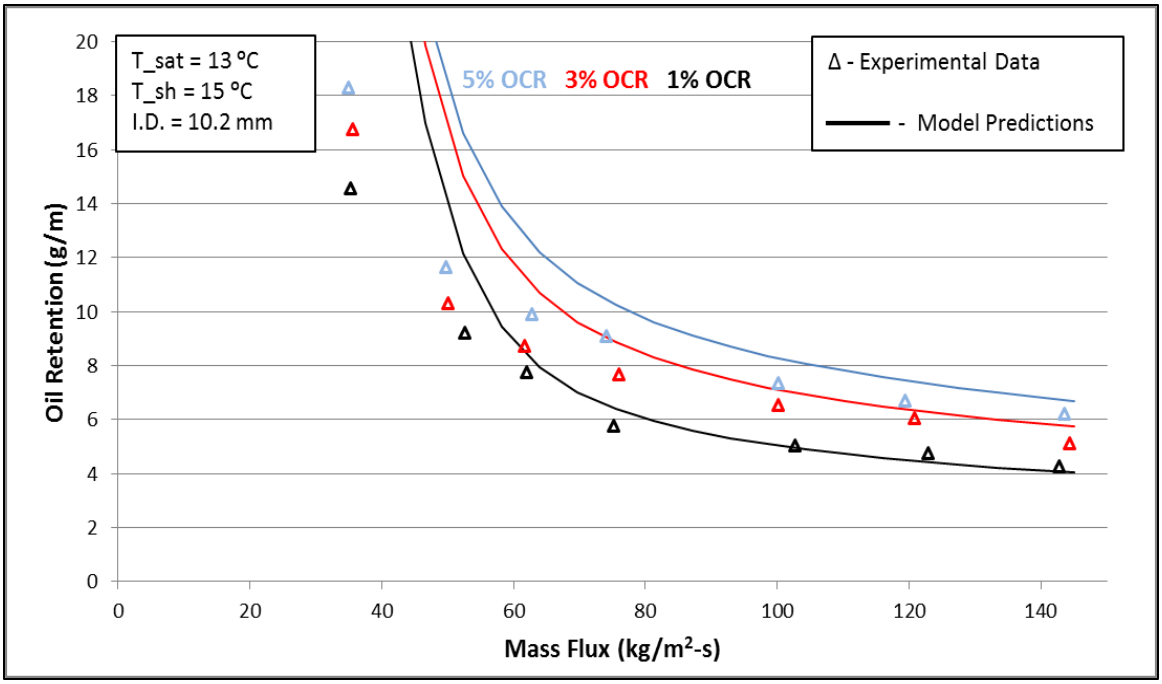

Figure 4.11 Experimental data and model predictions for variation of oil retention with mass flux in R1234yf/ POE 100

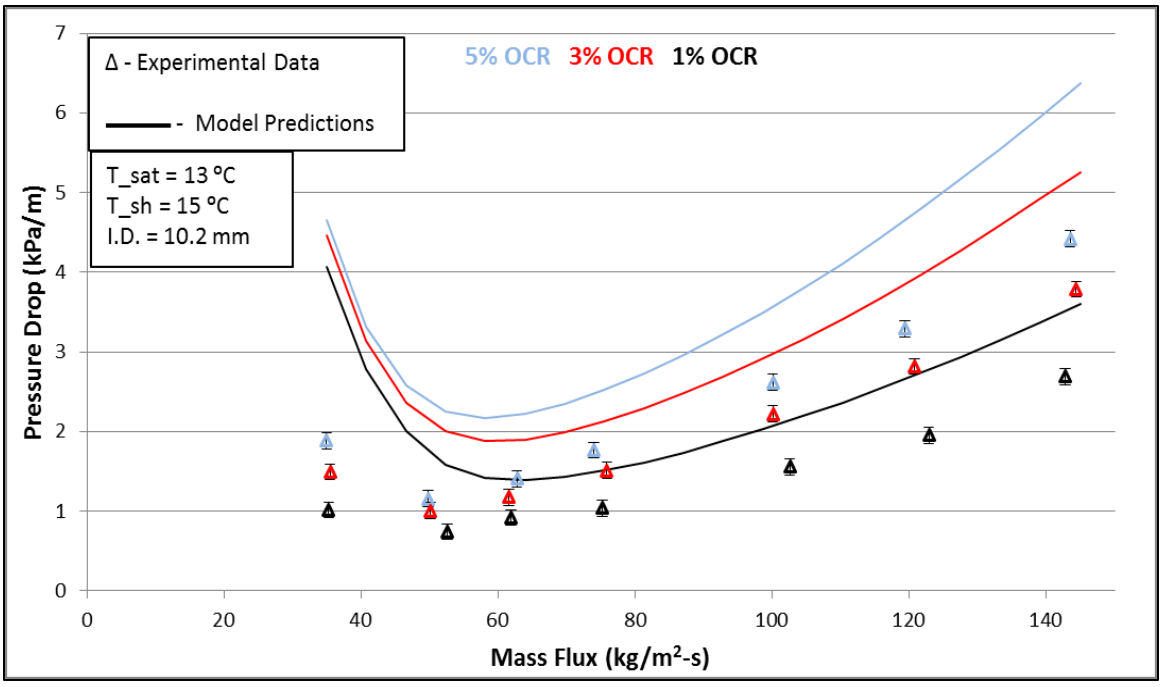

Figure 4.12 Experimental data and model predictions for variation of pressure drop with mass flux in R1234yf/ POE 100

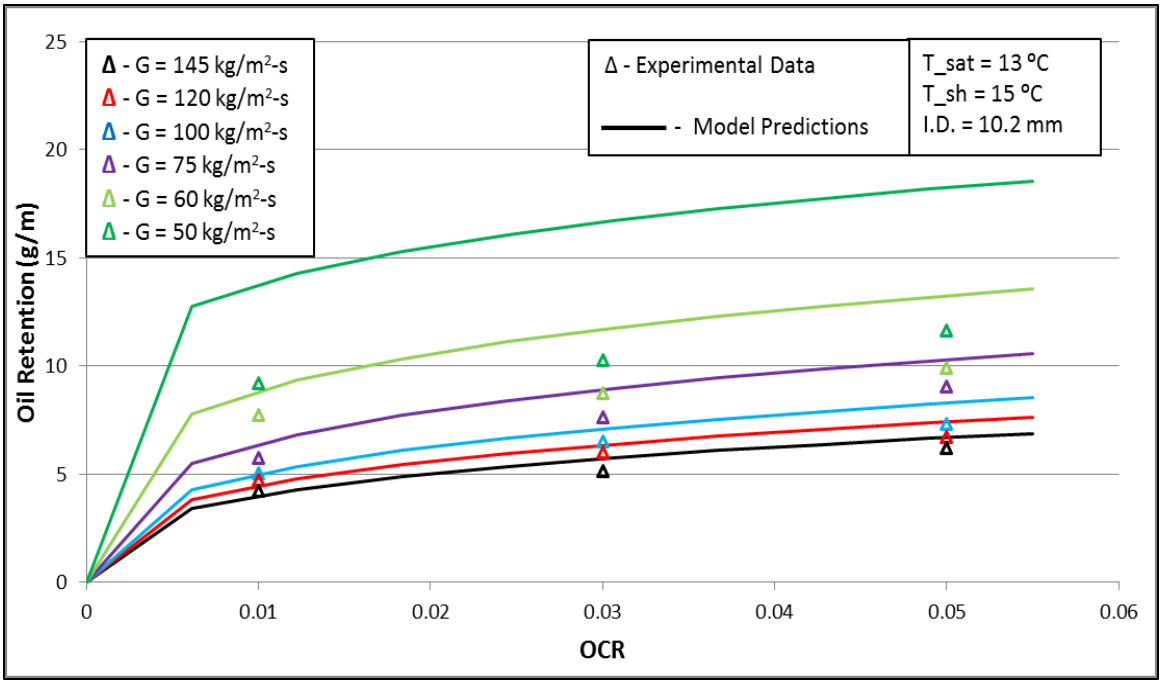

Figure 4.13 Experimental data and model predictions for variation of oil retention with OCR in R1234yf/POE 100

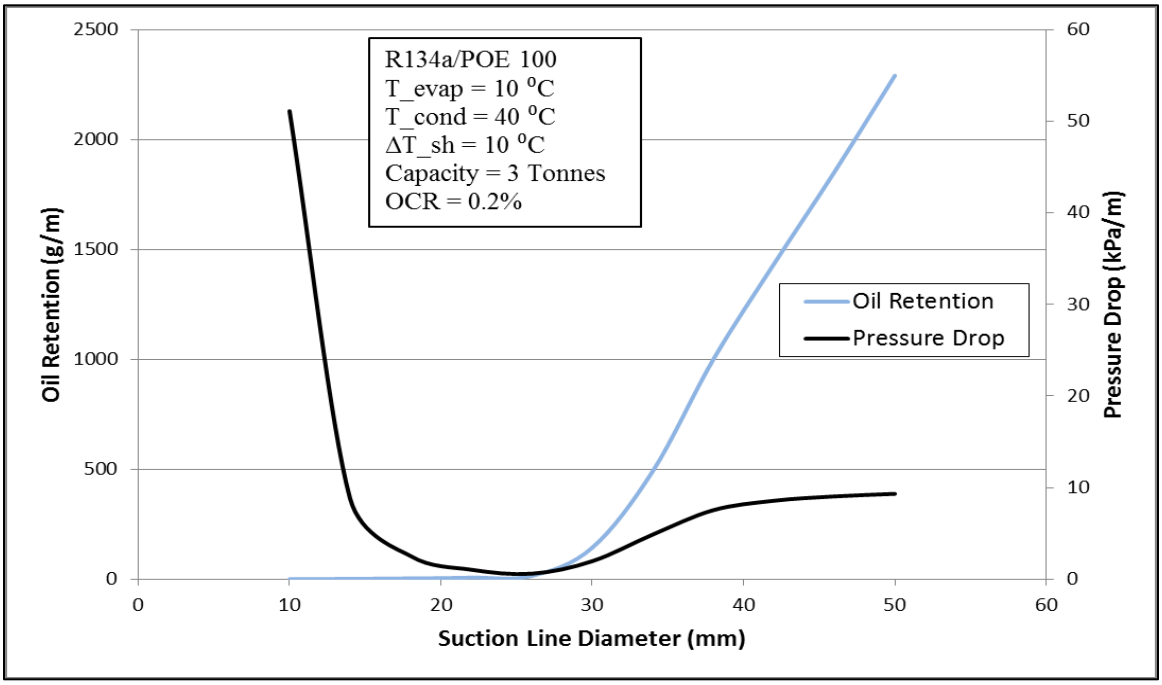

Figure 4.14 Parametric effect of suction line diameter on oil retention and pressure drop

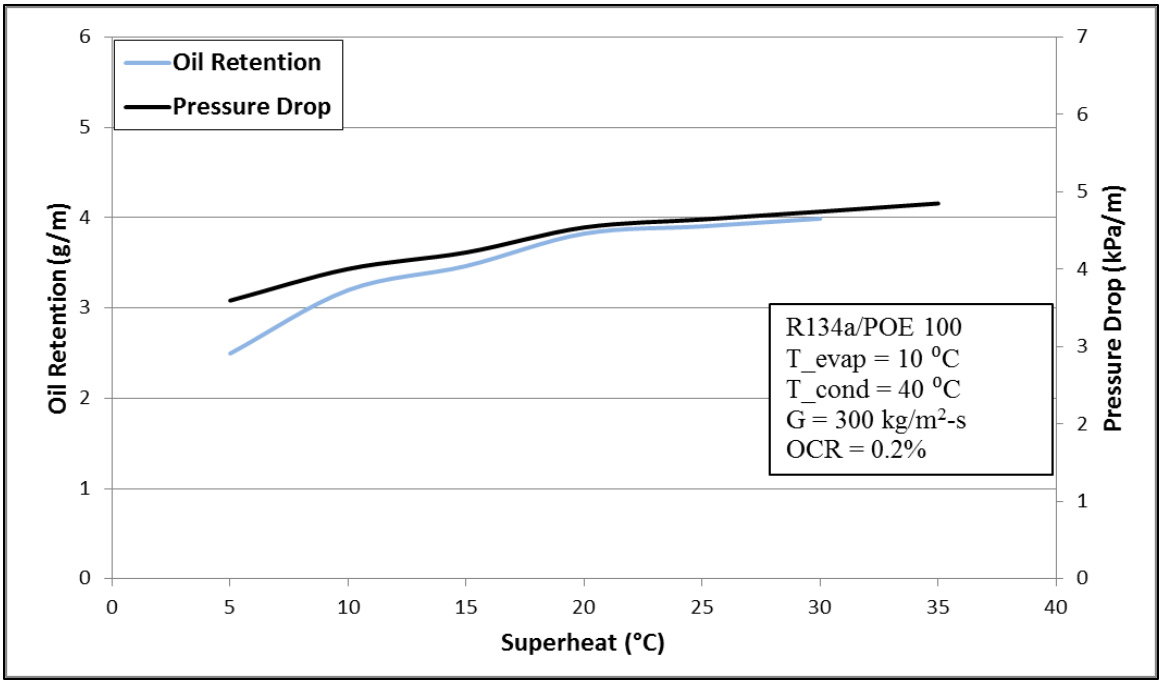

Figure 4.15 Parametric effect of degree of superheat on oil retention and pressure drop

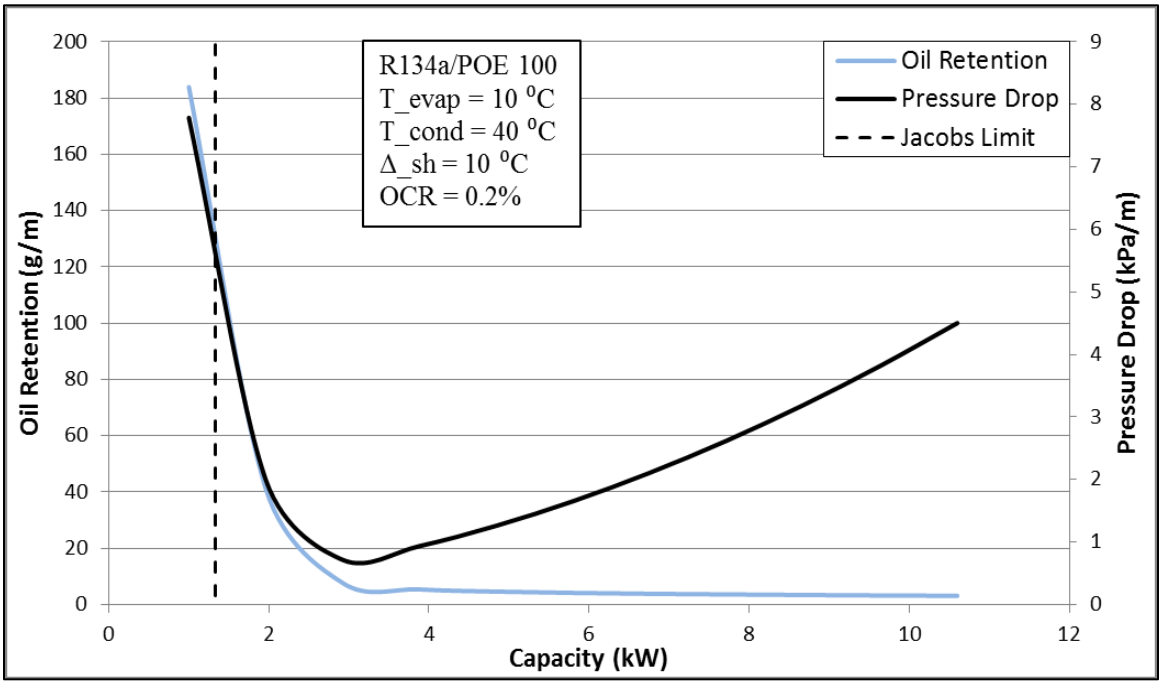

Figure 4.16 Parametric effect of cooling capacity on oil retention and pressure drop

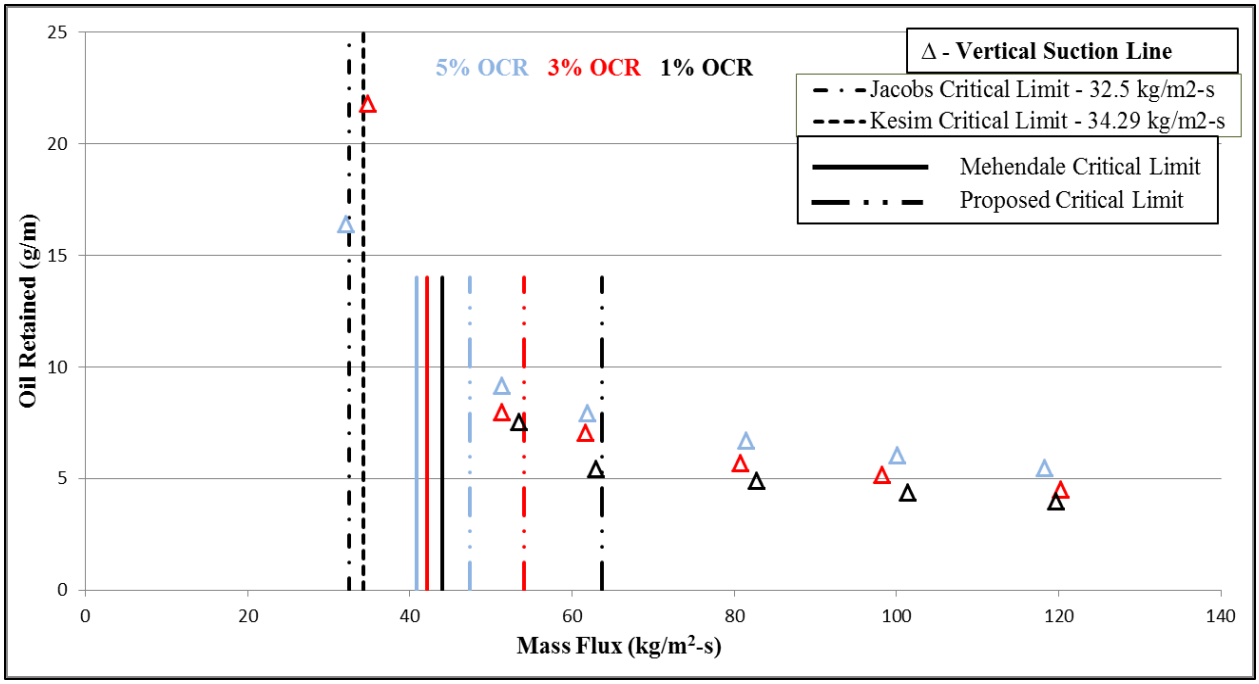

Figure 4.17 Oil Retention Data for R134a/POE 100 in 10.2 mm diameter suction line with various critical mass flux limits

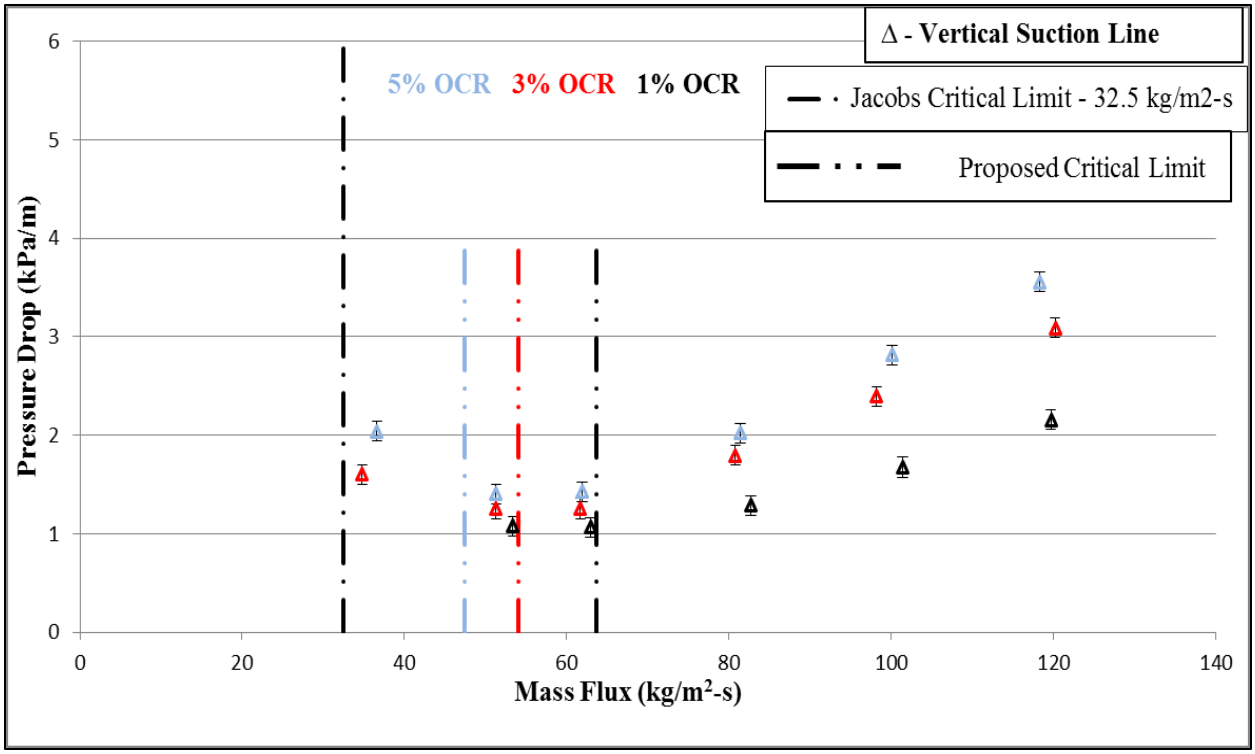

Figure 4.18 Pressure Drop Data for R134a/POE 100 in 10.2 mm diameter suction line with the proposed critical mass flux limits

Table 4.1 – Minimum Refrigeration Capacity (kW) based for Oil Entrainment up Vertical Suction Lines based on the current model (OCR of 0.1 %)

(Copper Tubing, ASTM 88M Type B, Metric Size)

Refrig-erant	Saturated Temp., °C	Suction Gas Temp., °C	Tube Nominal OD, mm												
			10	12	15	18	22	28	35	42	54	67	79	105	130
R134a	-10	-5	0.323	0.538	1.014	1.735	3.000	5.744	10.335	16.880	32.717	56.866	86.293	177.595	305.754
		5	0.301	0.507	0.968	1.676	2.932	5.720	10.314	16.692	31.975	55.068	83.023	171.062	295.319
		15	0.278	0.470	0.902	1.567	2.751	5.392	9.783	16.031	31.204	54.422	82.788	169.105	289.098
	-5	0	0.375	0.579	1.077	1.924	3.174	6.149	11.044	17.952	34.580	59.814	90.455	189.139	325.546
		10	0.334	0.560	1.061	1.825	3.121	5.937	10.703	17.489	33.917	58.980	89.533	184.369	317.544
		20	0.311	0.524	1.001	1.733	3.033	5.920	10.501	16.866	32.004	54.723	82.089	165.898	282.140
	5	10	0.422	0.696	1.308	2.235	3.857	7.409	13.212	21.353	45.837	70.431	106.962	220.417	379.820
		20	0.393	0.658	1.247	2.145	3.728	7.222	12.968	21.076	42.592	70.244	106.160	217.254	372.598
		30	0.370	0.623	1.190	2.062	3.610	7.052	12.757	20.857	40.478	70.205	105.811	215.226	367.608
	10	15	0.455	0.758	1.428	2.445	4.229	8.146	14.558	23.571	47.179	80.846	119.609	245.938	423.158
		25	0.422	0.711	1.354	2.340	4.088	7.964	14.373	23.455	45.412	77.866	117.405	241.266	411.921
		35	0.402	0.670	1.293	2.229	3.919	7.654	13.844	22.631	43.915	76.404	116.025	239.065	409.192

		Liquid Temperature, °C		
	Refrigerant	20	30	50
Correction Multipliers	134a	1.20	1.10	0.89

Table 4.2 – Minimum Refrigeration Capacity (kW) based for Oil Entrainment up Vertical Suction Lines based on the current model (OCR of 0.2 %)

(Copper Tubing, ASTM 88M Type B, Metric Size)

Refrig-erant	Saturated Temp., °C	Suction Gas Temp., °C	Tube Nominal OD, mm												
			10	12	15	18	22	28	35	42	54	67	79	105	130
134a	-10	-5	0.329	0.554	1.054	1.821	3.177	6.186	11.139	18.156	36.141	61.595	94.039	195.459	338.827
		5	0.299	0.509	0.981	1.714	3.026	5.971	10.896	17.971	35.097	60.876	92.241	189.380	327.506
		15	0.275	0.468	0.906	1.589	2.816	5.582	10.229	16.900	33.255	58.509	89.573	187.029	325.260
	-5	0	0.368	0.611	1.148	1.961	3.383	6.502	11.790	19.310	37.565	65.484	99.580	205.637	354.864
		10	0.337	0.568	1.089	1.892	3.319	6.495	11.577	18.569	36.392	63.820	97.473	202.722	351.576
		20	0.309	0.525	1.013	1.771	3.128	6.175	11.273	18.310	35.755	61.480	92.565	188.249	321.445
	5	10	0.429	0.720	1.367	2.356	4.102	7.962	14.322	23.309	46.972	79.886	120.888	245.103	420.108
		20	0.396	0.669	1.282	2.225	3.903	7.642	13.853	22.684	44.117	76.892	118.913	243.629	416.568
		30	0.367	0.664	1.204	2.106	3.720	7.348	13.422	22.110	43.382	76.124	116.317	241.387	414.835
	10	15	0.464	0.780	1.485	2.565	4.476	8.712	15.710	27.618	49.553	87.944	132.605	271.150	469.675
		25	0.422	0.715	1.377	2.402	4.234	8.339	15.196	25.993	48.889	85.606	130.348	267.785	460.469
		35	0.400	0.679	1.309	2.288	4.041	7.979	14.572	24.011	47.082	82.605	126.207	262.648	455.713

		Liquid Temperature, °C		
	Refrigerant	20	30	50
Correction Multipliers	134a	1.20	1.10	0.89

Table 4.3 – Minimum Refrigeration Capacity (kW) based for Oil Entrainment up Vertical Suction Lines based on the current model (OCR of 0.3 %)

(Copper Tubing, ASTM 88M Type B, Metric Size)

Refrig-erant	Saturated Temp., °C	Suction Gas Temp., °C	Tube Nominal OD, mm												
			10	12	15	18	22	28	35	42	54	67	79	105	130
134a	-10	-5	0.340	0.557	1.068	1.855	3.254	6.372	11.551	18.914	38.782	64.099	99.086	205.196	357.337
		5	0.295	0.504	0.979	1.719	3.025	6.063	11.131	18.419	36.315	63.295	97.452	201.166	347.054
		15	0.270	0.462	0.900	1.586	2.826	5.640	10.397	17.264	34.199	60.501	92.999	195.495	341.626
	-5	0	0.374	0.625	1.181	2.028	3.516	6.792	12.667	21.737	41.303	68.508	104.456	217.210	376.391
		10	0.335	0.568	1.095	1.913	3.375	6.655	12.137	19.995	39.103	66.267	101.605	212.692	370.562
		20	0.305	0.521	1.011	1.776	3.154	6.268	11.511	19.053	37.586	64.451	98.833	201.810	345.589
	5	10	0.431	0.727	1.389	2.407	4.214	8.232	15.890	24.342	47.236	82.180	124.792	257.116	447.005
		20	0.395	0.670	1.290	2.251	3.971	7.826	14.268	23.476	45.941	80.470	122.796	255.035	443.514
		30	0.363	0.619	1.201	2.111	3.750	7.455	13.697	22.683	44.776	78.989	121.167	253.841	441.872
	10	15	0.465	0.785	1.504	2.613	4.585	8.891	16.287	26.680	53.912	93.511	139.658	287.011	495.892
		25	0.418	0.711	1.377	2.415	4.280	8.466	15.554	25.766	50.605	89.075	136.415	284.347	490.787
		35	0.395	0.673	1.306	2.295	4.075	8.098	14.876	24.629	48.667	85.732	131.496	275.431	480.093

		Liquid Temperature, °C		
	Refrigerant	20	30	50
Correction Multipliers	134a	1.20	1.10	0.89

CHAPTER 5 – CONCLUSIONS

The current work presented data for oil retention and pressure drop in horizontal and vertical suction lines for four different refrigerant/oil mixtures, namely R134a/POE 100, R1234yf/POE 100, R410A/POE 100 and R410A/POE 32. Visualization was also performed in the transparent test sections in order to determine the flow regimes present and also the transition between one regime to another. This was followed by a semi-empirical analytical modeling, by means of which the oil retention and pressure drop were predicted. The following salient conclusions can be made from the current work:

- It is observed that the flow regime in the horizontal suction line is annular at high mass fluxes, which transitions into stratified wavy flow regime as the mass flux is reduced. Flow visualizations indicate that this transition occurs at a superficial vapor velocity of 4 m/s for R1234yf, 3 m/s for R410A and 5 m/s for R134a at 3-5 % OCR values.
- Flow visualizations also indicate that the flow regime in the vertical suction line is annular for all mass fluxes above the Jacobs critical limit. Flow reversal is noticed when the mass flux is reduced to 50 kg/m^2-s for R134a and R1234yf and at 60 kg/m^2-s for R410A. The Jacobs critical limit is characterized by a churn flow regime.
- It is observed that when the mass flux is reduced, oil retention in the vertical suction line continuously increases. As the mass flux is reduced, the oil retention in the horizontal suction line is characterized by an initial increase, after which it decreases and remains constant with subsequent reduction in mass flux. This is a consequence of the change in the flow regime from annular to stratified wavy. The film thickness in the stratified regime does not vary much with decrease in mass flux, resulting in constant oil retention.

- It is noted that the pressure drop in the horizontal suction line decreases continuously with reduction in mass flux. As the mass flux is reduced, the vertical suction line pressure drop decreases initially, passes through a minima point and increases again. This minima point coincides with the mass flux at which the flow reverses. The pressure drop again increases in the churn flow regime due to increase in the hydrostatic pressure drop component.
- It is observed that at the same mass flux and the same refrigerant, the oil retention increases upto 22 % in R134a, upto 38 % in R1234yf and upto 31% in R410A when the more viscous POE 100 is used in place of POE 32. Similarly, the horizontal suction line pressure drop increases upto 15 % in R134a, upto 27 % in R1234yf and upto 34 % in R410A. The pressure drop in the vertical suction line shows a steep increase of upto 55 % in R134a, upto 32 % in R1234yf and upto 63 % in R410A, when POE 100 is used. It is also observed that refrigerant/lubricant mixture property has preceding importance over pure lubricant properties.
- At the same superficial vapor velocity in POE 100, it is observed that R1234yf has higher oil retention and pressure drop values in comparison to R134a.
- For the same superficial vapor velocity in POE 32, it is noticed that R1234yf and R134a have similar oil retention, while a 20-30 % increase in pressure drop is observed in R1234yf. These results show that using R1234yf in the place of R134a as a drop-in replacement would definitely lead to a reduction in system performance.
- It is also seen that R1234yf shows a larger increase in oil retention and pressure drop in comparison to R134a for POE 100, while the magnitude of increase is observed to be smaller in the lower viscosity lubricant, POE 32.

- A semi-empirical model is developed in order to predict oil retention and pressure drop for upward annular film flow in vertical suction lines. The interfacial friction factor is expressed as a function of the liquid film Reynolds number, the vapor core Reynolds number, the non-dimensional annular film thickness and the mixture Weber number.
- The proposed model is validated using R134a/POE 32 data from Sethi and Hrnjak (2011), R410A/POE 32 data from Zoellick and Hrnjak (2010). It is observed that the model predicts more than 90% of the experimental oil retention and pressure drop data within limits of ± 35% and ± 40% respectively.
- Parametric variations were performed using the model. Oil retention and pressure drop are both found to increase when the degree of superheat increases. The mass flux at which the liquid film reversal starts is found to be a suitable critical mass flux value, with both the pressure drop and oil retention values being optimum. It is also determined that the Jacobs critical mass flux is unsuitable for sizing vertical suction lines, due to the high oil retention and pressure drop observed.
- The current work also presents a critical mass flux based on which vertical suction lines maybe sized properly. The mass flux at which the annular liquid film starts reversing is determined to be the critical mass flux limit. Tables denoting minimum system capacity values based on the proposed model are also presented for different OCR values.

APPENDIX A

Repeatability Test Results

Experiments were conducted in order to verify the repeatability of the test setup. Six experimental tests were conducted over a period of two weeks, with R134a being the refrigerant employed. POE 100 was the lubricant that was used. The operating condition was maintained at about 80 kg/m^2-s with an OCR of 3 %. The saturation temperature was calculated by means of measuring the absolute pressure in the test section. The saturation temperature was maintained at 13 °C, with a superheat of 15 °C provided. The detailed conditions of operation as well as the obtained test results are represented in Table A.1. The presented data included both oil retention and pressure drop in horizontal and vertical suction lines, with the results represented per unit length of the test section. At the outlet of the evaporator, both the temperature of the vapor core (T_{SH}) as well as the temperature of the tube wall (T_{TW}) was measured. These temperatures have to be close to each other in order to ensure that liquid and vapor phases are in equilibrium with each other, as it was observed in the measured tests. In general, the experimental results indicate that the tests are repeatable to a good degree of accuracy. However, minor fluctuations are encountered in the measured quantities. There are many reasons for these observed variations in oil retention, with the main one being the inability of closing the suction line ball valves at the same time and with the same precision every single time. Also, minor variations in the OCR, mass flux, etc. also lead to changes in the observed results. The average oil retention in the horizontal suction line was 3.99 g/m while it was 5.79 g/m in the vertical suction line, while the standard deviations were 0.12 g/m and 0.11 g/m respectively. Hence these variations account for 3 % and 2 % of the average oil retention values. Similarly, the average horizontal and vertical

pressure drops were 0.60 kPa/m and 1.79 kPa/m respectively, with standard deviations of 0.04 kPa/m and 0.05 kPa/m respectively.

Table A.1 Repeatability Test Data

T_{Sat}	G	T_{SH}	T_{TW}	OCR	$m_{oil,hor}$	$m_{oil,vert}$	dP_{hor}	dP_{vert}
[°C]	[kg/m^2-s]	[°C]	[°C]		[g/m]	[g/m]	[kPa/m]	[kPa/m]
13.3	80.9	28.3	27.6	0.0296	3.95	5.94	0.62	1.80
13.3	81.3	28.2	27.6	0.0309	4.09	5.83	0.66	1.86
13.0	81.3	28.2	27.6	0.0304	3.79	5.61	0.54	1.72
13.0	81.6	28.0	27.4	0.0304	4.02	5.73	0.59	1.77
13.0	81.7	27.9	27.2	0.0301	4.12	5.84	0.58	1.84
13.0	81.4	28.2	27.6	0.0313	3.99	5.79	0.60	1.78

APPENDIX B

EES Model Code for calculating oil retention and pressure drop in vertical suction lines

```
{1. Defined Quantities}

G =62.9                    {Total mass flux kg/m^2 s}

Psat = 0.455 [MPa]         {System saturation pressure in MPa}

w_inlet = 0.0103           {Oil concentration ratio, OCR}

T_evap_out = 28.1          {Evaporator outlet temperature in °C}

D=0.0102                   {Inner tube diameter in m}

L_vert = 1.89              {Length of Vertical Suction Line in m}

nu_l_cst = 18              {Viscosity of refrigerant oil mixture in cSt}

rho_l= 1035                {Density of refrigerant oil mixture in kg/m^3}

{Thome's (1995) Method for calculating local oil concentration}

{2. Determine local oil concentration in liquid at inlet of suction line}

{2.1 Interpolating two points just above and below P_sat}

Pabove = Psat +.005
Pbelow = Psat - .005
Tabove=Temperature(R134a,P=Pabove,x=.1)
Tbelow=Temperature(R134a,P=Pbelow,x=.1)

{2.2 Calculate a_0 and b_0 assuming zero w_inlet}

Tabove+273 = a_0 / (ln(Pabove) - b_0)
Tbelow+273 = a_0 / (ln(Pbelow) - b_0)

{2.3 a_1 to b_4 values are constants which are used along the calculated a_0 and b_0}

a_1 = 182.52
a_2 = -724.21
a_3 = 3868
a_4 = -5268.9

b_1 = -.72212
b_2 = 2.3914
b_3 = -13.779
b_4 = 17.066

{2.4 Finally calculate w_local}
```

A_w_local = a_0 + a_1*w_local + a_2*w_local^3 + a_3*w_local^5 + a_4*w_local^7
B_w_local = b_0 + b_1*w_local + b_2*w_local^3 + b_3*w_local^5 + b_4*w_local^7
T_evap_out+273 = A_w_local / (ln(Psat) - B_w_local)

{3. Determining Quality at inlet to the suction lines}

w_local*(1-x)= w_inlet

{4. Calculate Pure Vapor Density}

rho_v=Density(R134a,T=T_evap_out,P=Psat)

{5. Calculate Liquid Film Properties}

mu_v=Viscosity(R134a,T=T_evap_out,P=Psat)
mu_r=Viscosity(R134a,T=T_evap_out,x=0)
mu_l=rho_l * nu_l

nu_v = mu_v/rho_v {Kinematic viscosity of the vapor}
nu_l = nu_l_cSt*10^(-6) {Kinematic viscosity of the liquid}

{6. Calculating oil retention and pressure drop in the vertical suction line}

G_l=G*(1-x)

G_v=G*x

mdot_l=(G_l)*(3.14*D^2*0.25)

mdot_l=a+b

a=(2*3.14*rho_l/mu_l)*((tau_i*(0.5*D-delta)+((0.5*D-delta)^(2)/2)*(dpdz+rho_l*9.81))*(((0.5*D)^2-(0.5*D-delta)^2)/4-((0.5*D-delta)^(2)/2)*ln(1/(1-delta_by_R))))

b=(-1*3.14*rho_l/(8*mu_l))*(dpdz+rho_l*9.81)*((0.5*D)^2-(0.5*D-delta)^2)^2

delta_by_R=delta/(0.5*D)

dpdz+rho_v*9.81+(4*tau_i/(D*(alpha)^(0.5)))=0

alpha=((D-2*delta)/D)^2

tau_i=0.5*f_i*rho_v*v_v^2

v_v=G_v/(rho_v*alpha)

delta_plus=delta/(nu_v)*(tau_i/rho_v)^(0.5)

{6.1 Interfacial Friction Factor Correlation}

f_i/f_s=1+137240835.2*(delta_plus)^(1.0112)*Re_v^(-2.08)*(Re_lf)^(-0.0539)*(Weber_mix)^(0.864)

f_s=0.046*Re_v^(-0.2)

{6.2 Defining Various Non-Dimensional Terms in the Model}

Re_v=rho_v*v_v*D/mu_v

Re_lf=G*(1-x)*D/(4*mu_l)

sigma_r=SurfaceTension(R134a,T=T_evap_out)

sigma_o=46*10^(-3)

sigma_mix=(sigma_r)+(sigma_o-sigma_r)*(w_local)^(0.5)

Weber_mix=(G^(2)*D)/(sigma_mix*rho_l)

{6.3 Final Calculated Parameters}

Oil_retention_predicted=((3.14*D*delta*rho_l*w_local))*1000 {Oil Retention in g/m}

PressureDrop_Predicted = dpdz*(-1)/1000 {Pressure Drop in kPa/m}

EES Model Code for calculating critical refrigerant mass flux

{1. Defined Quantities}

G =62.9 {Total mass flux kg/m^2 s}

Psat = 0.455 [MPa] {System saturation pressure in MPa}

w_inlet = 0.0103 {Oil concentration ratio, OCR}

T_evap_out = 28.1 {Evaporator outlet temperature in °C}

D=0.0102 {Inner tube diameter in m}

L_vert = 1.89 {Length of Vertical Suction Line in m}

nu_l_cst = 18 {Viscosity of refrigerant oil mixture in cSt}

rho_l= 1035 {Density of refrigerant oil mixture in kg/m^3}

{Thome's (1995) Method for calculating local oil concentration}

{2. Determine local oil concentration in liquid at inlet of suction line}

{2.1 Interpolating two points just above and below P_sat}

```
Pabove = Psat +.005
Pbelow = Psat - .005
Tabove=Temperature(R134a,P=Pabove,x=.1)
Tbelow=Temperature(R134a,P=Pbelow,x=.1)
```

{2.2 Calculate a_0 and b_0 assuming zero w_inlet}

```
Tabove+273 = a_0 / (ln(Pabove) - b_0)
Tbelow+273 = a_0 / (ln(Pbelow) - b_0)
```

{2.3 a_1 to b_4 values are constants which are used along the calculated a_0 and b_0}

```
a_1 = 182.52
a_2 = -724.21
a_3 = 3868
a_4 = -5268.9

b_1 = -.72212
b_2 = 2.3914
b_3 = -13.779
b_4 = 17.066
```

{2.4 Finally calculate w_local}

```
A_w_local = a_0 + a_1*w_local + a_2*w_local^3 + a_3*w_local^5 + a_4*w_local^7
B_w_local = b_0 + b_1*w_local + b_2*w_local^3 + b_3*w_local^5 + b_4*w_local^7
```

T_evap_out+273 = A_w_local / (ln(Psat) - B_w_local)

{3. Determining Quality at inlet to the suction lines}

w_local*(1-x)= w_inlet

{4. Calculate Pure Vapor Density}

rho_v=Density(R134a,T=T_evap_out,P=Psat)

{5. Calculate Liquid Film Properties}

mu_v=Viscosity(R134a,T=T_evap_out,P=Psat)
mu_r=Viscosity(R134a,T=T_evap_out,x=0)
mu_l=rho_l * nu_l

nu_v = mu_v/rho_v {Kinematic viscosity of the vapor}
nu_l = nu_l_cSt*10^(-6) {Kinematic viscosity of the liquid}

{6. Calculating oil retention and pressure drop in the vertical suction line}

tau_i*(0.5*D-delta)/delta=0.5*(dpdz+rho_l*9.81)*(D-delta) {Wall Shear Stress Equated to Zero}

dpdz+rho_v*9.81+(4*tau_i/(D*(alpha)^(0.5)))=0

tau_i=0.5*f_i*rho_v*u_v^2

mdot_l=a+b

a=(2*3.14*rho_l/mu_l)*((tau_i*(0.5*D-delta)+((0.5*D-delta)^(2)/2)*(dpdz+rho_l*9.81))*(((0.5*D)^2-(0.5*D-delta)^2)/4-((0.5*D-delta)^(2)/2)*ln(1/(1-delta_by_R))))

b=(-1*3.14*rho_l/(8*mu_l))*(dpdz+rho_l*9.81)*((0.5*D)^2-(0.5*D-delta)^2)^2

delta_by_R=delta/(0.5*D)

dpdz+rho_v*9.81+(4*tau_i/(D*(alpha)^(0.5)))=0

alpha=((D-2*delta)/D)^2

tau_i=0.5*f_i*rho_v*v_v^2

v_v=G_v/(rho_v*alpha)

delta_plus=delta/(nu_v)*(tau_i/rho_v)^(0.5)

{6.1 Interfacial Friction Factor Correlation}

f_i/f_s=1+137240835.2*(delta_plus)^(1.0112)*Re_v^(-2.08)*(Re_lf)^(-0.0539)*(Weber_mix)^(0.864)

f_s=0.046*Re_v^(-0.2)

{6.2 Defining Various Non-Dimensional Terms in the Model}

Re_v=rho_v*v_v*D/mu_v

Re_lf=G*(1-x)*D/(4*mu_l)

sigma_r=SurfaceTension(R134a,T=T_evap_out)

sigma_o=46*10^(-3)

sigma_mix=(sigma_r)+(sigma_o-sigma_r)*(w_local)^(0.5)

Weber_mix=(G^(2)*D)/(sigma_mix*rho_l)

{6.3 Calculating Critical Mass Flux}

x=mdot_v/(mdot_v+mdot_l)

mdot_v=rho_v*0.25*D^2*3.14*u_v*alpha

G_critical=((mdot_v+mdot_l*(1-w_local))/(0.25*3.14*D^2))

APPENDIX C

R134a/POE 100 raw data – 10.2 mm pipe diameter

P_sat	T_sat	Total Mass Flux	OCR	T_ref_evap_out	T_r_e_wall	Mass Oil (Ho)	Mass Oil (Vert)	Pressure Drop (Ho)	Pressure Drop (Vert)
± 9 kPa	± 0.3 °C	(kg/m^2-s)		± 0.5 °C	± 0.5 °C	g	g	± 0.1 kPa	± 0.1 kPa
468	14.0	32.1	0.0515	29.1	28.0	21.81	32.78	0.14	4.08
467	13.9	51.3	0.0504	28.1	27.5	10.55	18.28	0.41	2.81
453	13.0	61.9	0.0495	28.0	27.3	10.16	15.85	0.67	2.85
454	13.0	81.4	0.0497	28.1	27.4	10.30	13.40	1.51	4.04
454	13.1	100.1	0.0505	28.0	27.3	11.53	12.05	3.18	5.63
453	13.0	118.3	0.0506	28.1	27.3	10.63	10.93	5.00	7.11
455	13.1	120.2	0.0300	28.0	27.3	8.83	9.02	4.39	6.18
454	13.0	98.2	0.0306	28.2	27.5	9.40	10.30	2.78	4.79
458	13.3	80.8	0.0313	28.0	27.4	7.78	11.37	1.33	3.59
454	13.0	61.7	0.0305	28.1	27.3	7.82	14.07	0.76	2.51
467	13.9	51.3	0.0305	28.2	27.5	7.69	15.93	0.39	2.50
470	14.1	34.8	0.0294	29.2	28.2	25.60	43.67	0.14	3.20
454	13.0	53.4	0.0114	28.2	27.5	6.35	15.05	0.37	2.15
455	13.1	62.9	0.0103	28.1	27.7	3.88	10.83	0.33	2.13
455	13.1	82.7	0.0118	28.1	27.8	5.52	9.77	0.92	2.57
454	13.0	101.4	0.0110	28.0	27.4	6.47	8.78	1.58	3.35
457	13.2	119.7	0.0104	28.1	27.5	7.09	7.96	2.91	4.31

R1234yf/POE 100 raw data – 10.2 mm pipe diameter

P_sat	T_sat	Total Mass Flux	OCR	T_ref_evap_out	T_r_e_wall	Mass Oil (Ho)	Mass Oil (Vert)	Pressure Drop (Ho)	Pressure Drop (Vert)
± 9 kPa	± 0.3 °C	(kg/m^2-s)		± 0.5 °C	± 0.5 °C	g	g	± 0.1 kPa	± 0.1 kPa
492	13.9	35	0.0510	29.2	28.5	22.50	36.62	0.13	3.77
492	14.0	49.8	0.0509	29.1	28.6	13.51	23.30	0.39	2.31
493	14.0	62.8	0.0500	29.2	28.7	12.22	19.83	0.57	2.81
478	13.0	74	0.0516	28.2	27.8	12.81	18.15	1.05	3.53
478	13.0	100.1	0.0501	28.1	27.3	13.51	14.67	3.04	5.23
479	13.1	119.4	0.0503	28.1	27.7	12.64	13.44	4.56	6.58
479	13.0	143.5	0.0505	28.0	27.6	12.16	12.46	6.53	8.84
491	13.9	35.5	0.0293	29.0	28.1	19.16	33.55	0.09	2.98
494	14.1	50.1	0.0312	29.1	28.2	10.61	20.60	0.41	2.01
492	14.0	61.6	0.0311	29.0	28.2	9.80	17.46	0.67	2.35
477	13.0	75.9	0.0304	28.1	27.5	9.74	15.32	0.94	3.02
478	13.0	100.1	0.0313	28.1	27.5	10.56	13.05	2.18	4.44
479	13.1	120.8	0.0309	28.1	27.4	11.24	12.07	4.10	5.63
479	13.0	144.4	0.0301	28.1	27.3	9.86	10.28	5.90	7.57
492	14.0	35.30	0.0132	29.2	28.8	16.11	29.11	0.00	2.03
494	14.1	52.6	0.0119	29.3	28.9	7.16	18.44	0.22	1.48
478	13.0	61.9	0.0109	28.3	27.8	6.74	15.52	0.45	1.84
478	13.0	75.2	0.0105	28.2	27.9	7.43	11.53	0.48	2.07
477	12.9	102.6	0.0104	28.0	27.8	8.03	10.08	1.51	3.11
477	12.9	122.9	0.0101	28.0	27.9	7.91	9.49	2.47	3.90
481	13.2	142.8	0.0102	28.2	28.0	7.52	8.50	4.01	5.38

R410A/POE 100 raw data – 10.2 mm pipe diameter

P_sat	T_sat	Total Mass Flux	OCR	T_ref_evap_out	T_r_e_wall	Mass Oil (Ho)	Mass Oil (Vert)	Pressure Drop (Ho)	Pressure Drop (Vert)
± 9 kPa	± 0.3 °C	(kg/m^2-s)		± 0.5 °C	± 0.5 °C	g	g	± 0.1 kPa	± 0.1 kPa
1169	14.0	46.4	0.0513	29.2	28.5	20.17	36.00	0.17	4.42
1138	13.0	60.8	0.0514	28.0	27.6	13.41	23.75	0.22	3.22
1137	13.0	82.6	0.0504	28.1	27.6	12.46	18.60	0.65	3.13
1139	13.0	125.3	0.0505	28.1	27.6	12.21	13.92	2.14	4.75
1140	13.1	164.8	0.0511	27.9	27.5	11.40	11.84	4.43	6.60
1170	14.0	45.1	0.0301	29.1	28.4	18.59	33.74	0.00	4.35
1140	13.1	62.4	0.0327	28.2	27.7	11.05	21.87	0.40	2.65
1138	13.0	83.1	0.0308	28.2	27.6	9.65	16.36	0.42	2.81
1140	13.1	124.9	0.0305	28.2	27.8	9.23	11.91	1.73	3.99
1140	13.1	165.0	0.0312	28.1	27.7	9.08	9.90	4.07	5.88
1170	14.0	48.0	0.0115	29.1	28.5	11.38	26.92	0.00	3.17
1136	13.0	62.2	0.0136	28.2	27.8	7.13	17.47	0.25	2.17
1137	13.0	83.4	0.0103	28.2	27.7	5.61	12.49	0.55	2.08
1138	13.0	124.8	0.0110	28.0	27.7	5.11	8.62	1.24	2.84
1143	13.2	166.5	0.0117	28.0	27.7	6.32	7.43	2.94	4.29

R410A/POE 32 raw data – 10.2 mm pipe diameter

P_sat	T_sat	Total Mass Flux	OCR	T_ref_evap_out	T_r_e_wall	Mass Oil (Ho)	Mass Oil (Vert)	Pressure Drop (Ho)	Pressure Drop (Vert)
± 9 kPa	± 0.3 °C	(kg/m^2-s)		± 0.5 °C	± 0.5 °C	g	g	± 0.1 kPa	± 0.1 kPa
1173	14.1	46.1	0.0514	29.1	28.5	18.34	33.95	0.02	3.70
1138	13.0	60.1	0.0508	28.0	27.5	11.33	23.81	0.19	2.42
1138	13.0	83.5	0.0499	28.2	27.8	9.93	16.73	0.27	2.00
1140	13.1	124.8	0.0511	28.1	27.5	10.06	12.66	1.44	3.19
1140	13.1	162.4	0.0506	27.9	27.4	11.15	12.08	3.50	4.56
1175	14.2	47.4	0.0285	29.0	28.5	14.61	32.68	0.00	2.94
1137	13.0	61.1	0.0305	27.9	27.5	8.93	20.78	0.17	2.06
1138	13.0	83.8	0.0293	28.0	27.7	7.35	14.27	0.42	1.89
1140	13.1	123.5	0.0307	28.0	27.5	8.46	11.60	1.29	2.62
1138	13.0	163.9	0.0304	28.0	27.6	8.39	9.38	2.83	3.77
1174	14.2	50.0	0.0098	29.1	28.5	8.03	24.13	0.08	2.31
1137	13.0	61.4	0.0108	28.0	27.7	6.00	17.88	0.12	1.48
1140	13.1	84.7	0.0114	28.2	27.9	5.03	11.97	0.34	1.28
1141	13.1	125.4	0.0102	28.3	27.9	4.65	8.12	0.85	1.88
1135	12.9	164.3	0.0106	28.0	27.6	5.70	7.08	2.00	2.62

REFERENCES

1. Abdolahi, F., Mesbah, A., Boozarjomehry, R.B. & Svrcek, W.Y., 2007, “The Effects of Major Parameters on Simulation Results of Gas Pipelines”, *International Journal of Mechanical Sciences*, vol. 49, no. 8: p. 989-1000.
2. Asali, J.C., Hanratty, T.J. & Andreussi, P., 1985, “Interfacial Drag and Film Height for Vertical Annular Flow”, *AIChE J.*, vol. 31, no. 6: p. 895–902.
3. ASHRAE, 1973, *Handbook and Product Directory, 1973 Systems*
4. Baker, O., 1954, "Simultaneous Flow of Oil and Gas", *Oil and Gas Journal*, vol. 53, no. 12: p. 185-190.
5. Belt, R.J., Van't Westende, J.M.C. & Portela, L.M., 2009, "Prediction of the Interfacial Shear-Stress in Vertical Annular Flow", *International Journal of Multiphase Flow*, vol. 35, no. 7: p. 689-697.
6. Biancardi, F.R, Michels, H.H., Sienel, T.H. & Pandy, D.R., 1996, “Study of Lubricant Circulation in HVAC Systems. Volume I – Description of Technical Effort and results”, *UTRC Technical Report*, United Technologies Research Center, East Hartford, CT.
7. Cremaschi, L., Hwang, Y. & Radermacher, R., 2005, "Experimental Investigation of Oil Retention in Air Conditioning Systems", *International Journal of Refrigeration*, vol. 28, no. 7: p. 1018-1028.
8. Cremaschi, L., 2004, “Experimental and Theoretical Investigation of Oil Retention in Vapor Compression Systems”, *PhD Thesis*, Center for Environmental Energy Engineering, University of Maryland, College Park, MD.
9. Crompton, J.A., Newell, T.A. & Chato, J.C., 2004, “Experimental Measurement and Modeling of Oil Holdup*”*, *ACRC TR-226*, Air Conditioning and Refrigeration Center, University of Illinois at Urbana-Champaign, Urbana, IL
10. F-Chart, 2010, Engineering Equation Solver (EES) (academic version), Madison, WI: F-Chart.
11. Jacobs, M.L., Scheideman, F.C., Kazem, S.M. & Macken, N.A., 1976, "Oil Transport by Refrigerant Vapor", *ASHRAE Transactions*, vol. 82, no. 2: p. 318-329.
12. Kesim, S.C., Albayrak, K. & Ileri, A., 2000, "Oil entrainment in Vertical Refrigerant Piping", *International Journal of Refrigeration*, vol. 23, no. 8: p. 626-631.

13. Lee, J.P., Hwang, Y., Radermacher & R., Mehendale, S.S., 2001, "Experimental Investigations on Oil Accumulation Characteristics in a Vertical Suction Line", *2001 ASME International Mechanical Engineering Congress and Exposition, November 11 - November 16, 2001,* American Society of Mechanical Engineers, New York, NY, United States, vol. 41, p. 63-69.
14. Lee, J.P., 2003, "Experimental and Theoretical Investigation of Oil Retention in Carbon Dioxide Air Conditioning System", *PhD Thesis*, Center for Environmental Energy Engineering, University of Maryland, College Park, MD.
15. Mehendale, S.S., 1998, "Experimental and Theoretical Investigation of Annular Film Flow Reversal in a Vertical Pipe" *PhD Thesis*, Center for Environmental Energy Engineering, University of Maryland, College Park, MD.
16. Mehendale, S.S. & Radermacher, R., 2000, "Experimental and Theoretical Investigation of Annular Film Flow Reversal in a Vertical Pipe: Application to Oil Return in Refrigeration Systems", *HVAC and R Research,* vol. 6, no. 1: p. 55-74.
17. Radermacher, R., Cremaschi, L. & Schwentker, R.A., 2006, "Modeling of Oil Retention in the Suction Line and Evaporator of Air-Conditioning Systems", *HVAC and R Research*, vol. 12, no. 1: p. 35-56.
18. Sethi, A. & Hrnjak, P., 2011, Oil Retention and Pressure Drop of R1234yf and R134a with POE ISO 32 in Suction Lines, *ACRC TR-281,* Air Conditioning and Refrigeration Center, University of Illinois at Urbana-Champaign.
19. Takaishi, Y. & Oguchi, K. 1987, "Measurements of vapor pressures of R22/oil solution", *Proceedings of the 18th International Congress of Refrigeration*, p. 217-222.
20. Thome, J.R., 1995, "Comprehensive Thermodynamic Approach to Modeling Refrigerant-Lubricating Oil Mixtures", *HVAC&R Research*, vol. 1, no. 2: p. 110-125.
21. Thome, J.R., 2004, *Engineering Data Book III*, Wolverine Tube Inc., chap. 12: p. 1-34.
22. van Rossum, J.J., 1959, "Experimental Investigation of Horizontal Liquid Films. Wave Formation, Atomization, Film Thickness", *Chemical Engineering Science*, vol. 11, no. 1: p. 35-52.
23. Wallis, G., 1969, *One Dimensional Two-Phase Flow*, McGraw-Hill Book Company, New York.

24. Wongwises, S. & Kongkiatwanitch, W., 2001, “Interfacial Friction Factor in Vertical Upward Gas-Liquid Annular Two-Phase Flow”, *Int. Comm. Heat Mass Transfer*, vol. 28, no. 3: p. 323-336.
25. Youbi-Idrissi, M. & Bonjour, J., 2008, “The Effect of Oil in Refrigeration: Current Research Issues and Critical Review of Thermodynamic Aspects”, *International Journal of Refrigeration*, vol. 31, no. 2: p. 165-179.
26. Zoellick, K.F. & Hrnjak, P.S., 2010, “Oil Retention and Pressure Drop in Horizontal and Vertical Suction Lines with R410A/POE ISO 32”, *ACRC TR-271*, Air Conditioning and Refrigeration Center, University of Illinois at Urbana-Champaign.